Advances in Regiocontrol and Bench Stability in

Nickel Catalyzed Reductive Couplings of Aldehydes and Alkynes

by

Evan P. Jackson

A dissertation submitted in partial fulfillment
of the requirements for the degree of
Doctor of Philosophy
(Chemistry)
in the University of Michigan
2015

Doctoral Committee:

Professor John Montgomery, Chair
Professor Melanie S. Sanford
Professor Johannes Schwank
Professor John P. Wolfe

Dedication

This dissertation is dedicated to my wonderful wife, Paige Jackson. Without her love, support, and encouragement I would not have made it this far.

Acknowledgements

I'd like to thank my advisor, Professor John Montgomery for all of his help and support over the years. He has helped me grow an incredible amount as a scientist and I'm grateful for his mentorship. Thank you to Professors Melanie Sanford, Johannes Schwank, and John Wolfe for serving on my committee and your feedback over the years.

I would also like to acknowledge Professor Ruben Martin at ICIQ for graciously letting me work in his lab for a summer as well as Dr. Josep Cornella who I worked closely with in the lab. It was a wonderful experience and I grew both as an individual and scientist. Thank you also to the members of the Martin lab for your hospitality and welcoming me to Tarragona.

Thank you to current and former Montgomery lab members who have played a valuable role in my education and I truly appreciate all of the support that I have received over the years. In particular, thank you to Dr. Ben Thompson and Dr. Zachary Buchan for mentoring me when I first started in the lab. Thank you to Dr. Jordan Walk who I've had the pleasure of sharing a cubby with for the past 5 years, I'm going to miss our scientific (and nonscientific) discussions.

Finally, thank you to my family and friends for your continued love and support.

Table of Contents

List of Schemes

List of Tables

List of Figures

List of Abbreviations

i-Pr-BAC•HBF_4 ..... 2,3-Bis(diisopropylamino)cycloprop-2-en-1-ylium tetrafluoroborate

n-Pr ..... *n*-propyl

i-Pr ..... *iso*-propyl

t-Bu ..... *tert*-butyl

acac ..... acetylacetone

Ad ..... adamantyl

COD 1,5-Cyclooctadiene

Cp ..... cyclopentadienyl

Cp* 1,2,3,4,5-pentamethylcyclopentadienyl

DMF ..... Dimethylformamide

DM-IPr•HCl ..... 1,3-bis(2,6-diisopropylphenyl)-4,5-dimethyl-1H-imidazol-3-ium chloride

dppp ..... 1,3-Bis(diphenylphosphino)propane

dppf ..... 1,1'-Bis(diphenylphosphino)ferrocene

Et ..... ethyl

equiv ..... equilivalent

GC-MS ..... gas chromatography mass spectrometry

GC-FID ..... gas chromatography flame ionization detector

IMes•HCl ..... 1,3-bis(mesityl)imidazolium chloride

IPr•HCl ..... 1,3-bis(2,6-diisopropylphenyl)imidazolium chloride

KIE ..... kinetic isotope effect

Mes ..... Mesityl

NHC .....N-Heterocyclic Carbene

PhMe ..... Toluene

PPh_3..... Triphenylphosphine

RDS.....rate determining step

rt .....room temperature

SIPr•HCl .....1,3-bis(2,6-diisopropyl-phenyl)-4,5-dihydroimidazolium chloride

TBS ..... *tert*-butyldimethylsilyl

THF .....tetrahydrofuran

Abstract

Advances in nickel catalyzed reactions have been achieved that allow for alteration and control of the rate- and regioselectivity determining step in nickel-catalyzed aldehyde-alkyne reductive couplings for the synthesis of allylic alcohols. Combinations of ligand, reducing agent, and reaction conditions have been identified that allow access to highly regioselective outcomes that were not possible using previously developed protocols. Previous mechanistic studies have shown the rate determining step to be metallacycle-forming oxidative cyclization, however this study shows that reaction conditions can be changed so that the rate determining step can be altered for one of the two product pathways. These modified conditions render metallacycle formation reversible for one of the product pathways and σ-bond metathesis becomes rate determining. This improved mechanistic understanding has allowed access to highly regioselective outcomes for a variety of substrates that were not previously possible. The selectivity for a variety of biased alkynes has been increased to >98:2 in many cases that had previously only been ~4:1.

Methodology has been developed to allow bench stable and inexpensive nickel sources to be used in reductive couplings, eliminating the need for a glove box or air sensitive reducing agents. Previous protocols have typically employed air sensitive Ni^0 sources or air-sensitive reducing agents, and this methodology eliminates the need for either of these. Two different protocols have been developed to efficiently couple a variety of aldehydes and alkynes using inexpensive and bench stable Ni^{II} pre-catalysts as well as bench-stable trialkylsilane reducing agents.

Chapter 1

Regiodivergent Catalytic Processes Using Alkynes

1.1 Introduction

Control of selectivity in catalytic reactions is a persistent challenge in synthetic organic chemistry. The control of enantioselectivity, regioselectivity, chemoselectivity, and site selectivity all present unique obstacles with different strategies devised to overcome the challenges in each of these cases. One particularly difficult challenge is the control of regiochemistry in reactions employing unsymmetrical π-components such as arenes, conjugated dienes, allenes, alkenes, and alkynes.[1] While many protocols have been developed that show high regioselectivity the development of regiodivergent protocols where either regioisomer can be accessed using catalytic methods is still quite rare and challenging. The control of regioselectivity as well as the development of regiodivergent processes is an extensive area of research from groups around the world, and the focus of this chapter will be on methods for regiodivergent functionalization of alkynes and mechanistic rational for the observed selectivity.

As shown in Scheme 1.1 various strategies can be employed to achieve high levels of regiocontrol in alkyne functionalization reactions. A commonly employed tactic for controlling regioselectivity is the use of directing groups where a motif may bind to a catalyst and direct the reaction at a specific site.[2] Directing groups are effective at promoting high levels of selectivity; however, they may present a challenge for both installation and removal from the desired product. In cases where directing groups are not employed, challenges arise from designing a catalyst that must operate in a non-directed fashion and be selective for the desired product. The

two strategies discussed in this chapter to afford high selectivity include fundamentally altering the metal employed in the reaction and altering the ligand scaffold on the metal to alter selectivity. Alteration of metal identity is commonly employed with biased π-systems such as terminal alkynes where the π-component presents a strong bias and promotes one pathway. Accessing the opposite regioisomer can be achieved in some cases by changing the metal employed which fundamentally alters the mechanism, thus providing a regiodivergent synthesis based on metal identity. In the second strategy, the ligand scaffold must now alter the catalyst substrate interactions such that a reversal in selectivity can occur. This strategy has been employed with both unbiased and biased alkynes to afford highly regiodivergent outcomes. In the cases described in this chapter, the major isomer is shown; however, not all protocols achieve perfect selectivity for the major isomer.

Scheme 1.1 Strategies to Achieve High Levels of Regiocontrol

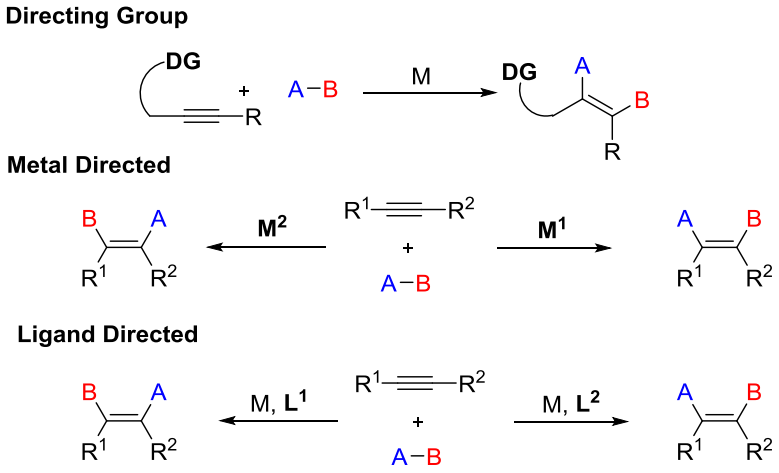

1.2 Regiodivergent Catalytic Processes Based on Metal Identity

One approach to accessing regiodiverent outcomes is though variation of the catalytic system by altering the metal employed which allows regiodivergent synthesis by fundamentally altering the mechanism of the reaction. This approach allows for highly regioselective outcomes

based on inherent reactivity of both the catalyst as well as typically a strong bias from the alkyne. However, accessing the opposite isomer generally requires an entirely different catalytic system being employed that proceeds through a distinct mechanistic pathway.

1.2.1 Triazole Synthesis

Perhaps the most well-known example of catalyst controlled regiodivergency is the copper and ruthenium catalyzed click reaction of azides and alkynes where either the 1,4- or 1,5-riazole products can be synthesized depending on metal catalyst employed. Use of a copper catalyst results in the 1,4 triazole product (Scheme 1.2, **1-1**) while use of a ruthenium catalyst affords the 1,5-triazole (Scheme 1.2, **1-2**). The origin for the observed regiodivergency in the reactions originates from fundamentally distinct mechanistic pathways for each metal.

Scheme 1.2 Synthesis of 1,4 and 1,5 Triazoles

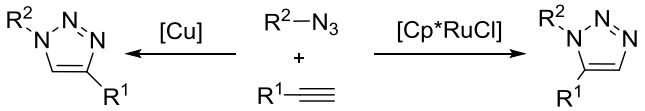

1-1 **1-2**

Synthesis of the 1,5-triazole is proposed to go through a ruthenacycle pathway where the regioselectivity is set in the oxidative coupling step by the coordination of the π-components. The mechanism for the ruthenium catalyzed pathway was investigated by Fokin and coworkers using DFT calculations, and 4 possible activated complexes for the π-components were proposed leading to 2 different possible regioisomeric outcomes. The lowest energy pathway was found to occur when the alkyne was coordinated to the catalyst with the larger substituent oriented away from the azide and the carbon substituted nitrogen of the azide coordinated to the Ru **1-3**, thus resulting in the observed selectivity (Scheme 1.3).[3] It should be noted that the authors observe a reversal in selectivity using $RuH_2(CO)(PPh_3)_3$ which leads to the 1,4 product, however no mechanistic discussion is presented.

Scheme 1.3 Regioseletivity Model for 1,5-triazole Synthesis

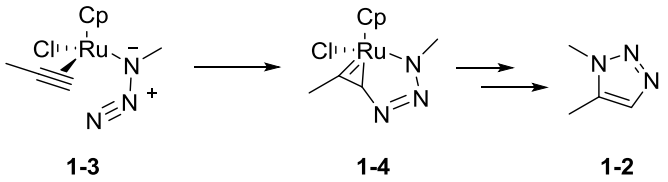

1-3 **1-4** **1-2**

Accessing the 1,4-triazoles product using a copper catalyst proceeds in a mechanistically distinct pathway from the previous ruthenium protocol.[4] Both mechanisms proceed through a metallacycle pathway, however, in a distinct mechanistic step the Cu catalyst forms a Cu-acetylide **1-5** prior to metallacycle formation. The regioselectivty of the reaction is determined during the cyclization step between a copper acetylide and the azide where the substituted nitrogen can coordinate to the metal and the electrophilic terminus of the azide aligns with the internal position of the alkyne (Scheme 1.4, **1-6**).

Scheme 1.4 Regioselectivity Model for 1,4-triazole Synthesis

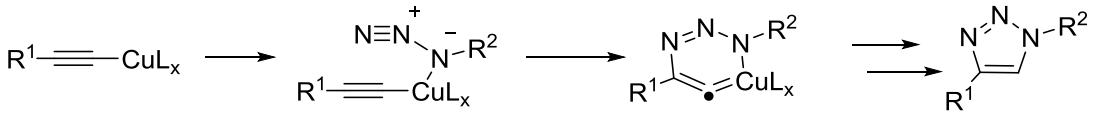

1-5 **1-6** **1-7** **1-1**

1.2.2 Alkyne Hydration

A variety of regiodivergent alkyne functionalization reactions have also been developed outside of click reactions based on metal identity. The hydration of alkynes is an attractive synthetic protocol to introduce either a ketone or an aldehyde depending on the reactive site on the alkyne. Nolan and coworkers showed that a Au-NHC complex was highly efficient at catalyzing the Markovnikov hydration of terminal alkynes (Scheme 1.5, **1-9**).[5] In addition to terminal alkynes, excellent yields were also observed for internal symmetrical alkynes, however, when unsymmetrical internal alkynes were used, a loss in selectivity was observed. Although no mechanistic studies were conducted, the proposed selectivity arises from the strong aurophilicity

of alkynes, with direct attack of water on the alkyne **1-8**. In a mechanistically distinct process, the anti-Markovnikov product can be accessed using a ruthenium catalyst and is proposed to proceeded through a Ru-vinylidene intermediate **1-9**.[6] The origin for selectivity arises from the Ru-vinylidene where the former terminal position on the alkynes becomes the most electrophilic site (Scheme 1.5). Although internal alkynes can be employed in the Nolan procedure, the Ru protocol can only employ terminal alkynes.

Scheme 1.5: Regiodivergent Hydration of Terminal Alkynes

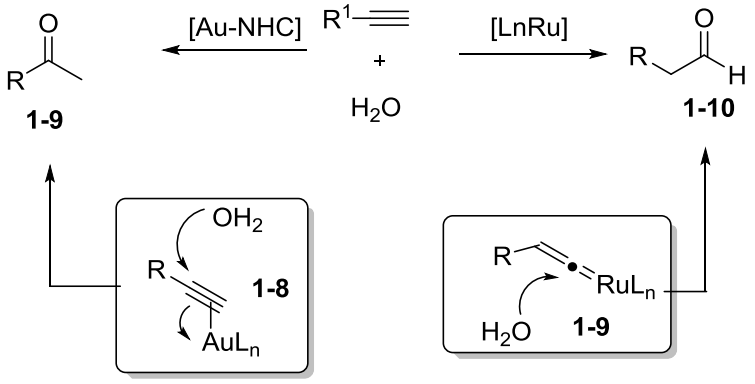

1.2.3 Hydroamination

Another example of metal controlled alkyne functionalization is the hydroamination of alkynes. Unlike the hydroamination of alkenes resulting in a secondary or tertiary amine, the hydroamination of alkynes leads to reactive imines or enamines which are attractive for further synthetic manipulations. Regiodivergence in intramolecular hydroamination developed by Looper and colleagues demonstrated a Ag^{I} catalyst was effective at promoting a 5-exo-dig cyclization and use of a Rh^{II} catalyst promoted the 6-endo-dig cyclization (Scheme 1.6).[7] The 5-exo-dig cyclization has been previously reported using transition metals; however the 6-endo-dig cyclization is much rarer. In mechanistic studies, the authors found that increasing the concentration of acetic acid when using $[Rh_2(oct)_4]$ reversed the selectivity of the reaction to favor the exo product **1-12**, suggesting that protonation of a vinyl rhodium intermediate (**1-14** or

1-16) is likely the rate limiting step. The authors also found that the ligand identity on the metal was crucial for the control of selectivity. Use of $[Rh_2(tfa)_4]$ favored the 5-exo product, however, use of $[Rh_2(oct)_4]$ favors the 6-endo product **1-13**. Both of these pieces of evidence suggest a Curtin-Hammett scenario where the initial cyclization is reversible and that stabilization of the kinetically favored 5-exo-dig intermediate results in the observed poor selectivity. This reversibility is proposed to lead to the preferential formation of the thermodynamic 6-endo product.

Scheme 1.6 Intramolecular Hydroamination

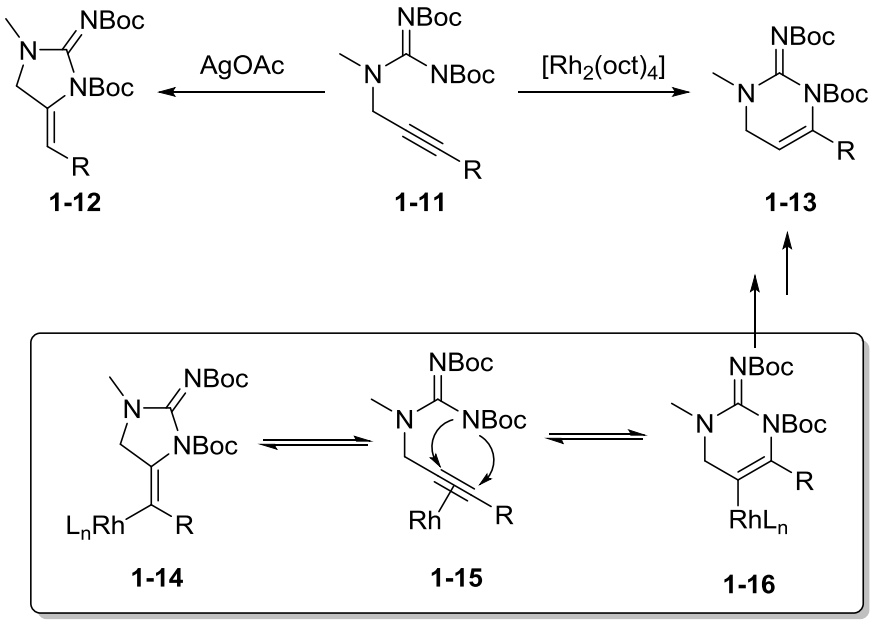

1.2.4 Hydrostannations

Accessing vinyl tin scaffolds is an important reaction due to their synthetic utility for a variety of C-C bond forming reactions. Metal identity has been shown to be crucial in regioselective hydrostannations of terminal alkynes[8] where use of a Mo catalyst generates the Markovnikov product (Scheme 1.7, **1-18**) and employing a Pd catalyst affords the anti-Markovnikov product (Scheme 1.7, **1-20**). Chong and coworkers showed that use of a Pd catalyst coupled with bulky trialkylphosphine ligands resulted in both high regio- and stereoselectivity

for the anti-Markovnikov product.[9] The mechanistic rational for the observed selectivity arises from steric interactions between the ligand and alkyne during the hydropalladation step favoring formation of the vinyl Pd species at the terminal position **1-19**. To access the anti-Markovnikov product **1-18**, Kazmaierand and coworkers have shown a Mo catalyst to be highly selective for the internal product.[10] In a distinct mechanistic pathway from the above protocol the selectivity arises from a stannyl metalation pathway (compared to a hydrometallation pathway with Pd) with the sterically larger Mo being added to the less hindered position on the alkyne **1-17**.

Scheme 1.7 Regiodivergent Hydrostannation

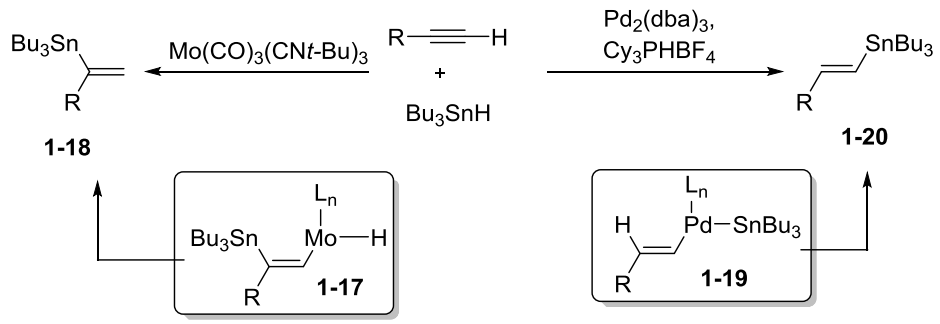

1.2.5 Hydrohydroxymethylation

Besides terminal alkynes, aromatic alkynes are another class of biased alkynes where there is a strong bias for one product pathway. Krische and Breit have shown that the selectivity on internal aromatic alkynes can be controlled by metal identity by employing either a Ni or Ru catalyst (Scheme 1.8).[11] In the optimized protocol, use of $[Ru(tfa)_2(CO)(PPh_3)_2]$ afforded high selectivity for C-C bond formation at the position adjacent to the aryl group **1-24** and use of $Ni(COD)_2$ affords the opposite isomer **1-22** with the new C-C bond formed adjacent to the methyl group on the alkyne. The authors propose fundamentally distinct pathways to account for the observed selectivity. Under Ru conditions, a Ru-H intermediate is proposed to undergo hydrometalation to generate a vinyl ruthenium **1-23** at the position adjacent to the aryl group, which sets the selectivity for the reaction. Alternatively, using a Ni catalyst generates a 5-

membered metallacycle **1-21** where the selectivity is set during oxidative cyclization. Although the authors did not conduct mechanistic studies in this report, both mechanistic manifolds have been well documented in analogous systems.[12,13] This methodology uses biased internal aromatic alkynes, and the authors do observe a loss of selectivity when non-aromatic substituted alkyne are used. Although internal alkynes can be employed, an inherent substrate bias needs to be present to achieve high levels of selectivity.

Scheme 1.8 Regiodivergent Allyilic Alcohol Synthesis

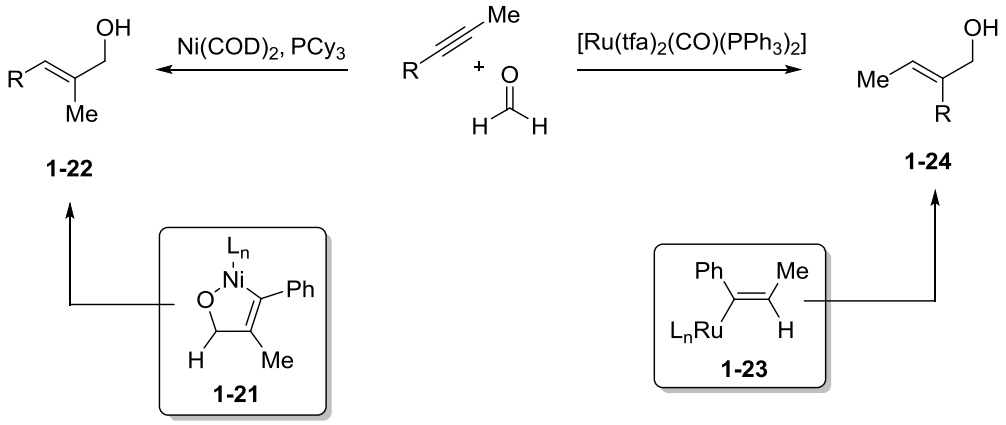

1.3 Regiodivergent processes based on ligand identity

Accessing regiodivergent outcomes with unsymmetrical alkynes using a single catalyst where the selectivity is controlled by ligand identity is a considerable challenge. In the cases described below, significant changes in either the ligand structure or a fundamental change in the kinetics are typically required to access high selectivity for both isomers.

1.3.1 Hydometallation

The ability to synthesize vinyl metal compounds by hydrometalation of alkynes is a particularly important synthetic transformation due to the prevalence of these compounds in cross coupling reactions. The hydroboration of alkynes to synthesize the anti-Markovnikov product has been well known for over half a century, however, accessing the Markovnikov

product is still quite challenging.[14] A regiodivergent protocol for the hydroboration of terminal alkynes has been developed by Hoveyda and coworkers employing a Cu-NHC catalyst where either regioisomer can be accessed in high selectivity depending on the ligand employed (Scheme 1.9).[15] The selectivity of the reaction is dictated by both steric and electronic effects from the ligand as well as electronic effects on the alkyne. The authors found that alkyl substituted NHC ligands favored formation of the anti-Markovnikov product **1-26** compared to less electron donating aryl groups which favored formation of the Markovnikov product **1-28**. Additionally, ligand sterics also dictated selectivity with aryl substituted NHC disfavoring formation of the terminal substituted product. The selectivity of the reaction is set in the binding of the alkyne to copper (**1-25** and **1-27**) followed by irreversible formation of the vinyl copper species. It should be noted that Hoveyda and coworkers have also reported a regiodivergent hydroalumination protocol where $Ni(PPh_3)_2Cl_2$ resulted in terminal substitution and use of $Ni(dppp)Cl_2$ afforded internal substitution, however no mechanistic rational is presented for the observed selectivity.[16]

Scheme 1.9 Cu-Catalyzed Hydroboration of Alkynes

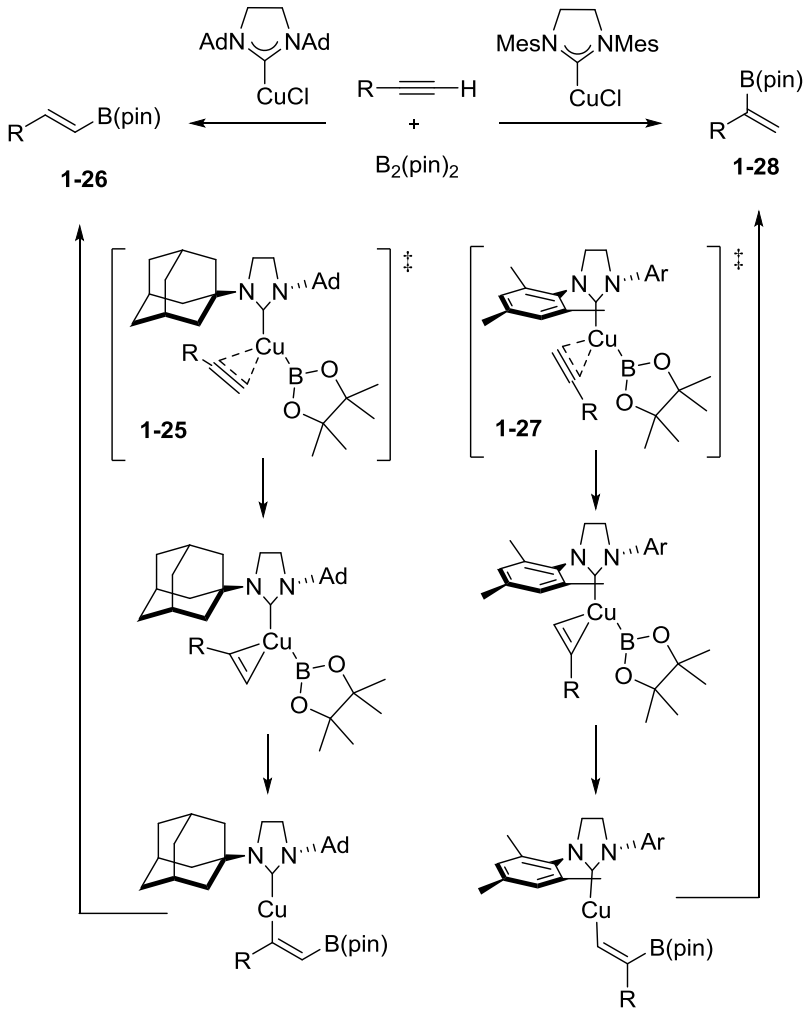

In addition to the hydroboration of alkynes, the hydrosilylation of alkynes is also an attractive reaction due the synthetic utility of vinyl silanes. Work from Trost and others have shown Ru catalysts to be effective at promoting the hydrosilylation of alkynes to afford not only the Markovnikov and anti-Markovnikov products, but both *E* and *Z* isomers of the anti-Markovnikov products selectively (Scheme 1.10).[17,18] A recent computational study helped elucidate the selectivity for the observed isomers in alkyne hydrosilylation. Houk and Wu found that a combination of both steric and electronic effects from the ligand dictate the observed selectivity.[19] Employing $[CpRu(i\text{-}Pr_3P)(MeCN)_2]^+$ results in the anti-Markovnikov product **1-29**, however, use of $[CpRu(MeCN)_3]^+$ generates the Markovnikov product **1-30**. In contrast to the

hydroboration mechanism where ligands dictate the binding preference of the substrates and both isomers are formed through similar reaction pathways, the hydrosilylation mechanism proceed though fundamentally different intermediates. Formation of the Markovnikov product proceeds though a hydrometalation pathway, however, the anti-Markovnikov product goes through a silylmetalation pathway. The anti-Markovnikov selectivity with $(i\text{-Pr})_3P$ arises from steric interactions between the bulky phosphine and silane resulting in the installation of silicon at the terminal position being most favored. Additionally, the NBO charge on the terminal carbon of the alkyne is more negative than the internal carbon, thus further favoring the positively charged silyl group installation at the terminal position when using $P(i\text{-Pr})_3$. Exchanging the $(i\text{-Pr})_3P$ ligand for MeCN results in high selectivity for the Markovnikov product. Selectivity arises from MeCN being less sterically bulky and the catalyst can better accommodate the bulky silyl group favoring hydrometalation on the alkyne generating a vinyl Ru species.

Scheme 1.10 Hydrosilylation of Alkynes

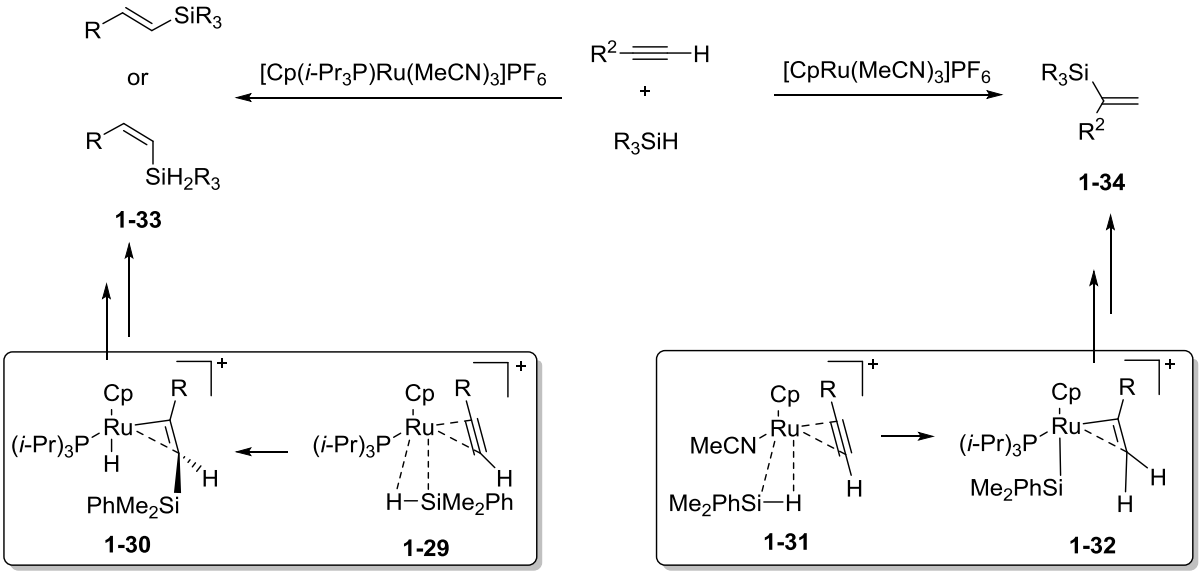

Although terminal alkynes possess an inherent steric and electronic bias, internal alkynes present a unique set of challenges due to a lack of bias between the substituents. Recently, Sun

and Wu showed that by switching between Cp and Cp* ligands in Ru catalyzed hydrosilylations of internal silyl alkynes, either regioisomer could be synthesized in high selectivity (Scheme 1.11).[20] Computational studies suggested that steric interactions between the ligand and silyl group on the alkyne were responsible for the observed selectivity with the Cp* ligated system favoring silane installation at the more sterically hindered position on the alkyne **1-39** and Cp favoring the opposite isomer **1-40**. The authors additionally found that silyl alkynes did not need to be employed, and use of a bulky *t*-Bu group afforded high levels of regiocontrol, although the selectivity was decreased from when TMS was employed. The selectivity of the reaction is proposed to be set in the hydrometalation step forming a vinyl Ru species **1-36** or **1-38** for both isomers.

Scheme 1.11 Internal Alkyne Hydrosilylation

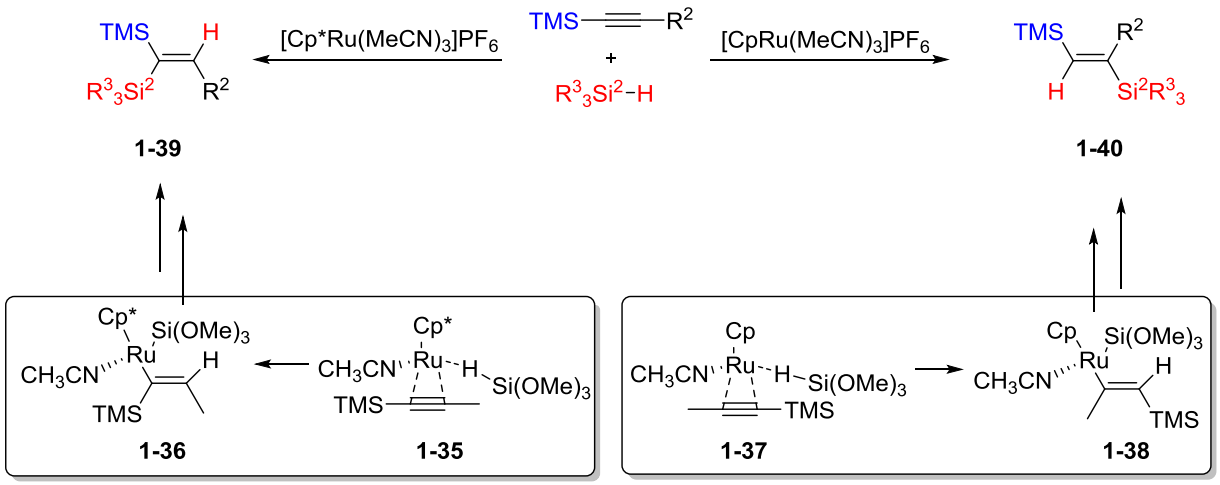

The installation of two functional groups across an alkyne to afford difunctionalized alkenes and the ability to reverse this selectivity is much rarer than just adding a single functional group. Suginome and coworkers have shown highly regiodivergent outcomes are possible in Pd catalyzed silaborations of terminal alkynes by altering the ligand employed (Scheme 1.12). Employing PPh_3 as a ligand in the Pd catalyzed reaction results in high selectivity for installation

of boron at the terminal position on the alkyne and delivering silane to the internal position **1-43**.[21] This selectivity can be reversed by employing a more electron rich and bulky phosphine to obtain the opposite regioisomer with installation of the boron on the internal position **1-44**.[22] Mechanistic studies suggested the origin for selectivity arises from reversible insertion of Pd into the alkyne (**1-41**) when bulky electron rich ligands are used, compared to this being an irreversible step when using PPh_3. The authors suggest that steric interactions between the ligand and alkyne may destabilize intermediate **1-41** pushing the equilibrium towards **1-42**.

Scheme 1.12 Regiodivergent Silaborations

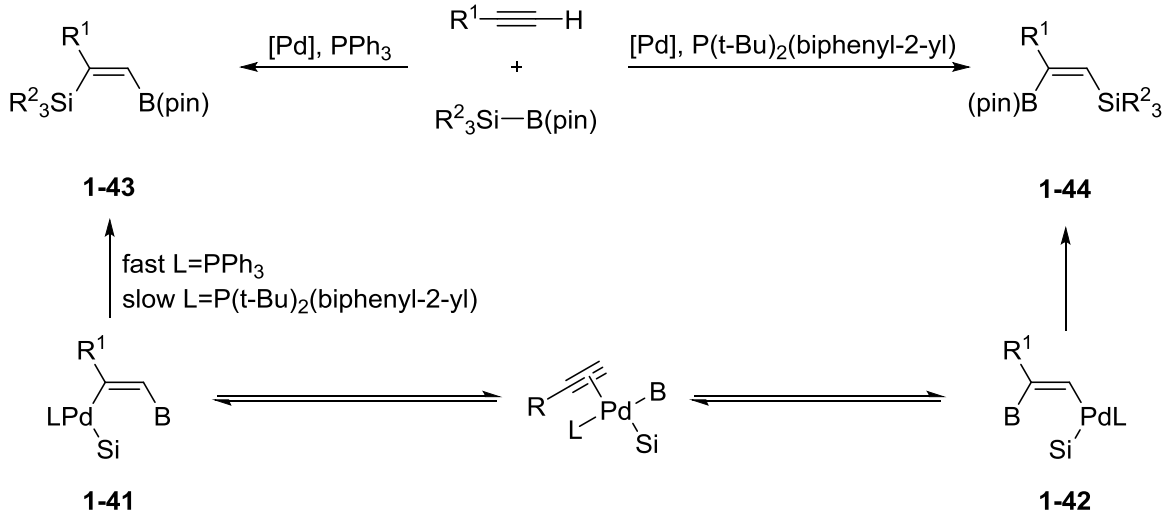

1.3.2 Cyclization Reactions

In comparison to the above reports for carbon-heteroatom bond formation, there are only a few reports of catalytic regiodivergent protocols for formation of new C-C bonds employing alkynes. The metal catalyzed [2+2+2] cycloaddition of alkynes has been well studied, however, limited reports exist of being able to access 2 regioisomers based on ligand identity.[23] Takeuchi and coworkers showed that employing dppe in Ir catalyzed cycloadditions led to primarily the meta product, however, use of sterically larger dppf affords primarily the ortho product (Scheme 1.13). The authors propose a fundamentally different mechanism for each pathway to account for

the selectivity. Both products are proposed to proceed through a common iridacycle intermediate, however, the ortho product is generated through a Diels-Alder mechanism where the alkyne coordinates to the open coordination site on Ir **1-45** and is directed with the R substituent oriented away from the sterically bulky methyl group. The meta product is proposed to go through a distinct insertion mechanism pathway **1-47** to **1-48**. In optimization studies for the ortho product, the authors found that increasing the length between the two phosphorus atoms in bidentate ligands enhanced selectivity towards the ortho product, suggesting that one of the phosphorus atoms could dissociate and form an open coordination site. In this pathway, the selectivity is determined by the catalyst where insertion of iridium occurs at the less hindered position on the alkyne.

Scheme 1.13 [2+2+2] Cycloaddition

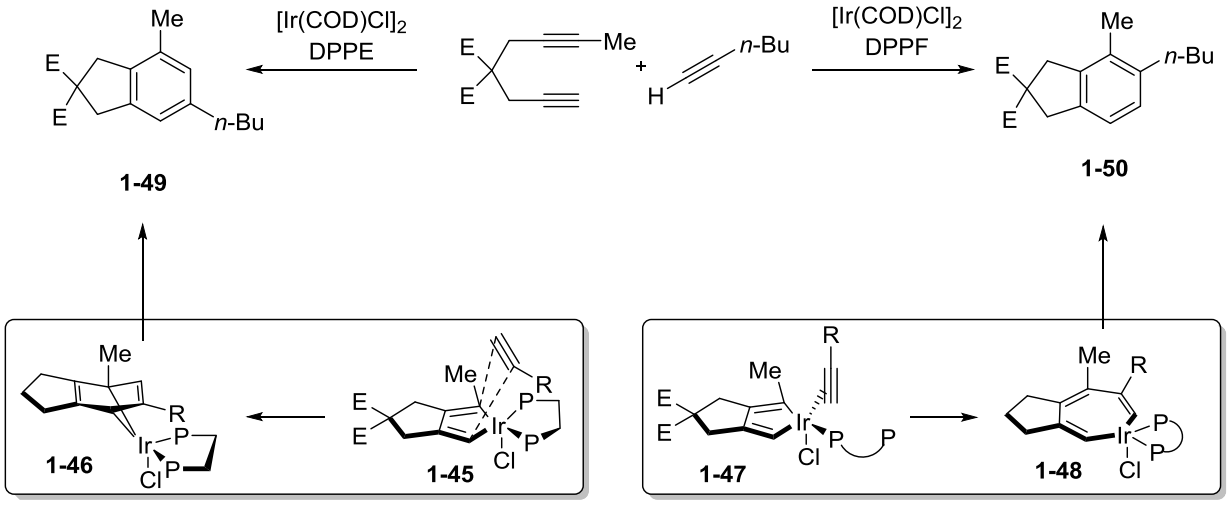

Ligand-controlled functionalization of alkynes in intramolecular cyclizations is particularly challenging due to a generally a strong kinetic preference for one product. This challenge has recently been overcome by Yorimitsu and colleges who demonstrated that both 5-exo and 6-endo products were accessible using a Pd catalyst in alkynol cyclizations by altering the ligand employed (Scheme 1.14).[24] The authors found that use of Xphos coupled with aryl

triflates favors the endo product **1-54** while use of Xantphos with aryl bromides favors the exo product **1-53**. Preliminary mechanistic studies suggested that the observed selectivity arises from different catalyst-substrate interactions where the oxidative addition adduct using aryl bromides would have an affinity for the hydroxyl group **1-52** favoring the 5-exo product; however the oxidative addition adduct using aryl triflates would interact with the ynamide moiety **1-51** and activate the alkyne for 6-endo cyclization.

Scheme 1.14 Alkynol Cyclization

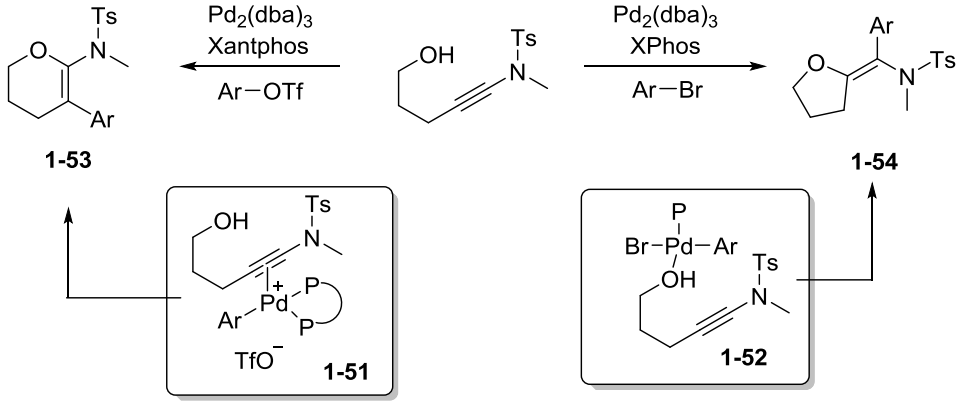

1.3.3 Aldehyde Alkyne Reductive Couplings

The development of catalyst directed regiodivergent protocols of various π-systems has been the interest of multiple projects in the Montgomery group. One focus of this interest is on the control of regiochemsitry in Ni catalyzed reductive coupling of aldehydes and alkynes to synthesize allylic alcohols. The first successful strategy to control selectivity in this class of reaction was developed by Jamison and coworkers who employed a remote alkene directing group on the alkyne where the directing effect may be turned on or off depending on ligand employed to afford either isomer in high selectivity (Scheme 1.15).[25] Mechanistic studies suggested that the observed selectivity arises from competition between the phosphine biding to the nickel compared to the remove olefin directing group.[26] The authors proposed three different

reaction pathways to account for the selectivity. In the type 1 pathway where phosphine is omitted from the reaction, selectivity is controlled by olefin binding to nickel which affords **1-56**. In the type 2 pathway substitution of L by bulky $PCyp_3$ affords **1-60** and subsequent displacement of the olefin by the aldehyde affords **1-61** leading to **1-55**. Finally in type 3 when tributylphosphine is used the reaction is unselective since both L as well as the olefin tether are displaced (**1-63**), leading to unselective displacement by the aldehyde (**1-64** or **1-65**). This methodology provides high levels of regiocontrol with unbiased alkynes, however, the requirement for use of a directing group adds further synthetic steps to install and remove if the group is not desired in the final product.

Scheme 1.15 Directing Group in Reductive Couplings

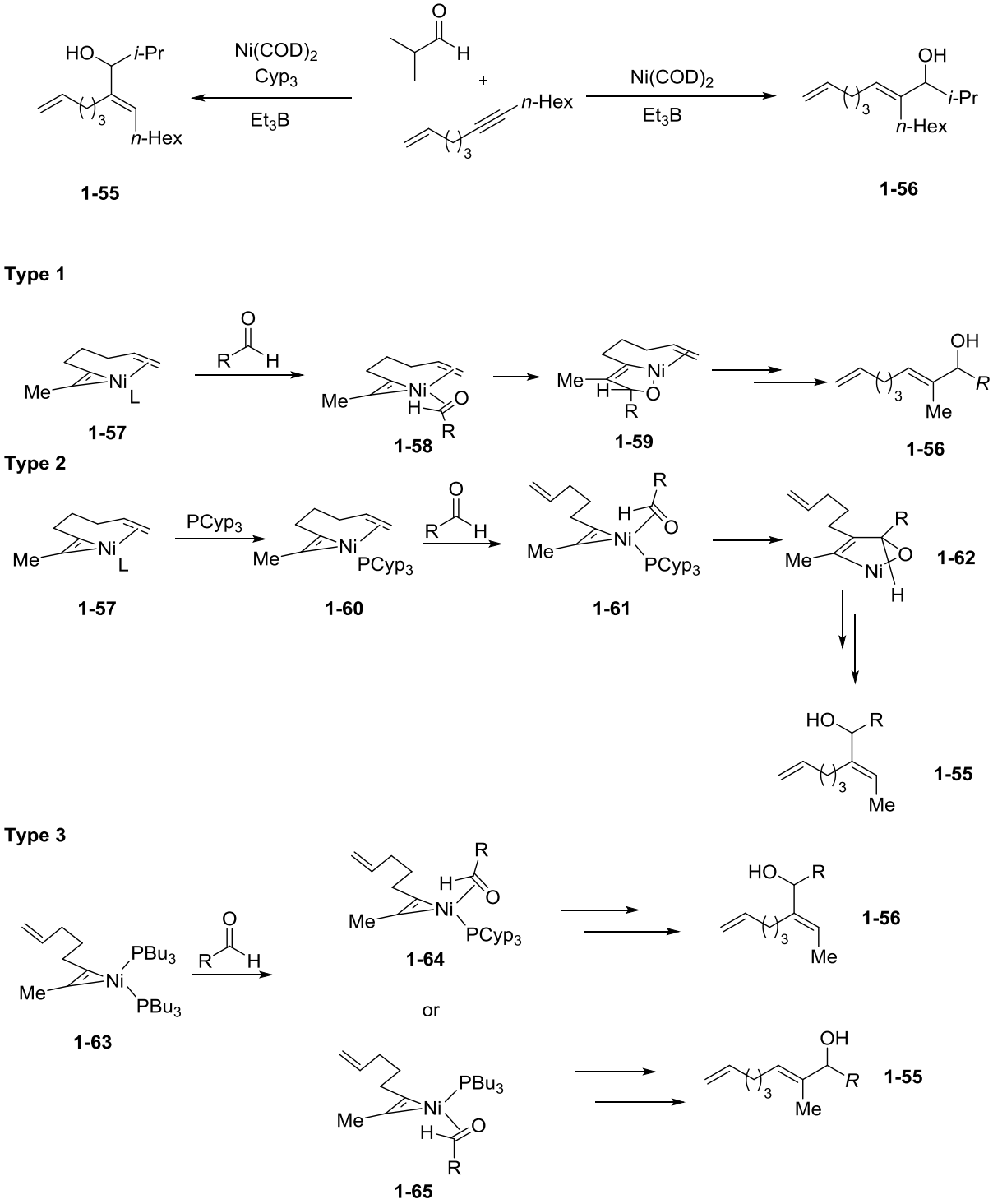

Not soon after the report from Jamison, our group reported a regiodivergent protocol for reductive couplings in a macrocyclization study in which switching ligand classes and reducing

agents afforded remarkably high levels of selectivity for both regioisomers (Scheme 1.16).[27] Use of IPr in combination with Et_3SiH as reductant generates primarily exocyclic product **1-66**, however, use of PBu_3 and Et_3B as reducing agent produced the endocyclic product **1-65**. It should be noted that these selectivities were observed employing substrates with methyl capped alkynes; however, the selectivity using aromatic or internal alkynes was only minimally impacted by ligand effects.

Scheme 1.16 Regiodivergent Macrocyclization

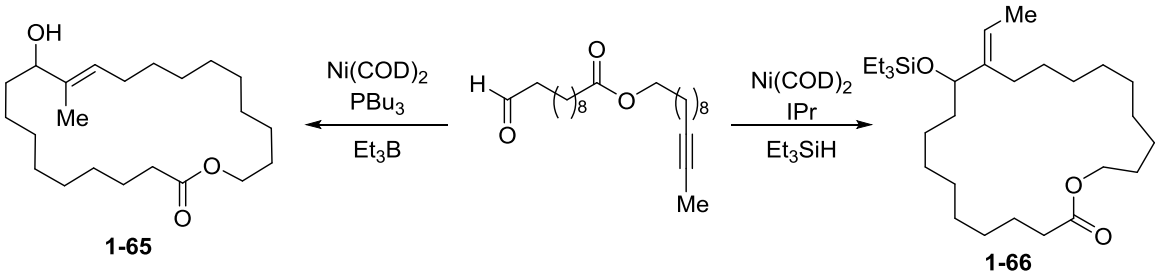

Subsequent developments from our group showed regiodivergent intermolecular reductive couplings where the selectivity was dictated by the steric bulk on the NHC (Scheme 1.17).[28] For cases where there was a small difference in alkyne substitution the use of *i*-Pr-BAC as a ligand was found to be optimal for C-C bond formation at the less hindered position on the alkyne favoring formation of **1-67**. Use of biased alkynes with IMes was previously reported and showed high selectivity for terminal and conjugated alkynes. While IPr was effective in reversing the regiochemical outcome in the intramolecular macrocyclization shown in Scheme 1.16, it was ineffective in the intermolecular variant. It was found that use of bulky SIPr was effective for unbiased alkynes; however the employment of bulkier DP-IPr was required to reverse selectivity with terminal alkynes to favor C-C bond formation and the more hindered position.

Scheme 1.17 Regiodivergent Intermolecular Reductive Couplings

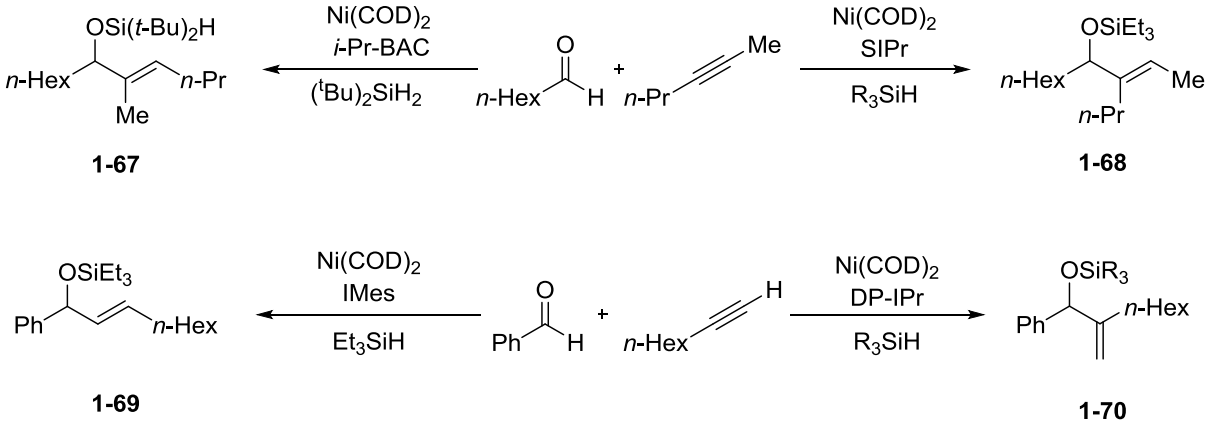

Ligands

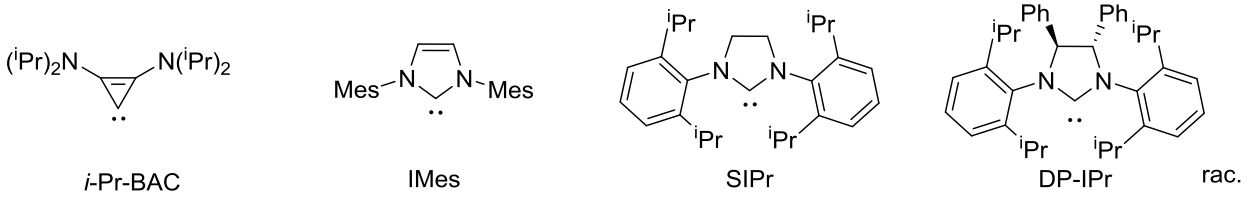

More recently this methodology was expanded in the total synthesis of 10-deoxymethynolide in a challenging macrocyclization step in which two different products could be selected for depending on the ligand employed. Use of IMes with the terminal alkyne afforded the endocyclized product **1-71** while use of DP-IPr afforded the exocyclized product **1-72** (Scheme 1.18).

Scheme 1.18 Regiodivergent Macrocycliztion in Total Synthesis

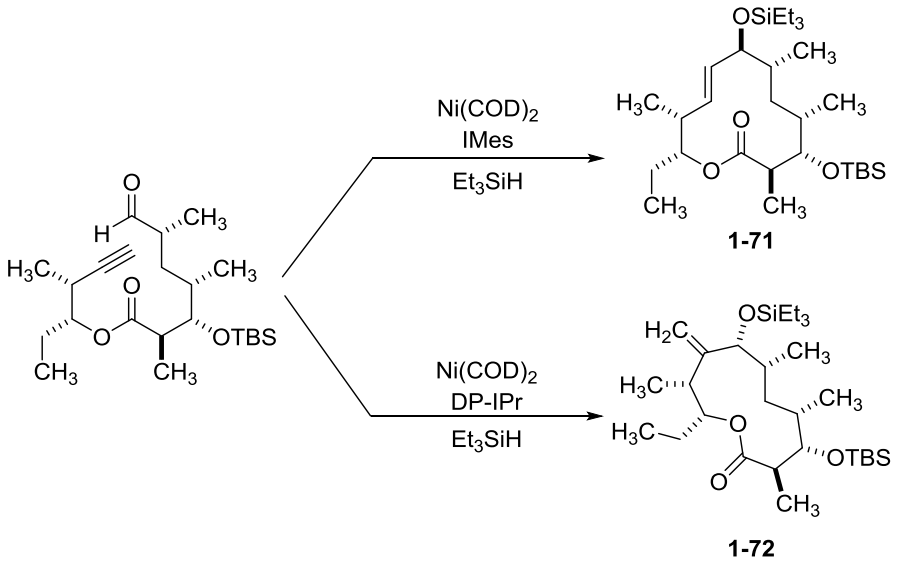

A full mechanistic discussion on Ni catalyzed reductive couplings will be provided in Chapter 2, however, computational studies from the Houk laboratory helped elucidate the origin of the observed selectivity trends with both large and small ligands in this chemistry.[29] Both products are proposed to proceed through a common metallacycle intermediate with selectivity of the reaction set at the oxidative cyclization step (Scheme 1.19).

Scheme 1.19 Mechanistic Rational for Observed Selectivity

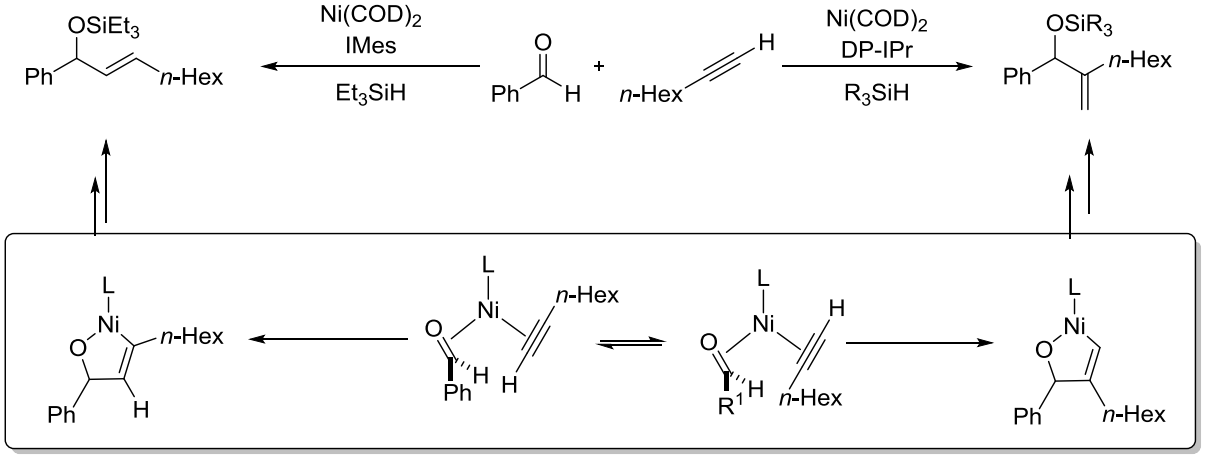

When small ligands were employed it was found that steric interactions between ligand and substrates were minor and the selectivity was primarily determined by steric interactions

between the alkyne and the aldehyde with distal transition state favored over the proximal (Figure 1.1a). However, when large ligands are employed, steric interactions between the ligand and alkyne were now significant and a reverse in selectivity observed for small ligands, thus now favoring the proximal pathway (Figure 1.1b).

Figure 1.1 TS for Oxidative Addition

a) TS for Oxidative Addition Small Ligand

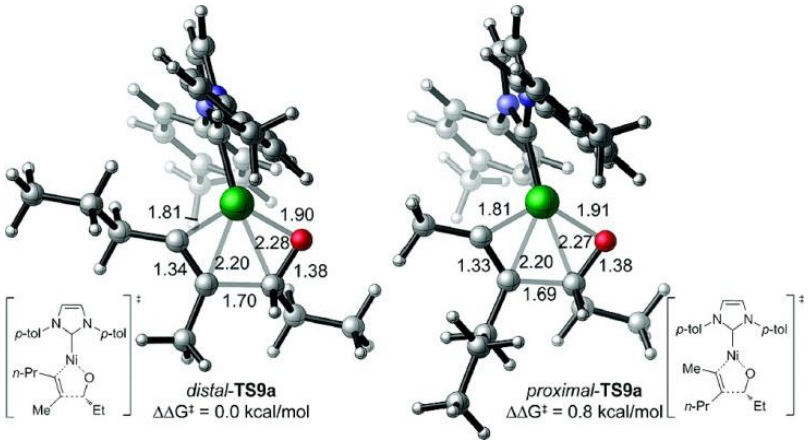

b) TS for Oxidative Addition Large Ligand

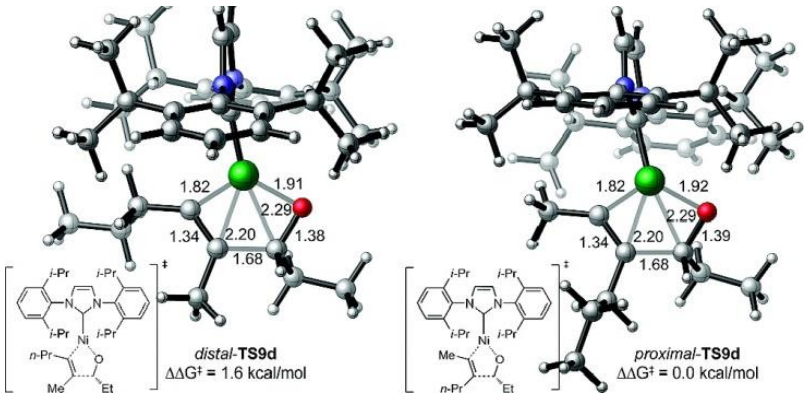

1.4 Conclusions

The ability to preferentially select for functionalization at one site on an unsymmetrical alkyne is a powerful tool for organic chemists. Various strategies have been devised to achieve highly selective regiodivergent outcomes for functionalization. The two strategies highlighted in

this chapter are fundamentally altering the catalyst by changing the metal to proceed through a mechanistically distinct pathway which generally also requires a strong bias on the alkyne. Alternatively, by altering the ligand environment on the metal, substrate catalyst interactions can be changed such that alternative binding modes can be favorable or the mechanism can be fundamentally changed to afford the opposite regioisomer.

Chapter 2

Regiocontrol in Catalytic Reductive Couplings through Alterations of Silane Rate Dependence

2.1 Introduction

Allylic alcohols are an important structural motif found in a variety biologically active natural products[30,31,32] as well as precursors for various synthetic transformations such as directed epoxidations,[33] cyclopropanations,[34] π-allyl chemistry,[35] as well as sigmatropic rearrangements.[36] Due to their importance to synthetic organic chemistry as well as medicinal chemistry, various protocols have been developed to synthesize allylic alcohols using both stoichometic and catalytic methods. Our group along with others have been interested in the Ni catalyzed reductive coupling of aldehydes and alkynes to synthesize allylic alcohols. A common challenge in this class of chemistry is the control of selectivity on the alkyne and as discussed in Chapter 1 various strategies have been employed to control selectivity. Typically, alkynes that possess a strong electronic and/or steric bias often afford high levels of regiocontrol, however, alkynes that have similar substitution proceed with poor regiocontrol and both isomers are typically observed. Two challenges in this class of chemistry are developing highly selective regiodivergent outcomes for alkynes that do not possess a stong bias as well as reversing the inherent reactivity of biased alkynes to afford the opposite regioisomer.

Figure 2.1 Allylic Alcohols in Natural Products and Synthetic Utility

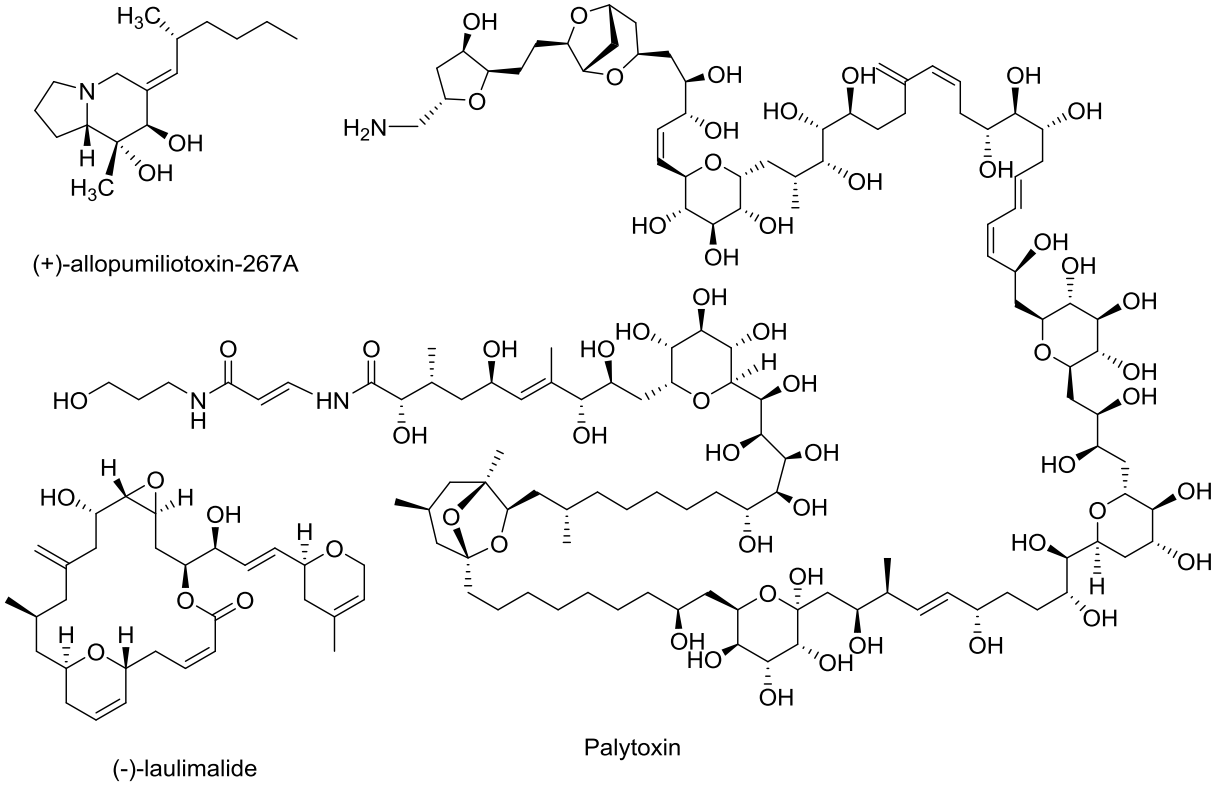

Synthetic Utility

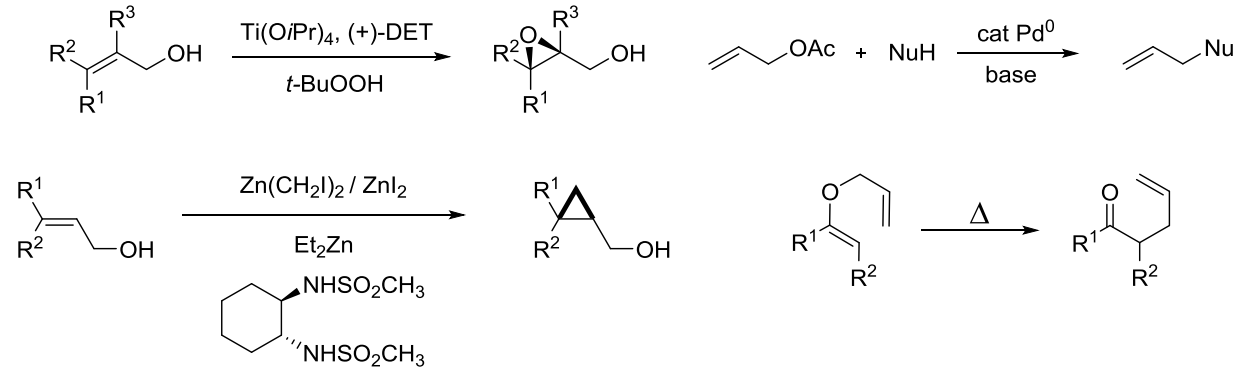

2.2 Synthesis of Allylic Alcohols

A variety of methods have been reported to synthesize allylic alcohols. Classically, allylic alcohols can be accessed from either reduction of a α,β−unsaturated ketone or addition of a

Grignard reagent to an aldehyde (Scheme 2.1a). While these methods have been well studied and commonly used, functional group compatibility and use of stoichiometric organometallic reagents make them less than ideal for assembly of complex molecules. A more contemporary method to synthesize allylic alcohols is the Nozaki-Hiyama-Kishi reaction which employs a nickel catalyst with a (generally) stoichometic quantity of chromium reducing agent (Scheme 2.1b).[37] While this reaction shows much better functional group compatibility, its use of both a predefined vinyl halide as well as stoichiometric chromium make it less than ideal from an environmental and synthetic step standpoint. An alternative synthetic route to the previous described methods is the nickel catalyzed reductive coupling of an aldehyde and alkyne with a reducing agent to synthesize allylic alcohols (Scheme 2.1c).

Scheme 2.1 Methods to Synthesize Allylic Alcohols

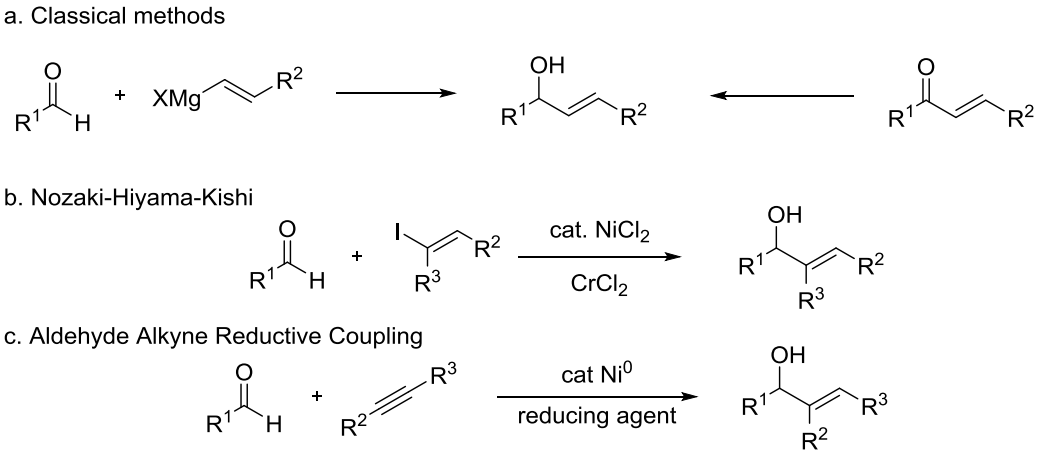

2.3 Aldehyde Alkyne Reductive Couplings

The Montgomery group first reported the intramolecular reductive coupling of an ynal **2-1** using a nickel catalyst and organozinc reducing agents (Scheme 2.2).[38] Pretreating $Ni(COD)_2$ with PBu_3 led to the reductive product **2-3** (transferring of a hydrogen substituent), while omission of PBu_3 led to the alkylative product **2-2**. This reaction was expanded to an

intermolecular alkylative variant, however the scope was narrow and only non-enolizable aldehydes were well tolerated.

Scheme 2.2 Ni Catalyzed Reductive or Alkylative Coupling

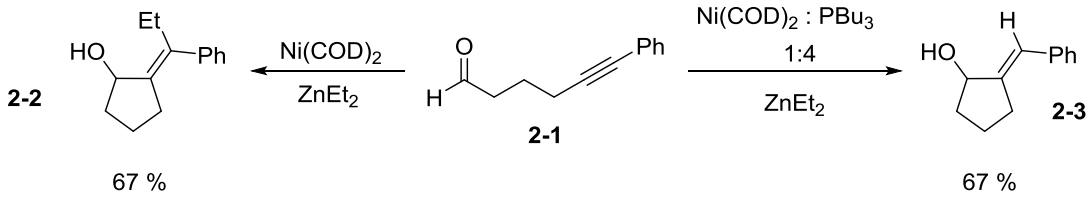

Subsequent advancements by Jamison and coworkers for the intermolecular variant showed that use of Et_3B in place of $ZnEt_2$ afforded exclusively the reductive product (Scheme 2.3, **2-4**).[39] A variety of substrate examples were shown, however, in all cases biased alkynes were employed showing high selectivity for one isomer.

Scheme 2.3 Intermolecular Reductive Couplings

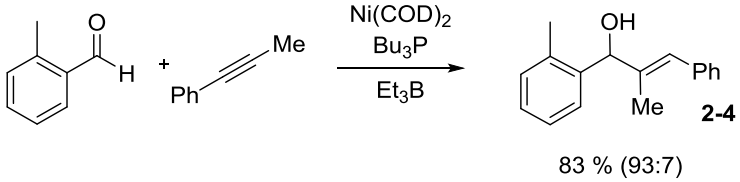

Another important development emerged from our lab showing that bench stable trialkylsilanes could be used in place of pyrophoric Et_3B or $ZnEt_2$ during studies for the total synthesis of (+)allopumilitoxin 267A. Unfortunately, this protocol employing trialkylsilanes could only be used for intramolecular cyclizations,[30] however, subsequent advancements showed that by switching ligand classes from phosphines to N-heterocyclic carbenes (NHC), silanes could be successfully employed in the intermolecular reaction to afford the silyl protected allylic alcohol **2-5** (Scheme 2.4a).[40] This methodology has been expanded to employ α-silyloxy aldehydes coupled with alkynes to produce 1,2 anti-diols **2-6** with high levels of diastereoselectivity (Scheme 2.4b).[41] Further advancements from our group showed that chiral

NHCs could be employed to achieve moderate to high levels of enantioselectivity in reductive couplings (Scheme 2.4c, **2-7**).[42]

Scheme 2.4 NHC and Silane Mediated Reductive Couplings

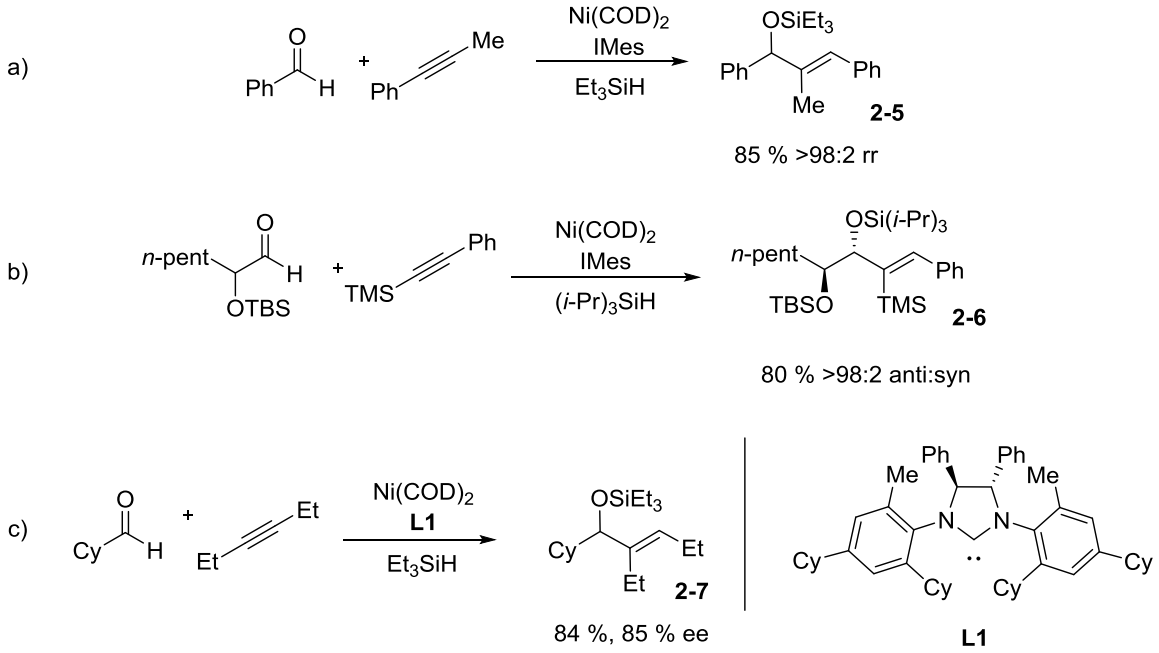

2.3.1 Regiodivergent Strategies

Although advancements had been made in this field since early reports employing $ZnEt_2$, a persistent challenge was still control of regioseletivity on the alkyne. The protocols listed above generally showed high regioselectivity, but this control was dictated by a strong substrate bias on the alkyne which strongly favored one regiochemical outcome. Terminal alkynes **2-9** or disubstituted alkynes where R^2 and R^3 were either sterically and/or electronically different (**2-11**) afforded highly regioselective outcomes. However, when R^1 and R^2 were similar **2-13**, a loss of regiocontrol was observed (Scheme 2.5c). An additional challenge was reversing regioselectivity with biased systems such as terminal alkynes. While highly selective outcomes were possible with biased systems, no methodology existed to afford C-C bond formation and the other position of the alkyne.

Scheme 2.5 Substrate Bias in Reductive Couplings

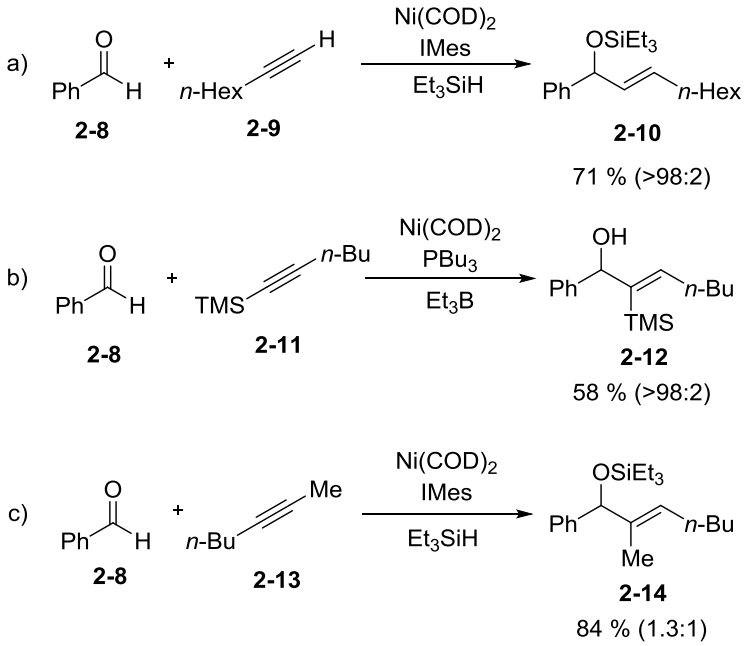

As discussed in Chapter 1, our group along with others have developed strategies to overcome the obstacle of regiodivergency by either employing a directing group or alteration of the ligand employed to access either regioisomer (Scheme 2.6).[25,28] In the protocol developed by Jamison, the alkene directing effect may be tuned depending on ligand employed in the reaction such that either regioisomer **2-15** or **2-16** can be accessed. In previous work for our group, ligand design has been employed to influence the rate of metallacycle formation and this is highly sensitive to ligand alterations. Employing small ligands afforded primarily C-C bond formation at the less hindered position on the alkyne **2-17**, while use of large ligands reversed this selectivity and favored C-C bond formation at the more hindered position **2-18**.

Scheme 2.6 Reductive Coupling Regiocontrol Strategies

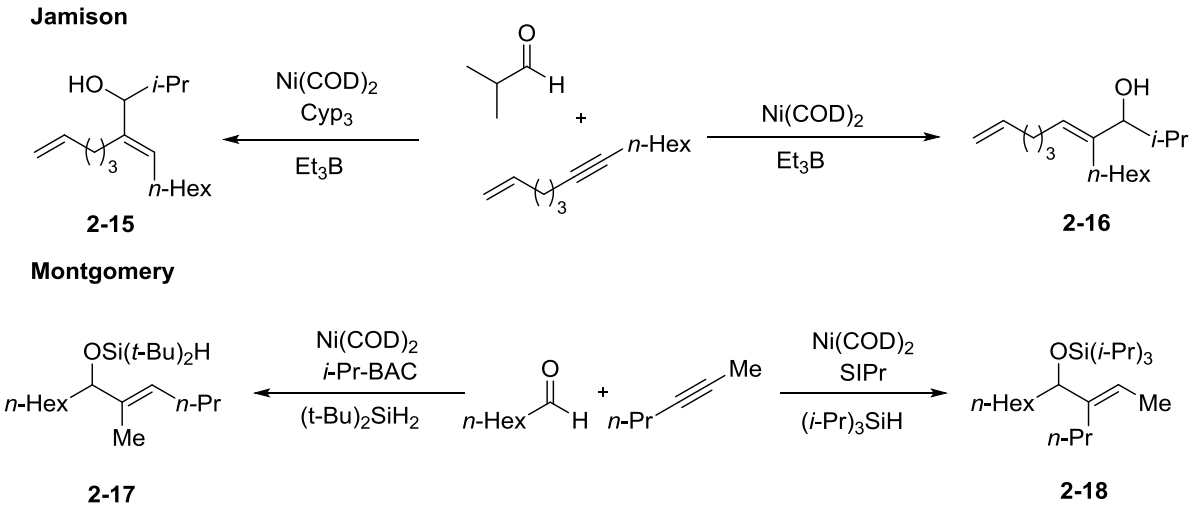

2.3.2 Reductive Coupling Mechanistic Studies

Regardless of strategy employed to control regiochemistry, the mechanism from previous studies is proposed to involve coordination of the aldehyde and alkyne a Ni^0 catalyst (**2-19**) followed by oxidative cyclization to for a five membered metallacycle **2-20**. Subsequent σ-bond metathesis with a silane affords a Ni-H species **2-21** which upon reductive elimination affords the silyl protected allylic alcohol **2-22** and regenerates the catalyst (Scheme 2.7). The metallacycle based pathway was first proposed by our group in the seminal report on Ni catalyzed reductive and alkylative couplings of aldehydes and alkynes[38] and this hypothesis was later supported by Ogoshi who isolated a dimeric Ni metallacycle from an aldehyde and alkyne.[12] Additionally, computational studies from our group,[29,43] as well as Jamison[44,45] and Krische[46] all in collaboration with Houk have uniformly proposed the metallacycle based pathway.

Scheme 2.7 Proposed Mechanism for Ni Catalyzed Reductive Couplings

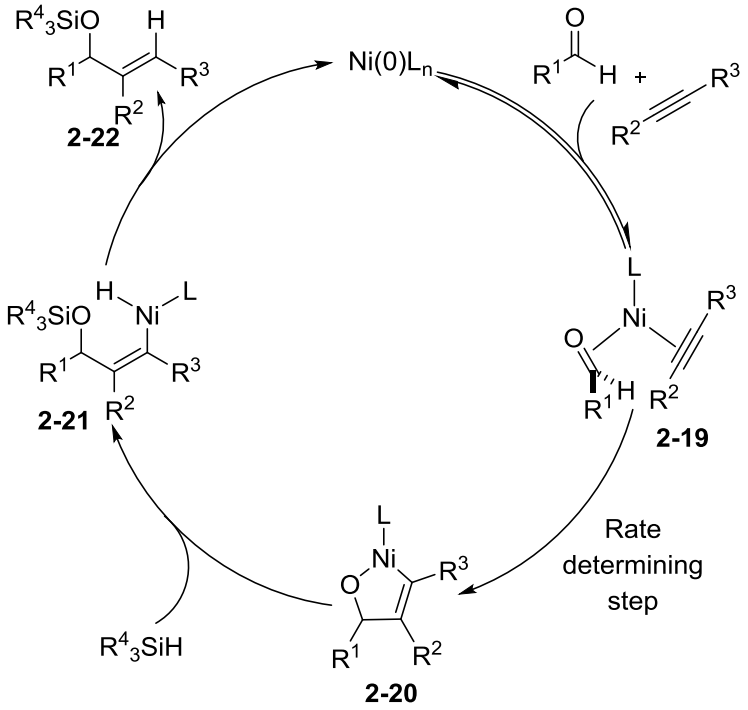

Our group first studied the kinetics of this reaction using an intramolecular reductive cyclization employing a Ni-phosphine catalyst.[47] Studying the initial rates by *in situ* IR monitoring showed a first order dependence on ynal **2-23** (Figure 2.2a) and catalyst (Figure 2.2b), and a zero order dependence on silane (Figure 2.2c). Additionally, kinetic isotope effect competition studies showed no KIE for the reaction, suggesting that the silane is not involved in the rate-determining step of the reaction.

Figure 2.2 Initial Rates for Intramolecular Cyclization

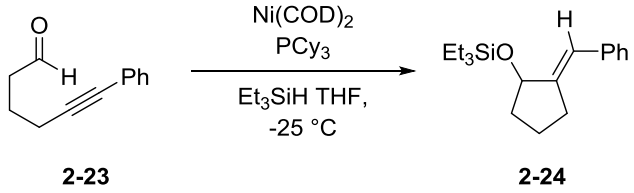

2-23 **2-24**

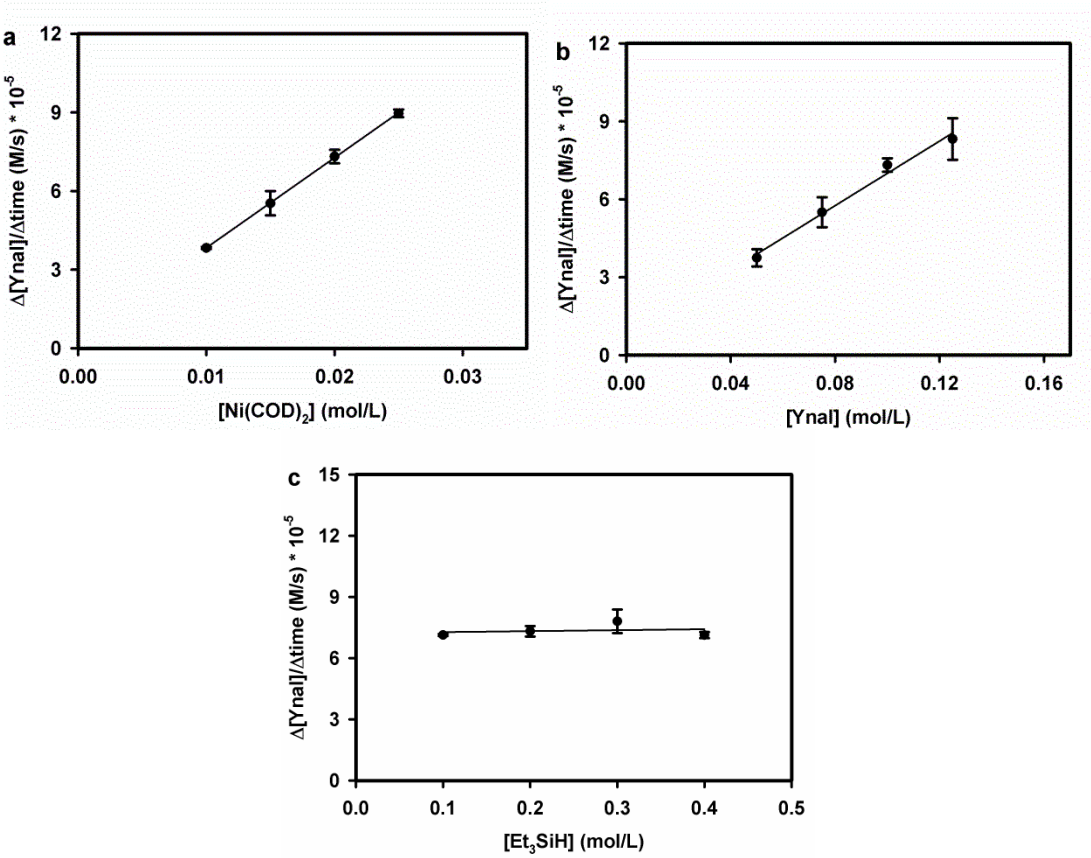

While there is strong evidence for metallacycle formation, a commonly proposed alternative mechanism for reductive couplings involves initial oxidative addition of Ni into the Si-H to generate a Ni^{II} complex (Scheme 2.8, **2-26**). Following oxidative addition, several different pathways can be proposed to arrive at the products. In path a, silylmetalation occurs across the aldehyde to generate **2-27** and subsequent migratory insertion on the alkyne affords two different vinyl Ni species which, upon reductive elimination from **2-28** or **2-29,** generates the product. In path b, hydrometallation across the alkyne generates a vinyl nickel species **2-31**

that can undergo migratory insertion across that aldehyde to generate an alkoxy-nickel intermediate **2-32** which upon reductive elimination generate the product.

Scheme 2.8 Alternative Mechanistic Proposal

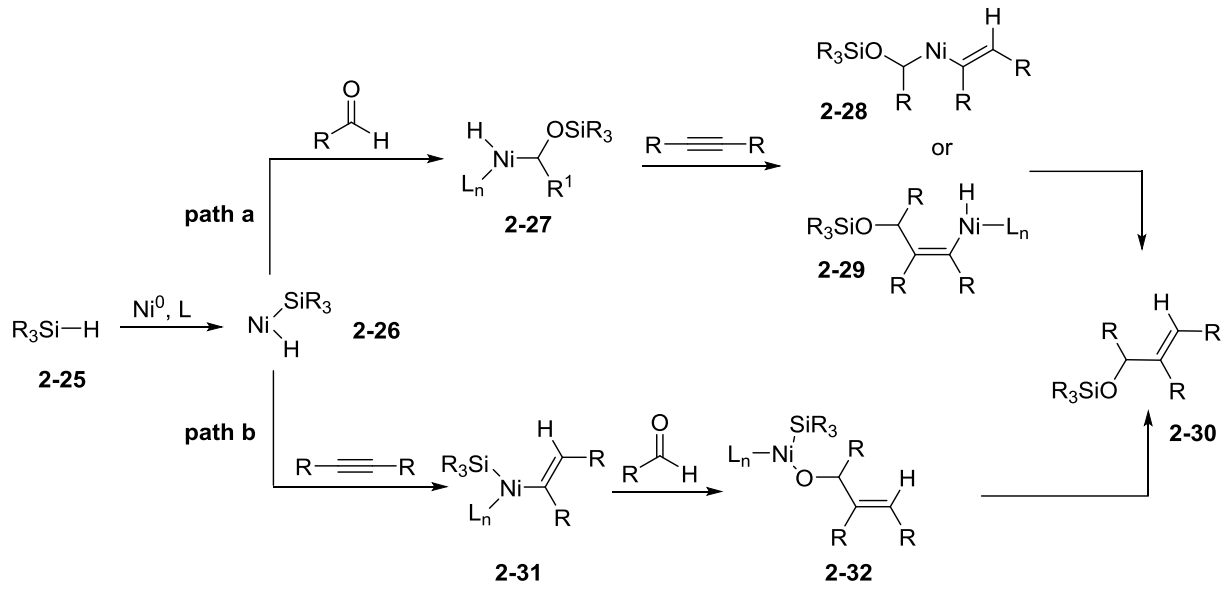

To distinguish the pathway in Scheme 2.8 from the metallacycle based mechanism a series a silane consumption experiments were conducted. No consumption, of silane was observed when in the presence of just the catalyst and further experiments showed that hydrosilation of either the alkyne or aldehyde was not competent under the reaction conditions. Finally, only when aldehyde, alkyne, and catalyst were present in solution was silane consumption observed. These results combined show that the mechanism is likely not operating under oxidative addition to the Si-H bond as shown in Scheme 2.8, but a metallacycle based pathway shown in Scheme 2.7.

All of the combined evidence suggests that the rate determining step for this reaction is oxidative cyclization to form the metallacycle. This has also been computationally supported in studies from Houk and Jamison[45,46] using a Et_3B and phosphine system as well as Houk and Montgomery[29] using a silane and NHC system. Regardless of ligand and reducing agent

employed, the rate determining step of the reaction is oxidative cyclization followed by a fast σ-bond metathesis with the reducing agent.

2.4 Initial Observation of Silane Dependence

In our previous report on regiodivergent reductive couplings to synthesize allylic alcohols both regioisomers could be accessed with moderate to high levels of regiocontrol depending on ligand employed.[28] Silane choice was primarily directed at suppressing undesired aldehyde or alkyne hydrosilylation and based on previous mechanistic studies silane identity should have no influence on selectivity, since it is involved after the regiochemistry has been set in the rate-determining oxidative cyclization step. Against the backdrop of previous work, we made a surprising discovery that the regioselectivity of the reaction of benzaldehyde coupled with phenyl propyne was highly sensitive to silane identity when using the ligand SIPr. During efforts to employ bench stable Ni^{II} pre-catalysts (discussed in Chapter 3) in reductive couplings we found that the regioselectivity of reactions were highly dependent on both temperature as well as silane identity when using SIPr (Table 2.1, entries 1-2). This result was unexpected since previous mechanistic studies had shown no involvement of the silane in the rate and regiochemistry determining step.[47] In sharp contrast to when SIPr was employed, varying silane structure with IMes showed no variation in selectivity (Table 2.1, entries 3-4).

Table 2.1 Regioselectivty Dependence on Silane using Ni^{II}

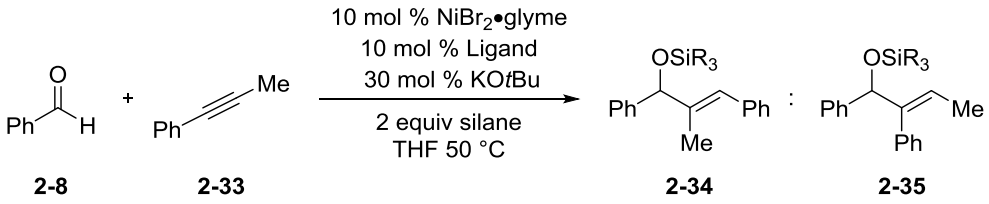

Entry	Ligand	Silane	**2-34**:**2-35** (% yield)
1	SIPr	Et_3SiH	38:62 (82)
2	SIPr	*i*-Pr_3SiH	8:92 (33)
3	IMes	Et_3SiH	96:4 (77)
4	IMes	*i*-Pr_3SiH	97:3 (76)

2.5 Optimization Studies

The regioselectivity dependence on silane when employing ligand SIPr was surprising and sparked a new interest in taking advantage of this previously unknown trend to improve selectivity. Equally as interesting as silane dependence was the selectivity for **2-35** when the reaction was heated (Table 2.1, entry 2). While typical reductive coupling protocols employing $Ni(COD)_2$ were productive when conducted at room temperature, it was found that optimal yields were observed for the protocol employing Ni^{II} pre-catalyst when reactions were heated to 50 °C. As discussed later in this chapter, both of these would be crucial for achieving high selectivities. Previous methodology had only been able to achieve ~80:20 selectivity for the desired isomer **2-35**, however, this protocol showed improved selectivity, albeit in decreased yield. To reduce the variability in the reaction conditions, the use of Ni^{II} pre-catalysts was avoided (to be later developed), and the above reactions were conducted using $Ni(COD)_2$ at room temperature. Not surprisingly, as shown in Table **2.2**, the selectivity for **2-35** showed a high dependence on silane when SIPr was employed.

Table 2.2 Ligand And Silane Effects

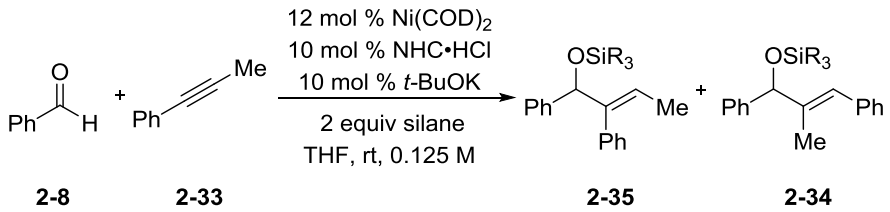

Entry	NHC	Silane	**2-35**:**2-34** (% yield)
1	IMes	Et_3SiH	<2:98 (84)
2	IMes	*i*-Pr_3SiH	<2:98 (83)
3	SIPr	Et_3SiH	58:42 (65)
4	SIPr	*i*-Pr_3SiH	83:17 (89)

Given the initial trends in Table 2.2 we decided to evaluate the influence of a variety of silanes for production of **2-35** in the above protocol. It became clear that as silane bulk increased, the selectivity for isomer **2-35** improved (Table 2.3).

Table 2.3 Silane Structural Effects

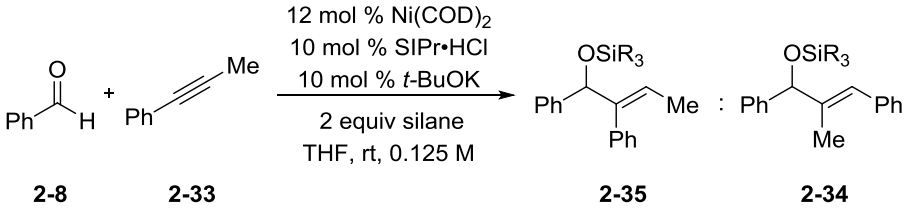

Entry	Silane	**2-35**:**2-34** (% yield)
1	Et_3SiH	58:42 (65)
2	Bn_3SiH	58:42 (ND)
3	$PhMe_2SiH$	60:40 (ND)
4	*t*-$BuMe_2SiH$	60:40 (83)
5	(*i*-Bu)$_3$SiH	63:37 (87)
6	*t*-$BuPh_2SiH$	77:23 (86)
7	(iPr)$_3$SiH	83:17 (89)
8	(tBu)$_2$MeSiH	>98:2 (61)
9	(*t*-Bu)$_3$SiH	NR

We initially rationalized this unexpected and surprising finding as originating from a change in the rate determining step, where metallacycle formation becomes reversible[48,49] and the silane is now involved in the rate determining step (Scheme 2.9, Path B).[50]

Scheme 2.9 Proposed Mechanism for the Origin of Silane Dependence

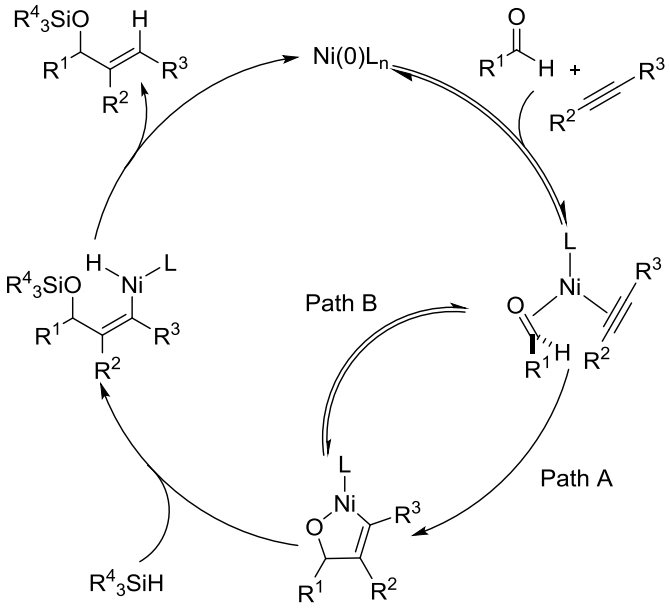

While it appears that protocols involving either small ligands with any silane or large ligands combined with small silanes favor path A, the use of large ligands with large silanes favor Path B and σ-bond metathesis is now the rate determining step. This hypothesis suggested further opportunities for controlling the relative rates of both metallacycle formation as well as σ-bond metathesis which would provide additional handles to control regiochemistry in the reaction. If σ-bond metathesis is now the RDS of the reaction, then altering silane concentration should alter the rate of σ-bond metathesis without changing the rate of metallacycle formation and thus alter regioselectivity. Additionally, previous computational studies[29] illustrated a significant entropic penalty associated with the σ-bond metathesis step since this is a bi-molecular reaction compared to the unimolecular reaction for metallacycle formation. This

entropic penalty would be maximized at high temperatures and is likely the origin for the improved selectivity in Table 2.1 employing $NiBr_2$glyme at elevated temperatures. Both of these variables are evaluated below using the benchmark example of benzaldehyde with phenylpropyne.

In protocols where metallacycle formation is rate limiting, the silane concentration should have no effect on selectivity of the reaction. This was observed with both IMes and SIPr when the concentration of Et_3SiH was varied (Table 2.4, entries 1-4). A marked contrast was seen when using bulky SIPr in conjunction with bulkier $(i\text{-Pr})_3SiH$ and the concentration was varied (Table 2.4, entries 5-7). As silane concentration was decreased the selectivity for **2-35** increased, however, increasing the concentration to 10.0 equiv reduced selectivity and it began to approach the levels observed when smaller Et_3SiH was used. When silane concentration was held constant and the reaction was diluted tenfold (Table 2.4, entry 8), excellent selectivity was observed. It should be noted that the optimized procedure for this protocol involved slow addition of aldehyde, alkyne, and silane over the course of 1 hour. While the concentration of reagents changes over the course of the reaction, the impacts of concentration as shown in Table 2.4 have a profound impact on selectivity.

Table 2.4 Silane Concentration Effects

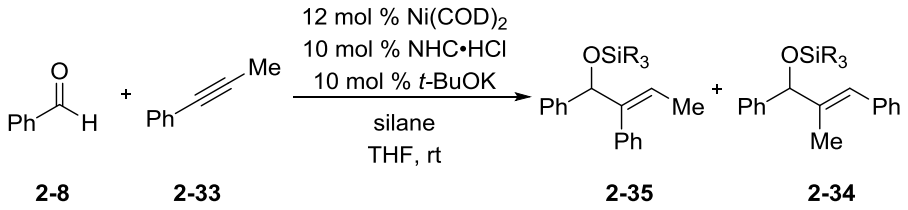

Entry	Ligand	Silane (equiv)	Conc	**2-35**:**2-34** (% yield)
1	IMes	Et_3SiH (2.0)	0.125 M	<2:98 (84)
2	IMes	Et_3SiH (1.1)	0.125 M	<2:98 (62)
3	SIPr	Et_3SiH (2.0)	0.125 M	58:42 (65)
4	SIPr	Et_3SiH (10.0)	0.125 M	58:42 (32)
5	SIPr	$(i\text{Pr})_3SiH$ (1.1)	0.125 M	95:5 (57)
6	SIPr	$(i\text{Pr})_3SiH$ (2.0)	0.125 M	83:17 (89)
7	SIPr	$(i\text{-Pr})_3SiH$ (10.0)	0.125 M	68:32 (93)
8	SIPr	$(i\text{-Pr})_3SiH$ (2.0)	0.0125 M	>98:2 (82)

Initial results from the Ni^{II} pre-catalyst project had suggested that at elevated temperatures, the selectivity of the reaction could improve when bulky ligands were used in conjunction with bulky silanes. To investigate this further, the reaction was conducted across a range of temperatures. As observed previously, when IMes was used with $(i\text{-Pr})_3SiH$ altering the reaction temperature had no effect on selectivity, however, when SIPr was used with $(i\text{-Pr})_3SiH$ heating the reaction had a dramatic effect on selectivity ranging from 68:32 at 0 °C to 98:2 at 95 °C (Table 2.5).

Table 2.5 Temperature Effects

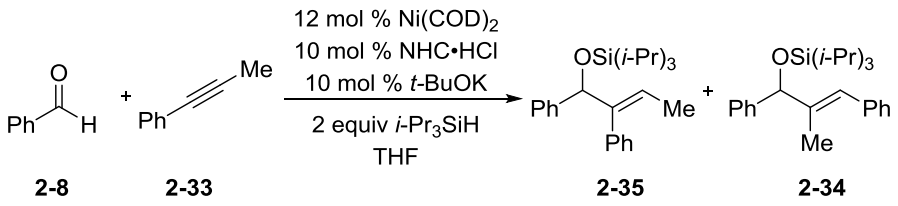

2-8 **2-33** **2-35** **2-34**

Entry	Ligand	Temp (°C)	**2-35**:**2-34** (% yield)
1	IMes	rt	<2:98 (84)
2	IMes	50	<2:98 (77)
3	SIPr	0	68:32 (81)
4	SIPr	rt	83:17 (89)
5	SIPr	50	94:6 (73)
6[a]	SIPr	95	98:2 (57)

[a]PhMe used as reaction solvent

2.6 Scope

Previous efforts to develop a regiodivergent protocol for reductive couplings showed good selectivity for unbiased internal alkynes, however, when biased alkynes were employed such as terminal or aromatic alkynes only moderate selectivities were observed for C-C bond formation at the more hindered position. Additionally, to obtain high selectivity for the exo-methylene product using terminal alkynes required the use of noncommercial DP-IPr which requires several steps to synthesize. With the observed trends in Tables 2.3-2.5 we sought to improve the selectivity of previous methodology.

2.6.1 Internal Alkynes

A variety of conditions were examined, however, it was found that heating the reactions to 50 °C and using $(i\text{-Pr})_3\text{SiH}$ proved most versatile for internal alkynes. Initial efforts focused on phenyl propyne as a coupling partner which had previously shown 83:17 selectivity and using newly developed conditions we could increase the selectivity up to >98:2 when coupled with

aromatic and aliphatic aldehydes (Table 2.6, entries 1-4). We were also interested in determining how far removed steric differences could be from the alkyne and found that differences in the homopropargylic position were well tolerated (Table 2.6, entries 5-6); however, the limit to this methodology is currently *n*-Pr vs Et substitution (Table 2.6, entry 7). Previous work from the group has focused on using the electronic bias in propargyl alcohols to obtain high selectivities;[51] however, using modified reaction conditions, we can now override the bias and obtain good selectivities for **2-36** (Table 2.6, entry 8). Finally, when steric differences were increased closer to the alkyne, excellent selectivity was maintained regardless of aldehyde employed (Table 2.6, entries 9-11).

Table 2.6 Scope with Internal Alkynes

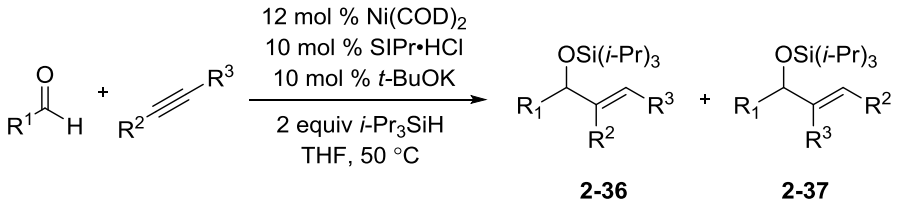

Entry	R^1	R^2	R^3	**2-36**:**2-37** (% yield)
1	Ph	Ph	Me	>98:2 (82)
2	4-FC_6H_4	Ph	Me	93:7 (85)
3	*n*-Hept	Ph	Me	>98:2 (77)
4	*c*-Hex	Ph	Me	>98:2 (90)
5	Ph	*i*-Bu	Et	94:6 (86)
6	*n*-Hept	*i*-Bu	Et	93:7 (66)
7	Ph	*n*-Pr	Et	68:32 (56)
8	Ph	*n*-Pr	CH_2OH	89:11 (59)
9	2-furyl	*n*-Pr	Me	93:7 (76)
10	Ph	*i*-Pr	Me	>98:2 (78)
11	*c*-Hex	*i*-Pr	Me	>98:2 (75)

2.6.2 Terminal Alkyne Scope

When the optimized conditions for internal alkynes were attempted with terminal alkynes, a significant decrease in yield was observed due to competing hydrosilylation of the alkyne. It became very apparent that, although heating was an effective method to improve selectivity with terminal alkynes, the dramatic decrease in yield was not synthetically useful (Table 2.7, entries 1-3). Further optimization showed that variables from tables 2.3-2.5 other than temperature could be used to improve selectivity. Decreasing the reaction concentration (Table 2.7, entry 4) as well as increasing the silane bulk (Table 2.7, entry 5) affords high selectivities,

although catalyst loading needed to be increased. Exploratory efforts were also directed towards finding a new ligand to improve selectivity for terminal alkynes, and it was found that DM-IPr was a suitable ligand that was easily synthesized in one step from commercially available starting materials and showed selectivity between SIPr and DP-IPr with terminal alkynes. While smaller silanes could be used with DM-IPr with moderate selectivity, its lack of commercial availability as well as the decreased yield with very bulky silanes made it less than ideal as a ligand and SIPr was selected for terminal alkynes. It should be noted that DP-IPr worked well with this protocol, however, it is not commercially available and requires several steps to synthesize, and SIPr was chosen as a more user-friendly ligand.

Table 2.7 Terminal Alkyne Optimization

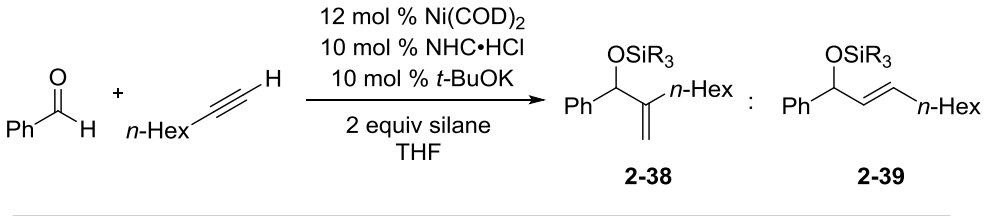

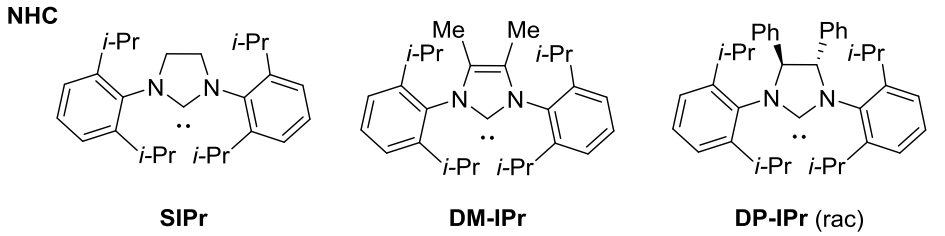

Entry	Ligand	Silane	Temp (°C)	[M]	**2-38**:**2-39** (% yield)
1	SIPr	$(i\text{Pr})_3\text{SiH}$	rt	0.125	45:55 (70)
2	SIPr	$(i\text{Pr})_3\text{SiH}$	50	0.125	57:43 (46)
3[a]	SIPr	$(i\text{Pr})_3\text{SiH}$	95	0.125	92:8 (34)
4	SIPr	$(i\text{Pr})_3\text{SiH}$	rt	0.0125	59:41 (79)
5[b]	SIPr	$(t\text{-Bu})_2\text{MeSiH}$	rt	0.0125	95:5 (69)
6	DM-IPr	$(i\text{Pr})_3\text{SiH}$	rt	0.125	80:20 (62)
7	DM-IPr	$(i\text{Pr})_3\text{SiH}$	rt	0.0125	86:14 (70)
8	DM-IPr	$(t\text{-Bu})_2\text{MeSiH}$	rt	0.125	94:6 (42)
9	DP-IPr	Et_3SiH	rt	0.125	90:10 (72)
10	DP-IPr	$(i\text{Pr})_3\text{SiH}$	rt	0.125	98:2 (63)

[a]PhMe reaction solvent, [b]20 mol % catalyst

Terminal alkynes are biased towards formation of **2-41** and reversing this inherent bias is quite challenging and rare. While previous methodology employed non-commercially available DP-IPr, we sought to use commercially available SIPr and examined the reactivity across a variety of terminal alkynes (Table 2.8). Both aliphatic and heteroatom substituted alkynes were reactive with benzaldehyde. Unfortunately, when aliphatic aldehydes were examined under the same conditions only recovered starting material was observed with no product formation (Table

2.8, entry 7). While this methodology improves the practicality of reductive couplings, it appears that the DP-IPr ligand is still necessary for aliphatic aldehydes and terminal alkynes.

Table 2.8 Terminal Alkyne Scope

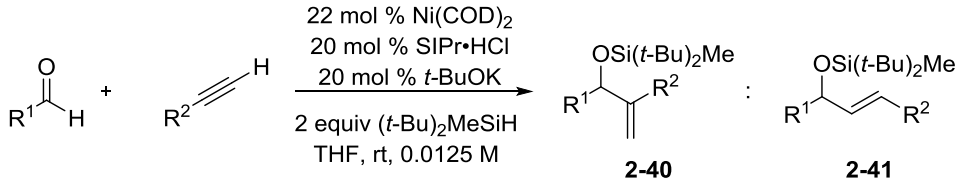

Entry	R^1	R^2	**2-40**:**2-41** (% Yield)
1	Ph	*i*-Pr	>98:2 (61)
2	Ph	*n*-Hex	95:5 (69)
3	Ph	CH_2TMS	>98:2 (58)
4	Ph	Bn	>98:2 (35)
5	Ph	CH_2OPMB	97:3 (46)
6	Ph	CH_2OTBS	71:29 (40)
7	*n*-Hept	*n*-Hex	SM

2.7 Origin for Regioreversal

As shown in this chapter, new experimental conditions were identified that showed significant improvements in regioselectivity across a broad range of substrates. The unique capabilities of this regioreversal are well demonstrated with benzaldehyde and phenylpropyne across a range of conditions where selectivities range from >98:2 for **2-34** using IMes to >98:2 for **2-35** using SIPr. The simplest explanation for the above trends is a change in the rate determining step where silane is now involved in the rate determining step **2-43** to **2-44** and metallacycle formation (**2-42** to **2-43**) is reversible. Conditions employing IMes are operating under the regime where metallacycle formation is rate determining (Scheme 2.10a, **2-42** to **2-43**), however, when SIPr is employed with a large silane, σ-bond metathesis is now the rate

determining step (**2-43** to **2-44**) and metallacycle formation is reversible (Scheme 2.10b). This reversible oxidative cyclization would preferentially lead to the formation of **2-35**.

Scheme 2.10 Initial Mechanistic Hypothesis

a) Standard protocol

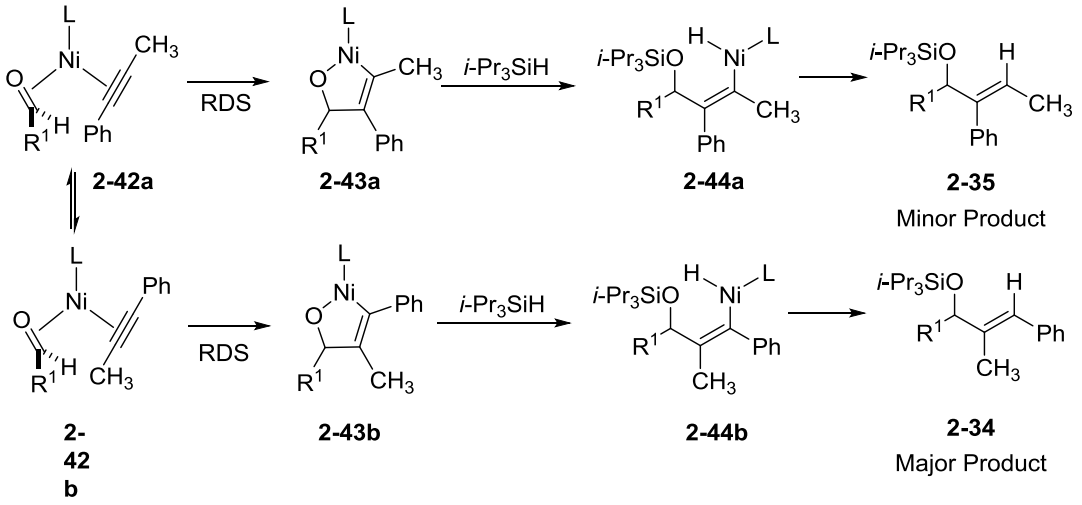

b) Large Ligand & Large Silane

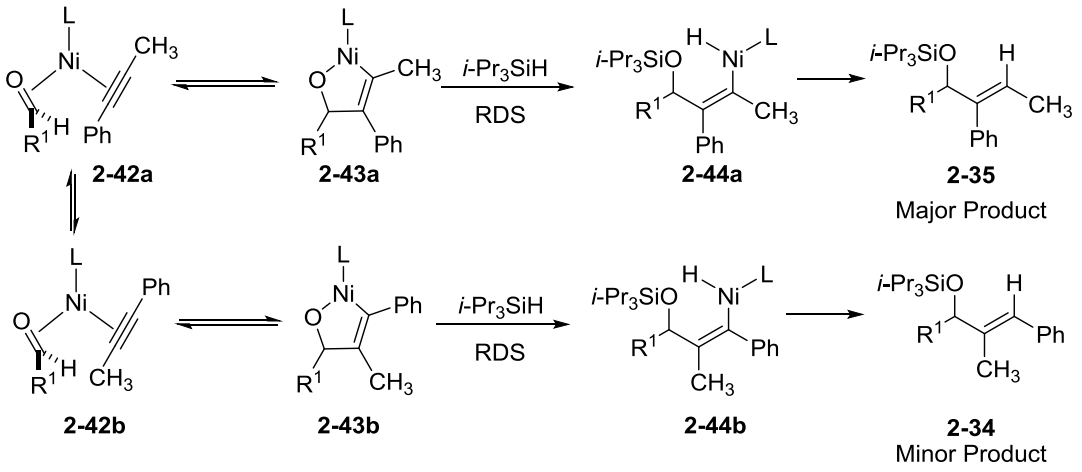

While unprecedented for this reaction type, reversible metallacycle formation has been documented with nickel as well as other metals in related processes.[48,49] Previous mechanistic[47] and computational studies[29] have not supported this hypothesis and we sought to gain evidence to support this mechanistic proposal. Perhaps the simplest and common probe for the rate determining step is the kinetic isotope effect where a reactive site is labeled with an isotope. To

probe the possibility of silane being involved in the rate determining step (i-Pr)$_3$SiD was synthesized and in both competition experiments as well as comparison of initial rates showed a small KIE of ~1.5 k_H/k_D. The small KIE was initially unexpected, however it was not surprising given that primary kinetic isotope effects for silane σ-bond metathesis can be as small as 1.15.[52] Additionally, previous computational studies showed that the σ-bond metathesis step proceeds by coordination of silane to nickel followed by an interaction between oxygen and silicon during the transition state.[29] As shown in Figure 2.3 there is only a minor change is Si-H bond length in the transition state energy maximum, and cleavage of the Si-H bond occurs after the energy maximum. For this reason, even if the silane is involved in the rate determining step, the expected KIE values would be small. However, altering the concentration of silane will alter the rate of σ-bond metathesis irrespective of the extent and timing of the Si-H cleavage. For this reason, we opted to study the reaction by initial rates and avoid the limitations of KIE experiments.

Figure 2.3 TS of σ-bond Metathesis

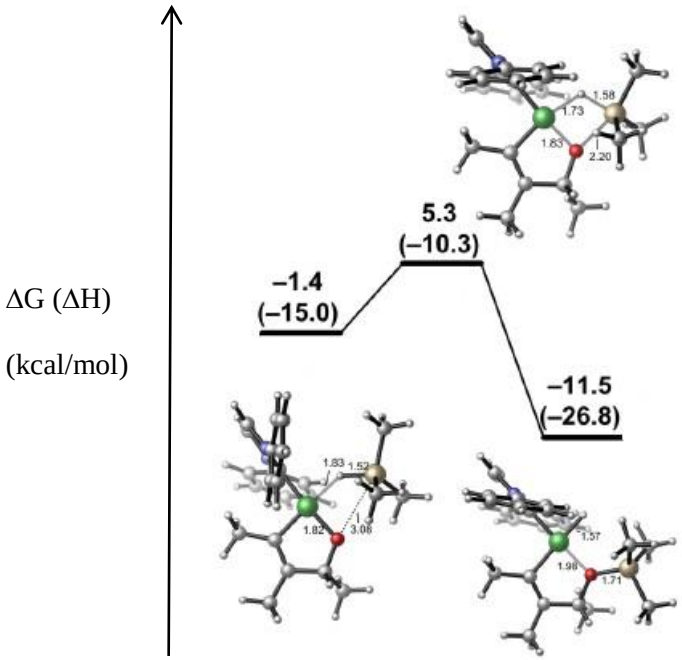

Previous mechanistic studies have observed the initial rate through *in situ* IR monitoring of the aldehyde stretch, and this technique works well for biased intramolecular cyclizations or intermolecular couplings employing symmetrical alkynes. No information about the rate of formation for each isomer can be gained for intermolecular reactions employing non-symmetrical alkynes. To overcome this challenge, GC-FID analysis was used with reaction sampling to determine initial rates for each regioisomer.

It should be noted that the dependence of initial rates on silane concentration was examined with modified reaction conditions from those described earlier. Highest yields were achieved when aldehyde, alkyne, and silane were added via syringe drive; however, this protocol was not suitable for initial rates analysis. Although a decrease in yield was observed, productive catalyst turnover could be achieved without slow addition when the reaction was diluted 10-fold to 0.0125 M.

With modified reaction conditions in hand, examining the rate of total product formation showed only a small rate dependence on silane (Figure 2.4a). This result was surprising; however, the origin of this effect became clear when the rate of formation for each isomer was plotted separately. As shown below, the rate dependence for each isomer varied significantly between plots for the minor isomer **2-34** compared to major isomer **2-35**. When silane concentration was varied from 2.0 to 6.0 equiv the rate dependence for the major isomer (**2-35**) remained near zero order (Figure 2.4b). However, under the same conditions the rate dependence for the minor isomer (**2-34)** showed an approximately first order dependence on silane (Figure 2.4c). The effect can also be seen when plotting the ratio of the rate of minor isomer production over the major isomer (Figure 2.4d). The observed trends from table 2.4 can be seen in the ratio plot in Figure 2.4d that as silane concentration increases the regioselectivity of the reaction

decreases which is consistent with the observed trend that high selectivity is observed at low silane concentrations.

Figure 2.4 Initial Rates

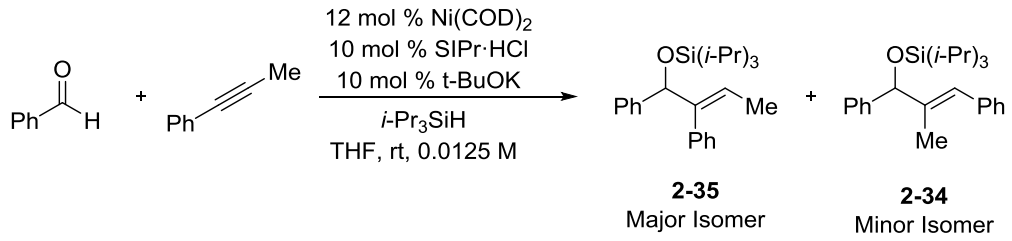

a) Rate of Total Product Formation

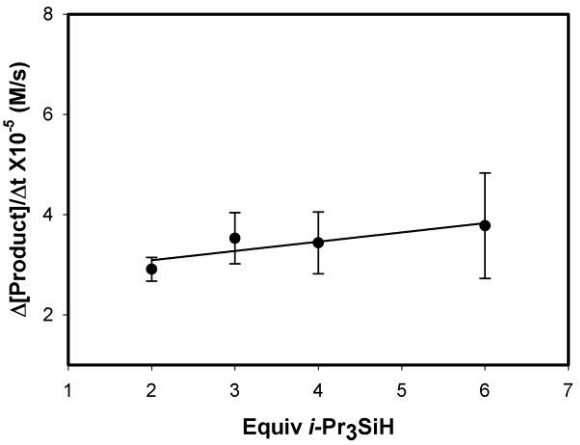

b) Rate of Major Isomer Formation

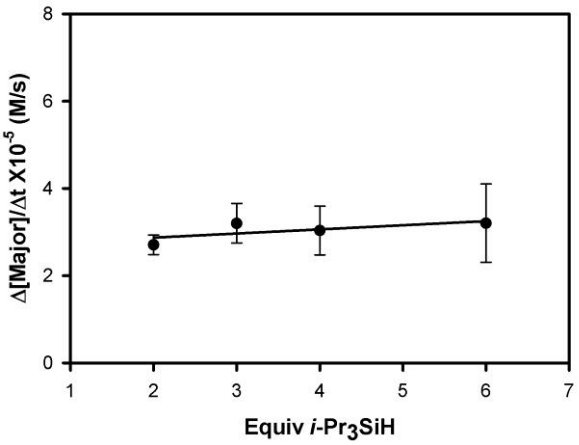

c) Rate of Minor Isomer Formation

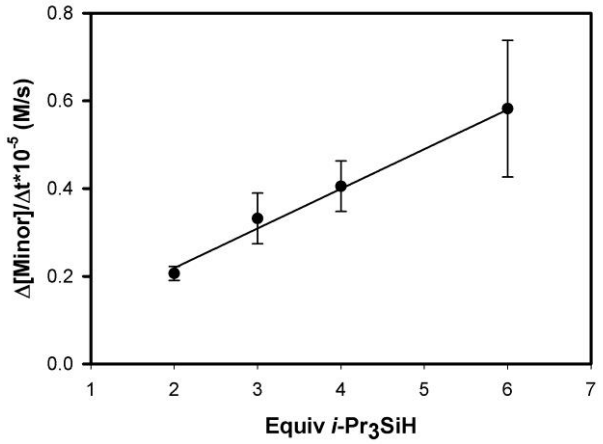

d) Ratio of rate of Minor/Major

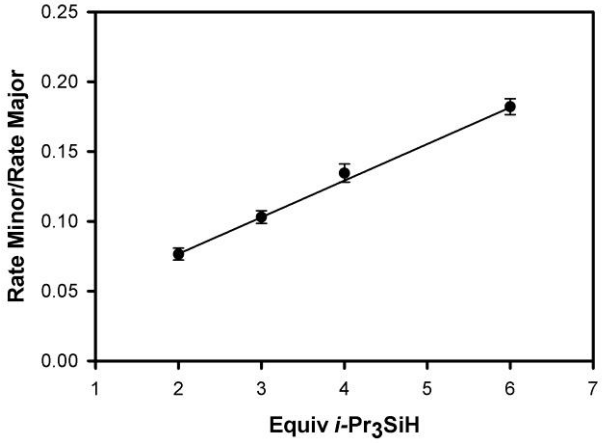

The data in Figure 2.4 suggested that, at least under the fast addition protocol used to study initial rates, the origin for the trends observed in Tables 2.3-2.5 is a fundamentally different rate-determining step for each pathway. For the formation of major isomer **2-35**, the rate-determining step is oxidative cyclization (Scheme 2.11, **2-42a** to **2-42b**) consistent with previous mechanistic studies. However, for minor isomer **2-34**, the rate-determining step is now σ-bond metathesis (Scheme 2.11, **2-43b** to **2-44b**) and metallacycle formation is reversible.

Scheme 2.11 Mechanism Invoking Different Rate-Determining Steps

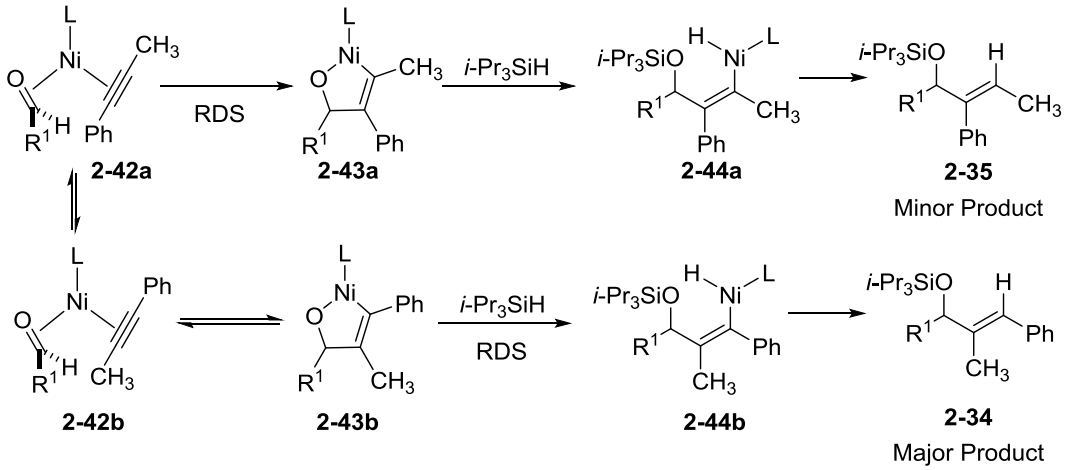

The difference in these two pathways can be rationalized by a more crowded nickel center for the minor isomer due to the large alkyne substituent being adjacent to the nickel center. All of the observed trends in Tables 2.3-2.5 can be explained by and are consistent with a mechanistic model involving rate determining σ-bond metathesis of just the minor isomer pathway. The concentration effects observed in Table 2.4 can be rationalized by a mechanism involving different rate determining steps for each isomer, since formation of the minor isomer will only depend on silane concentration while the major will remain independent. As silane concentration is increased the rate of σ-bond metathesis will increase for only the minor isomer and thus reduce selectivity of the reaction. Temperature effects observed in table 2.5 can also be rationalized using the model in Scheme 2.11. In the mechanistic pathway the oxidative cyclization step is a unimolecular rearrangement, however, σ-bond metathesis is a bimolecular reaction. In the unimolecular reaction the expected entopic penalty would be small, however, in the bimolecular reaction involving two bulky components a significant penalty would be expected, thus when the reaction is heated, the entropic penalty is maximized for the minor isomer pathway with little effect on the major isomer pathway.

2.8 Initial Rates using Et_3SiH

The rate dependence on Et_3SiH was also examined using the conditions listed previously for $(i\text{-Pr})_3SiH$. As expected, an approximate zero order dependence was seen for both isomers, although there was a slight increase in rate when comparing initial rates at low concentrations of silane to high concentrations for both major and minor isomer. These trends are consistent with the proposed mechanism (Scheme 2.10a) when employing a combination of large ligand and small silane no rate dependence on silane is observed due to oxidative cyclization being the rate determining step for both pathways of the reaction (Figure 2.5).

Figure 2.5 Initial Rates using Et_3SiH

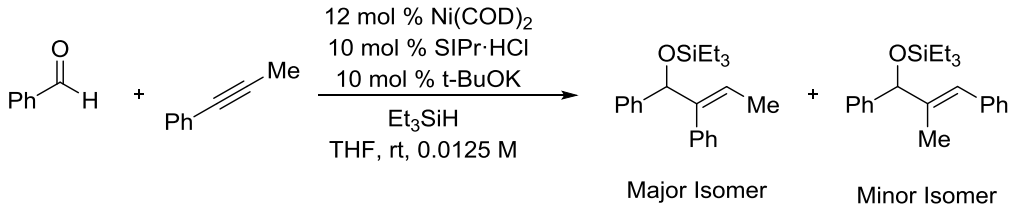

a) Rate of Major Isomer

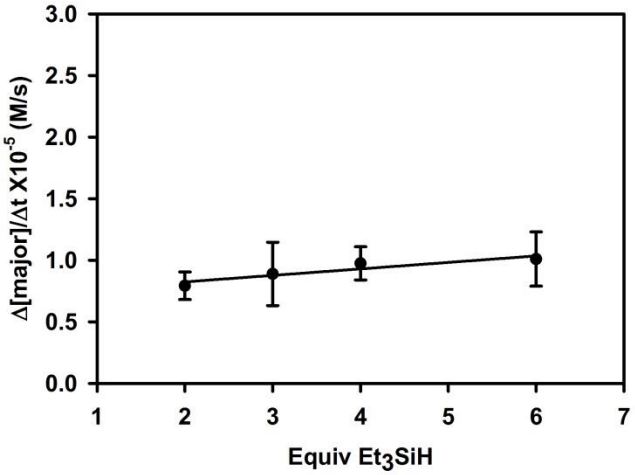

b) Rate of Minor Isomer

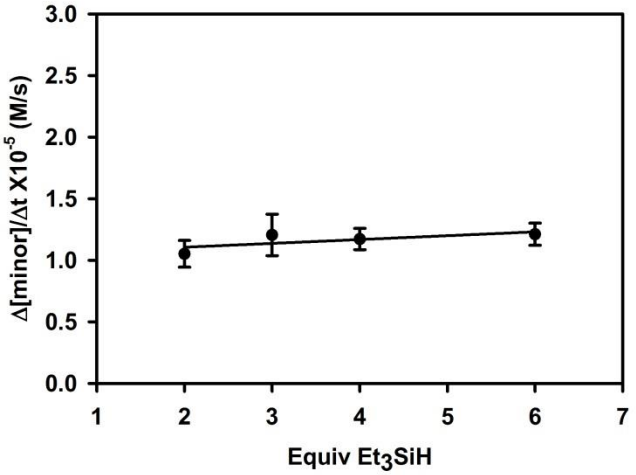

Although the above rate dependence on silane is consistent with the mechanistic proposal, to our surprise the initial rate for the minor isomer is actually larger than for the major (Figure 2.6a). However, as the reaction progresses the rate of the major isomer formation increases and overtakes the minor isomer. This effect can also be seen in the change in regioselectivity over the course of the reaction initially favoring minor isomer in 70:30 selectivity; however, as the reaction progress the selectivity reverses to 39:61 favoring the major isomer (Figure 2.6b). Additionally, the combined rate for both products using Et_3SiH is slower than when $(i\text{-Pr})_3SiH$ is used. This result is surprising given that $(i\text{-Pr})_3SiH$ is bulkier and one would expect the rate of σ-bond metathesis to be slower when larger silanes are used.

Figure 2.6 Reaction Progression using Et_3SiH

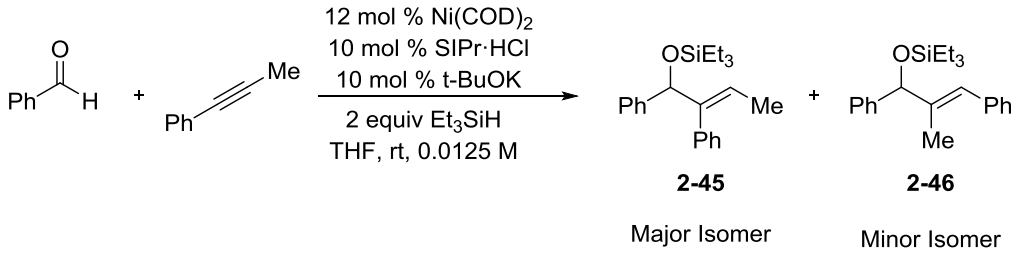

a) Reaction progression

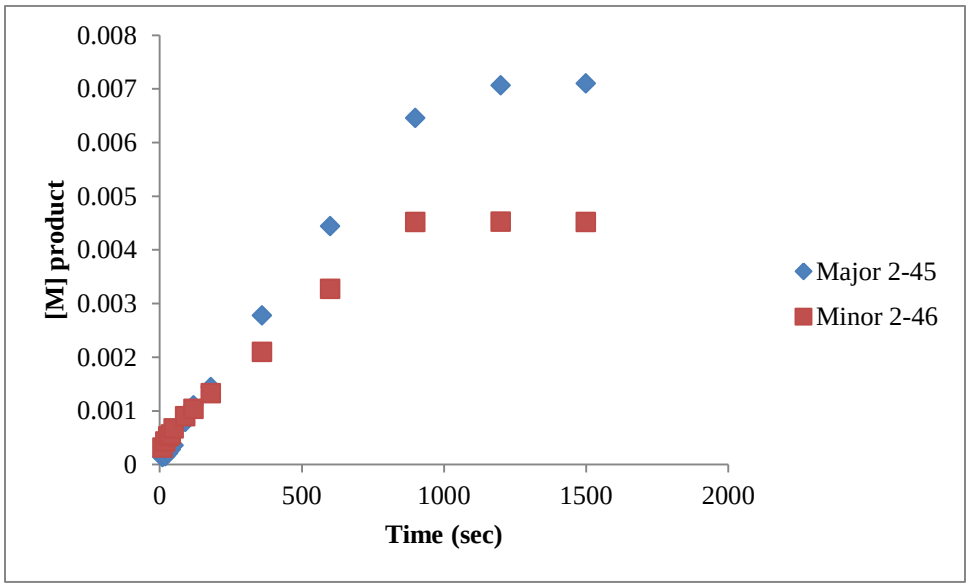

b) Regioselectivity of Reaction

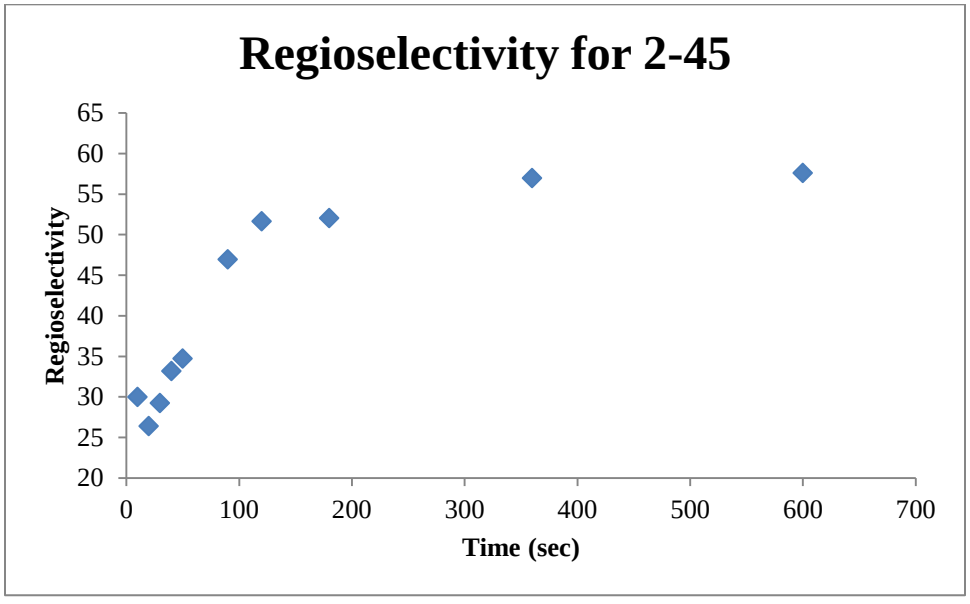

The large change in selectivity over the course of the reaction is surprising given that there is only a minor decrease in selectivity over the course of the reaction when using (*i*-Pr)$_3$SiH. No effect on regioselectivity from silane concentration is observed in this protocol indicating that silane is not involved in the rate determining step. Furthermore, this effect can be observed across all silane concentrations studied. It is likely that this effect arises from changing substrate concentration, not a change in the rate determining step of the reaction when small silanes are employed.

Previous efforts from the group have attempted to develop a full intermolecular kinetic profile for the NHC-silane mediated system and efforts to date have found this to be a complex system that does not show integer rate dependence on the aldehyde and alkyne.[53,54] This evidence suggests that the catalyst mixture could contain several substrate-bound complexes whose concentrations are highly sensitive to aldehyde and alkyne concentration. Previous computational studies showed that the catalyst resting state to be equilibrating between two different species **2-48** and **2-49**, with the minimum energy pathway for oxidative cyclization from **2-49** to **2-50**, however it is conceivable that as the concentration of substrates varied this would affect the relative concentrations of species.[44] This picture is further complicated when unsymmetrical alkynes are employed leading to two different binding modes of the alkyne to the metal (Scheme 2.12, **2-47a** to **2-47b**). It is likely that there are several off cycle intermediates that could be affecting the selectivity of the reaction when Et$_3$SiH is used in this protocol likely leading to the observed change in selectivity.

Scheme 2.12 Equilibration of Catalyst Complexes before Rate Determining Step

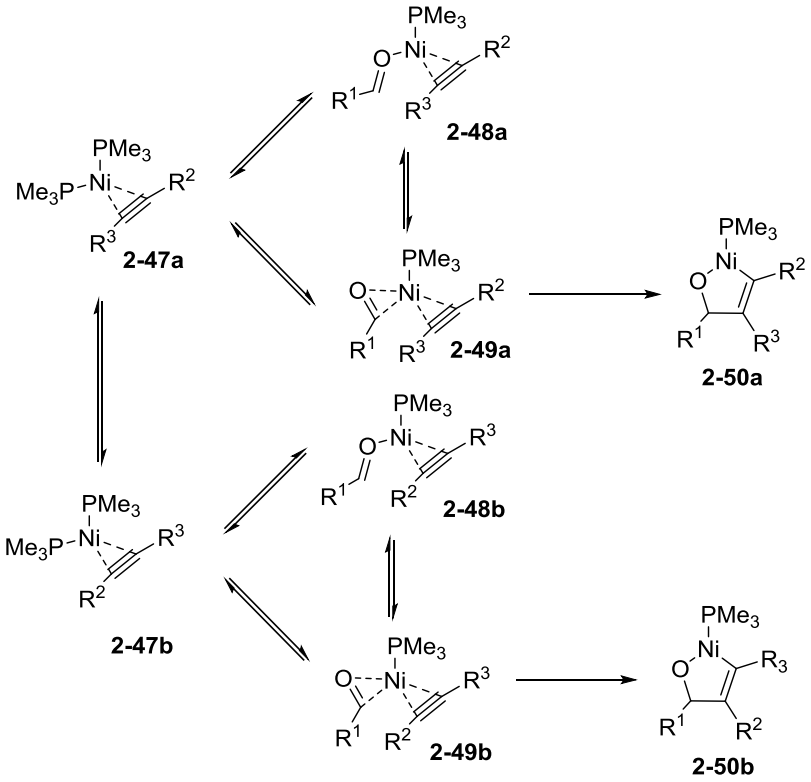

2.9 Alternative Mechanistic Considerations

Previously, mechanistic studies have ruled out initial oxidative addition to the Si-H bond as depicted in Scheme 2.8, however, the reaction conditions in this study are different enough that it is conceivable that this protocol could be operating under a different mechanistic manifold. While not directly probed, several pieces of evidence argue against initial oxidative addition to the Si-H bond. First, increasing silane bulk required to introduce the silane rate dependence would disfavor oxidative addition on steric grounds.[55,56,57,58] Second, different rate dependence for each isomer would not be expected for a mechanism involving initial oxidative addition. Third, silane oxidative addition pathways typically afford the hydrosilylation of either the aldehyde[59] or alkyne[60] and control reactions in which either alkyne or aldehyde were omitted showed no productive hydrosilylation indicating that this pathway is likely not operative under

these conditions. Finally, the aldehyde hydrosilylation proceeds with an inverse KIE which was not observed under these conditions.[47]

2.10 Conclusions

In summary a new regiocontrol strategy has been developed that employs commercially available ligands and silanes and is a significant advancement over previous protocols. This study illustrates that a rational change in that rate and regioselectivity-determining step for aldehyde alkyne reductive couplings. The improvement in selectivity arises from a change in the rate determining step for one isomeric pathway in which silane is now involved in the rate determining step. This methodology possesses broad scope and improves the selectivity for C-C bond formation at the more hindered position on the alkyne across a variety of substrate combinations.

Chapter 3

Ni-Catalyzed Reductive Couplings using Bench Stable and Inexpensive Ni^{II} Pre-catalysts

3.1 Introduction

Ni-catalyzed reactions have emerged as a powerful tool for a variety of transformations;[61,62,63,64] however, a persistent challenge in nickel catalysis is the stability and cost of Ni^0 sources. While nickel metal itself is quite inexpensive compared to 2nd or 3rd row transitions metals, commonly used Ni^0 sources such as $Ni(COD)_2$ are orders of magnitude more expensive than many Ni^{II} compounds when commercially purchased. Although the economic challenges can be overcome by the end user synthesizing $Ni(COD)_2$ from inexpensive $Ni(acac)_2$ using DIBAL[65] or $AlEt_3$,[66] this method requires an extra step for purification and may not always be practical. An additional and probably larger challenge to using $Ni(COD)_2$ is its instability to air, and all manipulations must be conducted under an inert atmosphere.

One commonly employed strategy to overcoming the challenge of Ni^0 bench stability is to employ a bench-stable Ni^{II} pre-catalyst and conduct the reduction *in situ* to generate an active Ni^0 catalyst, thus obviating the need for $Ni(COD)_2$. This strategy is commonly employed for a variety of cross-coupling reactions where the nucleophile also serves as the reducing agent; however a majority of these protocols employ air and moisture sensitive organometallic compounds which limit their practicality.[67,68,69,70,71] In cases where the nucleophile is not sufficiently reactive, a catalytic amount of organometallic reducing agent can be added to reduce

the pre-catalyst although these are generally still pyrophoric.[72] Limited reports exist that employ both a bench stable pre-catalyst as well as bench stable reducing agent, and these strategies will be discussed in this chapter.

An additional benefit of synthesizing Ni^0 *in situ* compared to using $Ni(COD)_2$ is the elimination of COD in the reaction. While commonly proposed to be a spectator ligand, recent studies have shown that COD can actually play a non-innocent role in Ni catalysed reactions.[73,74,75,76] This is significant given that $Ni(COD)_2$ is commonly employed in a variety of reactions. Developing alternative methods that can access Ni^0 without the use of $Ni(COD)_2$ will likely open up new avenues for reactivity that have previously been inhibited by COD.

3.2 *In Situ* Reductions using Bench Stable Reducing Agents

While well-defined air-sensitive organometallic reagents such as organozincs or magnesiums are effective at reducing Ni^{II} pre-catalysts for cross-coupling, the use of boronic acids or trifluoroborates as nucleophiles is attractive due to their bench stability. Various protocols have been developed for Suzuki-Miyaura reactions employing both bench stable catalysts and reagents.[77] Han has recently reported a particularly user friendly protocol employing inexpensive and bench stable $NiCl_2$(dppp) for Suzuki-Miyaura couplings with boronic acids.[78] Work from the Molander group has also shown Ni^{II} pre-catalysts to be efficient for coupling aryl and vinyl-trifluoroborates with alkyl halides.[79,80] Both of these protocols employ bench stable reagents and can be setup without the use of a glovebox (Scheme 3.1).

Scheme 3.1 Bench Stable Cross Couplings

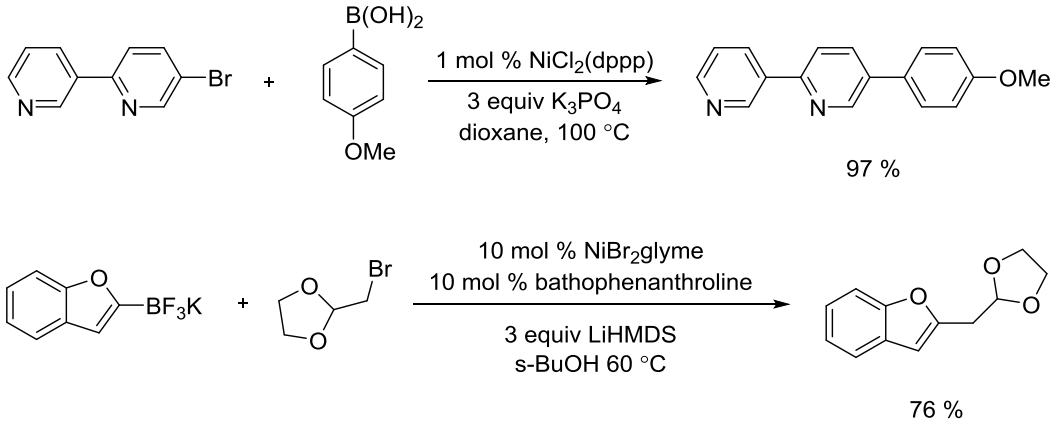

An alternative strategy to using well defined organometallic reagents for pre-catalyst reduction is to use Zn or Mn dust as the reductant. Initially employed as a reductant in Ni catalysis for arene homocoupling, Zn[81] and Mn[82] dust are economical and bench stable reducing agents that are capable of reducing a variety of Ni^{II} pre-catalysts. More recently this strategy has been employed by the Weix group for electrophile-electrophile cross coupling reactions using either Mn or Zn powder as a reducing agent for NiX_2.[83,84,85] Both Mn and Zn are proposed to act as the reducing agent for initial reduction of the Ni^{II} pre-catalyst as well as serve as the terminal reductant in the catalytic reaction. Employing Mn or Zn as reducing agents has also been applied by Martin and co-workers for Ni catalysed carboxylation reactions (Scheme 3.2).[86,87,88]

Scheme 3.2 Contemporary Uses of Zn and Mn Dust as Reducing Agents

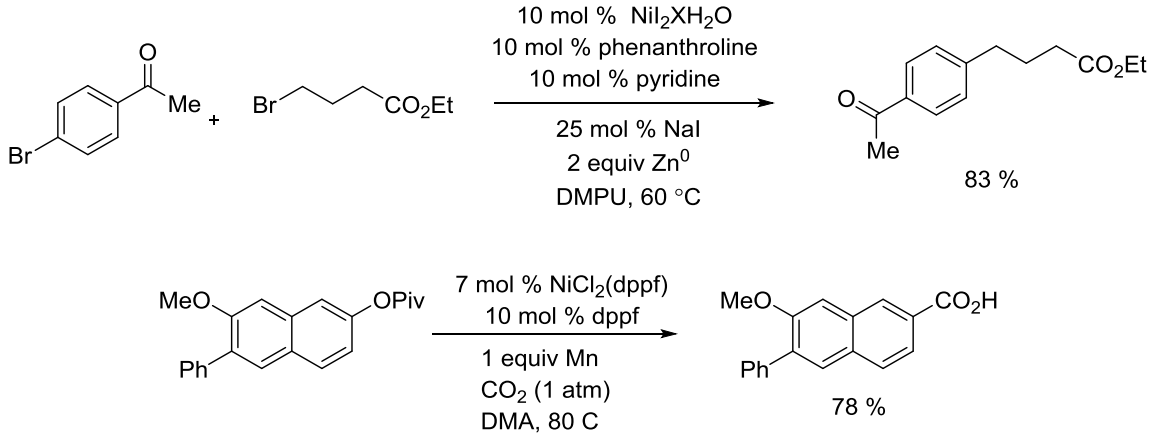

Limited reports exist of Ni catalyzed reductive couplings employing both bench stable pre-catalysts and reducing agents. Previous efforts from our group[89,90,91] have employed alcohols bearing β-hydrogens as a reductant, however, these methods still required the use of $Ni(COD)_2$ and thus necessitated the use a glovebox for reaction setup. An improvement by the Jamison group demonstrated that *i*-PrOH can serve as an effective reducing agent in Ni-catalyzed intramolecular reductive couplings of epoxides and alkynes using a bench stable Ni^{II} pre-catalyst (Scheme 3.3).[92] This method improves previous methodology which required the use of $Ni(COD)_2$ and Et_3B as a reducing agent.[93]

Scheme 3.3 Epoxide Alkyne Reductive Coupling

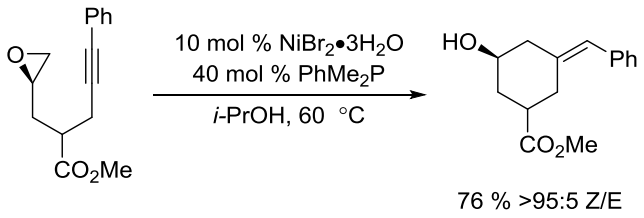

3.3 Developing a Bench Stable Reductive Coupling Protocol

Previous efforts from the our group have shown that $Ni(COD)_2$ can be synthesised *in situ* from $Ni(acac)_2$ using DIBAL (Scheme 3.4).[94] In this protocol, only a small decrease in chemical yield was observed when comparing $Ni(COD)_2$ to the *in situ* prep from $Ni(acac)_2$. While these reactions can be setup without the use of a glovebox, they still employ air sensitive DIBAL and an additional drawback to this method is the potential for residual reducing agent in solution which could lead to poor functional group compatibility.

Scheme 3.4 *In Situ* Generation of $Ni(COD)_2$

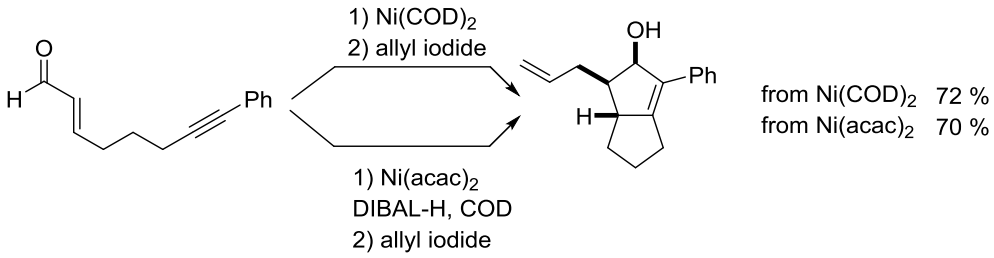

The goal for this project was to develop a user-friendly protocol that did not require the use of a glovebox for reaction setup or employment of air and moisture sensitive reducing agents. As discussed in Chapters 1 and 2, our group has previously reported Ni catalysed reductive coupling of aldehydes and alkynes to synthesize allylic alcohols. While early variants used pyrophoric organozincs[38] or organoboranes[39] as reducing agents, more recent advancements have shown that bench stable trialkylsilanes[40] can be employed as effective reducing agents in the system. Although bench stable trialkylsilanes can be used, protocols to date from our laboratory have required the use of $Ni(COD)_2$.

Inspired by previous work showing Mn or Zn to be an effective reducing agent for Ni^{II} pre-catalysts, we began our studies examining Mn as a pre-catalyst reductant using a variety of Ni^{II} sources for the reductive coupling of benzaldehyde and phenylpropyne (Table 3.1). Early efforts identified commonly used $NiBr_2$•glyme as a suitable pre-catalyst for reductive couplings. When then catalyst was weighed out in the glovebox, excellent yields were observed (Table 3.1, entry 1); however, when the catalyst was weighed out in regular atmosphere on the bench, a large decrease in yield was seen (Table 3.1, entry 2). The origin for this effect is likely the volatility of glyme when exposed to vacuum.[84] To overcome this challenge, inexpensive and bench-stable $Ni(acac)_2$ was selected as the pre-catalyst with initially anhydrous $Ni(acac)_2$ being used, however, during optimization studies it was found that the hydrate behaved similarly.

$Ni(acac)_2$ proved advantages over other nickel sources in that it is indefinitely stable to air, inexpensive, and exposure to vacuum does not reduce reactivity which was observed previously with $NiBr_2$•glyme.

Table 3.1 Pre-catalyst Screen

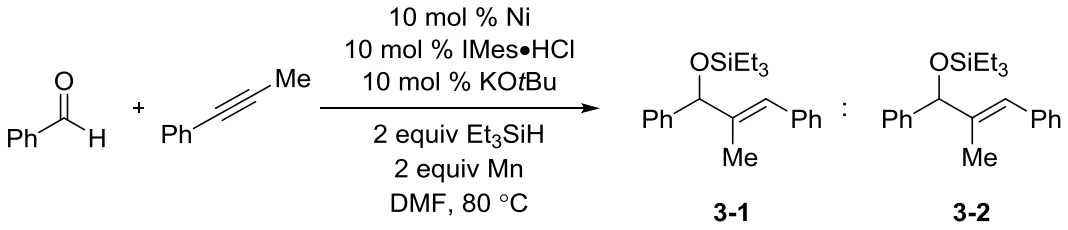

3-1 **3-2**

Entry	Ni	% Yield (**3-1**:**3-2**)
1	$NiBr_2$glyme	97 (94:6)
2[a]	$NiBr_2$glyme	11-40 (96:4)
3	$NiBr_2$	52 (95:5)
4	$Ni(acac)_2$	56 (93:7)
5[b]	$NiCl_2(PCy_3)_2$	28 (96:4)

[a]reaction setup on bench, [b]no NHC/base added

Further optimization showed that reactions could be cooled to room temperature without a reduction in yield, and to our surprise, omission of manganese had no effect on the yield during a control reaction (Table 3.2, entry 2). Although originally thought to be critical for pre-catalyst reduction, Mn appears to have no effect on yield and is not participating in the reaction. To make the reaction more user friends we sought to use more volatile solvents and unfortunately found that use of highly polar aprotic DMF was necessary. Attempts to use DMF as a cosolvent were moderately successful with good yields observed when used in a 1:1 ratio with PhMe, however efforts to decrease the ratio of DMF or use THF as a cosolvent all resulted in a decreased yield (Table 3.2, entry 3). Conducting the reaction in pure PhMe resulted in only recovered starting material (Table 3.2, entry 6). To our delight, further optimization showed that we could

circumvent the necessity for DMF by increasing the equivalents of KO*t*Bu in the reaction which achieved similar yields to when DMF was employed (Table 3.2, entry 7).

Table 3.2 Solvent Screen

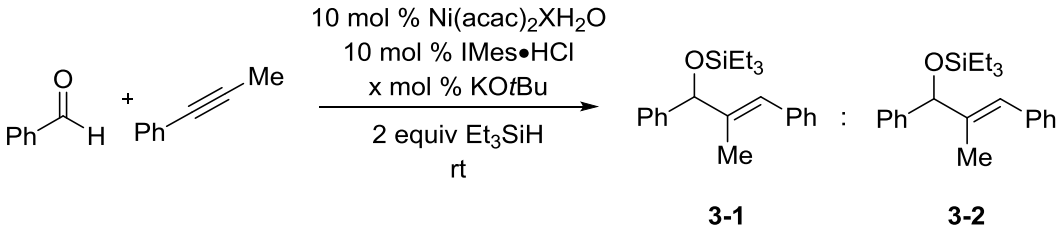

3-1 **3-2**

Entry	Solvent	Additive	mol % KO*t*Bu	GC Yield (**3-1**:**3-2**)
1	DMF	Mn	10	95 (97:3)
2	DMF	-	10	97 (97:3)
3	1:1 DMF:THF	-	10	50 (98:2)
4	1:1 DMF:PhMe	-	10	98 (98:2)
5	1:10 DMF:PhMe	-	10	70 (98:2)
6	PhMe	-	10	NR
7	PhMe	-	35	88 (97:3)*

*isolated yield

Although the origin of the solvent effect is not well understood, it is possible that DMF is sufficiently polar to allow the hydrosilylation with the acac ligand while a ligand displacement is required with *t*BuOK in PhMe. A similar mechanism has been proposed by Nolan and coworkers for reduction of Cu-NHC catalysts for the hydrosilylation of ketones.[95] Additionally, σ-bond metathesis to generate a Ni-H complex has been demonstrated with silanes and Ni-alkoxide pincer complexes.[96] Two possible mechanistic pathways are shown in Scheme 3.5 for the reduction of the pre-catalyst. In the pathway using DMF, σ-bond metathesis generates the silyl enol ether **3-4** and a Ni hydride **3-5**. Subsequent reductive elimination generates the active catalyst **3-7** and an equivalent of acac. When PhMe is used as a solvent, initial ligand exchange with *t*-BuOK generates a Ni alkoxide **3-6** and subsequent σ-bond metathesis generates common

intermediate **3-5**. This would be consistent with the observed requirement for excess base in reactions employing purely PhMe.

Scheme 3.5 Possible Reduction Mechanisms

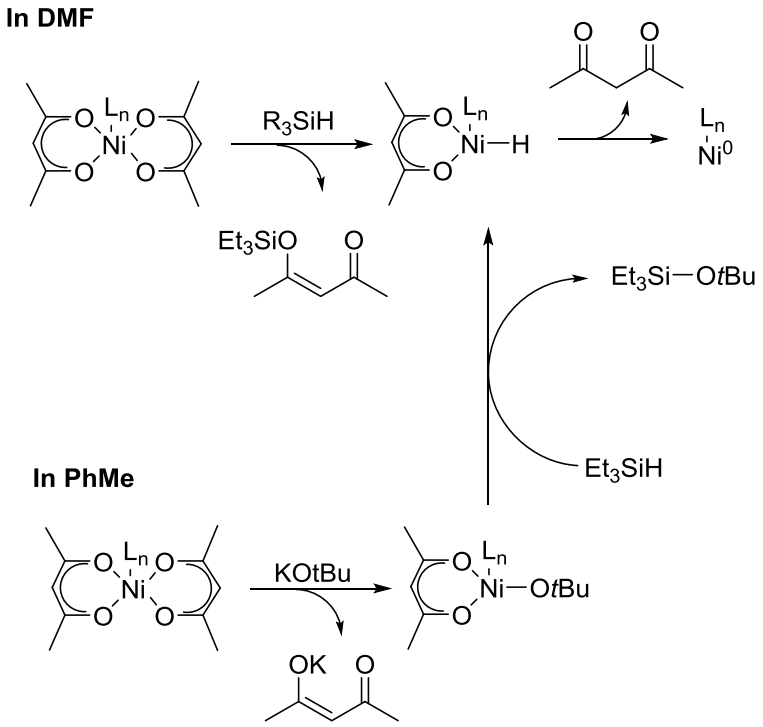

Early efforts on this project focused on developing regiodivergent protocols to access both isomers as previously discussed in Chapter 1.[28] As shown in Chapter 2, to obtain high selectivity using bulky NHCs required the use of bulky silanes in the protocol.[50] Although productive yields were observed with SIPr and Et_3SiH, a large erosion in selectivity was seen (Table 3.3, entry 5), however, use of *i*-Pr_3SiH to obtain high selectivity resulted in a dramatic decrease in yield (Table 3.3, entry 6). IMes was found to be the optimal ligand with regioselectivity primarily determined by alkyne bias. It is likely that the system is just too sterically hindered for the precatalyst reduction to take place efficiently when using SIPr and *i*-Pr_3SiH.

Table 3.3 Ligand Silane Screen

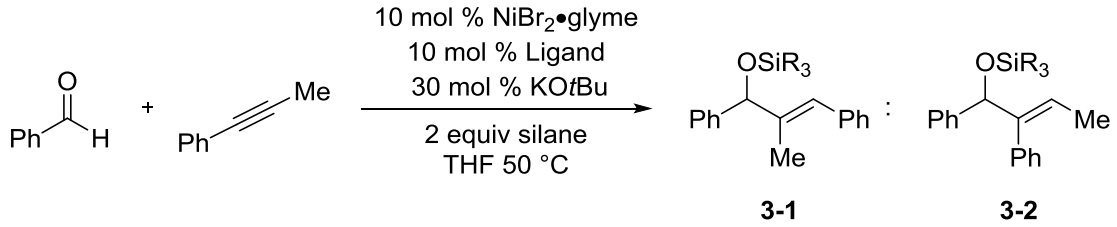

Entry	Ligand	Silane	**3-1**:**3-2** (% yield)
1	IMes	Et_3SiH	96:4 (77)
2	IMes	iPr_3SiH	97:3 (76)
3	IPr	Et_3SiH	57:43 (74)
4	IPr	iPr_3SiH	15:85 (21)
5	SIPr	Et_3SiH	38:62 (82)
6	SIPr	iPr_3SiH	8:92 (33)

3.4 Scope

With an optimized procedure in hand for conducting reactions without the use of a glovebox, we sought to examine the scope of coupling partners. Generally the system behaved comparably to when $Ni(COD)_2$ was employed with a variety of aldehydes and alkynes being efficiently coupled. Conjugated alkynes were efficiently coupled to both aliphatic and aromatic aldehydes (Table 3.4, entries 3a-c). Terminal alkynes were also efficiently coupled with both aromatic as well as aliphatic aldehydes, although a significant decrease in yield was observed when an aliphatic aldehyde was employed (Table 3.4, 3d-f). Examination of pyridine substituted aldehydes initially showed no reactivity, however, further optimization showed that addition of $AlMe_3$[97] and PPh_3 as well as heating the reaction to 100 C allowed for productive reactions employing pyridine (Table 3.4, 3g,h). Addition of PPh_3 appears to have a stabilizing effect on the catalyst and resulted in increased yield when reactions were heated. Finally the Jamison group has studied reductive couplings of aldehydes and allenes[98,99] and we found that cyclohexyl allene

was tolerated under these reaction conditions to obtain the exomethylene product albeit in lower yield (Table 3.4, 3i).

Table 3.4 Substrate Scope

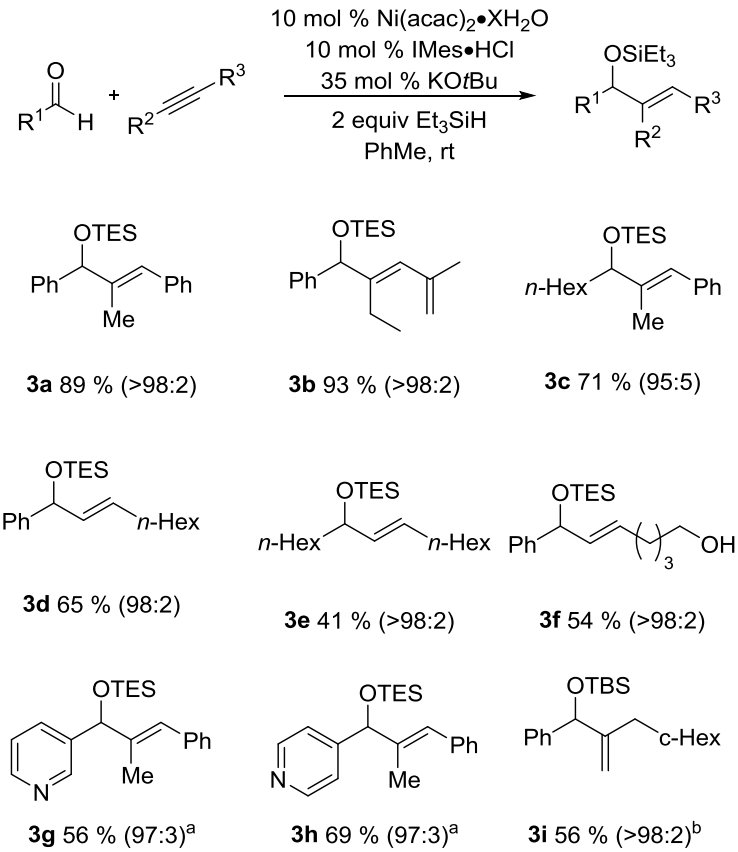

[a]10 mol % PPh_3, 10 mol % $AlMe_3$, 100 °C [b]cyclohexyl allene used

3.5 Other Ni-NHC Silane Mediated Reactions

Having observed the success for the above system for conducting reductive coupling reactions without the use of a glovebox, we sought to examine this catalytic system across different Ni-NHC catalyzed reactions employing silanes. The Harwig and Martin laboratories have shown successful aryl ether bond cleavage using either Ni-NHC or Ni-phosphine based catalysts employing silanes or H_2 as the reducing agent.[100,101] Both of these protocols employ $Ni(COD)_2$ and developing an alternative catalyst generation strategy would expand the utility of

the chemistry. To investigate if our protocol was effective at this transformation, the reduction of 2-methoxynaphthalene was briefly examined and it was found that while catalyst turnover was observed, significant optimization would need to be done to produce a catalytic system that is comparable to the Harwig or Martin protocols (Table 3.5).

Table 3.5 Aryl Ether Cleavage

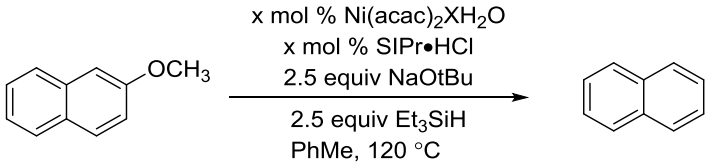

Entry	X mol % Ni	X mol % SIPr	GC Yield
1	10	10	30 %
2	10	20	66 %
3	20	20	66 %
4	20	40	59 %

Previous work from our group has shown Ni-NHC catalysts to be effective for the hydrosilylation of alkynes generating vinyl silanes.[102] When this protocol was attempted with the bench stable catalytic system, no product was observed. This result was surprising given that this product or the hydrosilylated dimer is typically observed as a by-product in reductive couplings. Additionally, no trimerization of the alkyne was observed in this reaction suggesting that no active Ni^0 catalyst was formed. It is possible that in this system, the aldehyde could be involved in pre-catalyst reduction, or COD could be a critical ligand for the hydrosilylation reaction to occur.

Scheme 3.6 Attempted Hydrosilylation of Alkynes

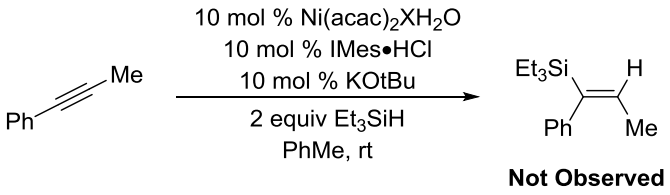

3.6 Alternative Reducing Agents

Alternative reduction protocols to the base-silane protocol described previously were also investigated. Inspired by work form the Masubara and coworkers showing NaH to be a competent reducing agent for $Ni(acac)_2$[103] we examined the competency of NaH as a reducing agent in Ni catalysed reductive couplings (Table 3.6). To our surprise, we found that NaH appears to be capable of reducing $Ni(acac)_2$ in reductive couplings. Omitting NaH and using the free carbene showed no product formation indicating that the base was doing more than just deprotonating the NHC (Table 3.6, entry 3). While the mechanism for this reduction is not well understood, it provides an unconventional route to access catalytically active Ni.

Table 3.6 Exploration of NaH as a Reducing Agent

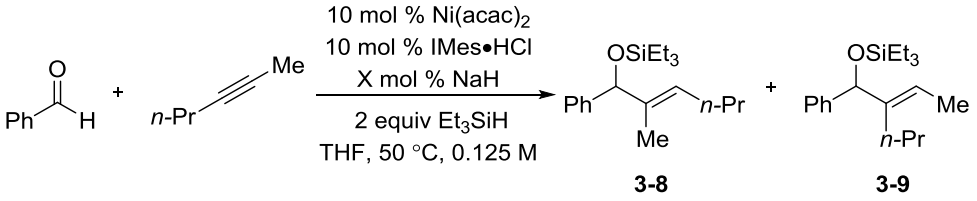

Entry	X mol % NaH	Yield (**3-8**:**3-9**)
1	20	71 (64:36)
2	30	52 (62:38)
3*	-	NR

*free carbene used

3.7 Conclusions

A user-friendly and bench-stable protocol for nickel catalysed intermolecular reducing couplings of aldehydes and alkynes has been developed. This methodology is characterized by use of non-pyrophoric reducing agents as well as allowing reactions to be completely setup without the use of a glove box. While it was initially thought that use of Mn was necessary for pre-catalyst reduction, control reactions showed that silane was capable of reducing the precatalyst in DMF and as well in modified conditions in more nonpolar solvents. This route provides two pathways to successful catalyst formation depending on the desired conditions. Although regiodivergent methods cannot be employed yet, a variety of aldehydes and alkynes can be efficiently coupled with comparable reactivity to $Ni(COD)_2$.

Chapter 4

Conclusions and Outlook

Use of transition metal catalysts is a powerful tool to assemble organic frameworks; however, the control of selectivity as well as practicality in these protocols is a persistent challenge that remains the focus of many research groups from around the world. Our group has had a long standing interest in the reductive coupling of aldehydes and alkynes to synthesize allylic alcohols as they are important structural motifs for a variety of biologically active molecules as well as their utility for various synthetic transformations. While many methods exist to synthesize allylic alcohols, they generally require pre-functionalized precursors or employ organometallic reagents with poor functional group compatibility. The reductive coupling of aldehydes and alkynes is attractive because it circumvents both of these issues; however, a persistent challenge is the control of regioselectivity on the alkyne. As shown in Chapter 2 a new protocol has been developed which allowed unprecedented levels of regiocontrol in Ni catalyzed reductive couplings of aldehydes and alkynes by altering the silane employed in the reaction. This discovery was made during the investigation of bench stable pre-catalysts discussed in Chapter 3. Mechanistic studies showed that the origin for this selectivity arises from a change in the rate determining step for one of regioisomeric pathways thus making selectivity tunable. Following this initial discovery, the regioselectivity for a variety of aldehyde and alkyne partners was substantially increased. Additionally, a new protocol has been developed that allows for some of our group chemistry to be completely employed without the use of a glovebox, and similar results were observed with the benchtop protocol compared to the

glovebox $Ni(COD)_2$ procedure. This protocol will undoubtedly expand the utility of our chemistry by allowing groups without access to a glovebox to conduct Ni catalyzed reductive couplings. Several long standing issues with reductive couplings have been solved, however, there are still future projects that would further the utility and understanding of this chemistry.

4.1 Development of a Intermolecular Kinetic Profile

Previously work from our group has developed a kinetic profile for the intramolecular Ni-phospine catalysed reaction; however, a kinetic profile has not been fully elucidated for the Ni-NHC intermolecular reaction that has proven most synthetically versatile. Efforts from previous group members have made progress towards developing a full kinetic profile; however these efforts have been hindered by a non-integer rate dependence for [aldehyde], [alkyne], and [catalyst] as well as varying induction periods in the reaction. Partial progress was made towards elucidating this picture in Chapter 2 by studying the rate dependence on [silane], however no rate information on [aldehyde], [alkyne], or [catalyst] was obtained. One potential source for this variability is poor catalyst formation since the Ni catalyst needs to be formed *in situ* by mixing $Ni(COD)_2$, NHC•HCl, with a base and the amount of active catalyst is not known. A possible solution to this challenge is to use discrete Ni-NHC complexes for studying the rate (Figure 4.1). Work currently being done in our lab has shown discrete Ni^0-NHC complexes can be synthesized and are effective catalysts for reductive coupling. Use of these discrete complexes could prove valuable for mechanistic studies since the amount of catalyst in solution can be accurately determined. Developing a full kinetic profile may also help elucidate the cause for the selectivity change over the course of the reaction when Et_3SiH was used discussed in section 2.9.

Figure 4.1 Discrete Ni-NHC Complexes

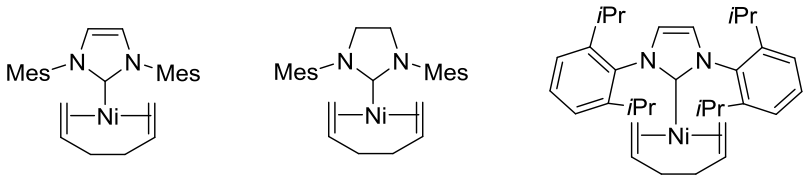

4.2 Internal Redox

The use of silanes is advantageous over organozincs or boranes as reducing agents in reductive couplings due to their bench stability, however, they still suffer from expense as well as generating the silyl ether which requires an additional step for deprotection. As discussed in Section 3.2 previous efforts from our group and others have shown alcohols bearing β-hydrogens to be effective reducing agents in reductive couplings. Unfortunately, when alcohols were attempted as reducing agents in intermolecular reductive couplings in the investigation in Chapter 3 only starting material was observed. Future efforts should be directed at employing alcohols as reducing agents as both the pre-catalyst reductant as well as the reducing agent for reductive couplings. Part of this goal was recently achieved by the Matsubara and co-workers who showed that alcohols bearing a β-hydrogen were capable of undergoing internal redox for Ni catalysed reductive couplings.[104] While this methodology was able to employ inexpensive alcohols, it still suffers from use of $Ni(COD)_2$ and developing methods that employ bench stable Ni precursors would further advance this field. An ideal reaction mechanism for this protocol is shown in Scheme 4.1.

Scheme 4.1 Internal Redox Mechanism

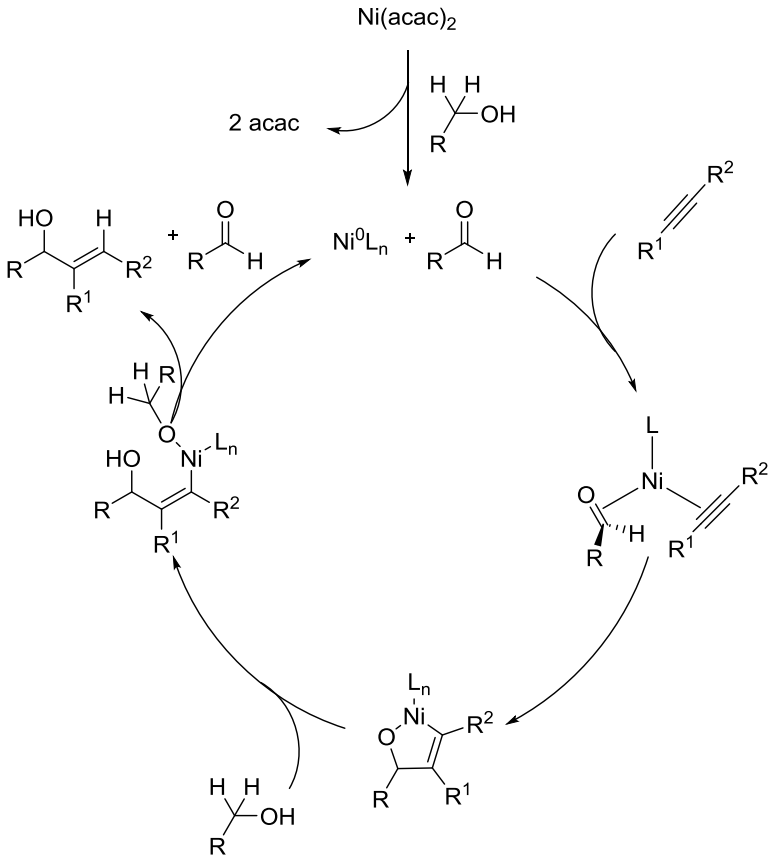

4.3 Summary

The two projects described in this thesis are directed towards providing chemists with more advanced tool for the synthesis of allylic alcohols. In Chapter 2, new methodology was developed that allowed for unprecedented levels of regiocontrol in reactions based on silane identity. In Chapter 3, a new protocol was developed for reductive couplings employing bench stable Ni^{II} precursors and did not require the use of air and moisture-sensitive organometallic reagents. Both of these projects expanded the utility of Ni-catalyzed reductive couplings and future work will be directed at developing full mechanistic models for the intermolecular variant and employing alternative reducing agents.

Chapter 5

Experimental

5.1 General Experimental Details Chapter 2

All reactions were conducted in flame-dried or oven dried (120 °C) glassware with magnetic stirring under an atmosphere of dry nitrogen. Solvents were purified under nitrogen using a solvent purification system (Innovative Technology, Inc. Model # SPS-400-3 and PS-400-3). Unless otherwise noted, alkynes were used as received. Aldehydes were distilled prior to use. Et_3SiH, *i*-Pr_3SiH (Aldrich) and *t*-Bu_2MeSiH ($82/10 g, Gelest & Chem-Impex) were passed through basic alumina before use and stored under nitrogen. $Ni(COD)_2$ (Strem Chemicals, Inc), *N*-heterocyclic carbene salts (Sigma Aldrich, Strem), and *t*-BuOK (Strem) were stored and weighed in an inert atmosphere glovebox.

^1H and ^{13}C were obtained in $CDCl_3$ at rt on a Varian Unity 500 MHz or Varian Unity 700 MHz instrument. Chemical shifts of ^1H NMR spectra were recorded in parts per million (ppm) on the δ scale from an internal standard of residual chloroform (7.24 ppm). Chemical shifts of ^{13}C NMR spectra were recorded in ppm from the central peak of $CDCl_3$ (77.0 ppm) on the δ scale. High resolution mass spectra (HRMS were obtained at the University of Michigan Mass Spectrometry Laboratory on a VG-70-250-s spectrometer manufactured by Micromass Corp. (Manchester UK). Regioisomeric ratios were determined on crude reaction mixtures using either ^1H NMR or GC. GCMS analysis was carried out on a HP 6980 Series GC system with HP-5MS column (30 m x 0.250 mm x 0.25 μm). GCFID analysis was carried out on a HP 6980N Series GC system with a HP-5 column (30 m x 0.32 mm x 0.25 μm).

General Procedure A for $Ni(COD)_2$/SIPr Promoted Reductive Coupling of Internal Alkynes, Aldehydes and Triisopropylsilane:

2 mL of THF was added to a solid mixture of $Ni(COD)_2$ (0.06 mmol), SIPr•HCl salt (0.05 mmol), and *t*-BuOK (0.05 mmol). The resulting solution was stirred for 5 min at rt until the solution turned dark brown. The alkyne (0.5 mmol), aldehyde (0.5 mmol), and triisopropylsilane (1.0 mmol) were combined together with 2 mL of THF. The catalyst was immersed in a 50 °C oil bath and the mixture of aldehyde, alkyne, and silane was added over the course of 60 minutes using a syringe pump. The reaction mixture was allowed to stir until starting materials were consumed. The reaction mixture was filtered through silica gel eluting with 50 % v/v EtOAc/hexanes. The solvent was removed *in vacuo*, and the crude residue was purified via flash chromatography on silica gel to afford the desired product.

General Procedure B for Ni(COD)2/SIPr Promoted Reductive Coupling of Terminal Alkynes, Aldehydes and Di-tert-butyl(methyl)silane:

38 mL of THF was added to a solid mixture of $Ni(COD)_2$ (0.11mmol), SIPr•HCl salt (0.1 mmol), and *t*-BuOK (0.1 mmol). The resulting solution was stirred for 10 min at rt until the solution turned light brown. The alkyne (1.2 equiv, 0.6 mmol), aldehyde (1.0 equiv, 0.5 mmol), and di-tert-butyl(methyl)silane (2.0 equiv, 1 mmol) were combined together with 2 mL of THF and the mixture was added over the course of 60 minutes using a syringe pump at rt. The reaction mixture was allowed to stir until starting materials were consumed. The reaction mixture was filtered through silica gel eluting with 50 % v/v EtOAc/hexanes. The solvent was removed *in vacuo*, and the crude residue was purified via flash chromatography on silica gel to afford the desired product.

(E)-((1,2-diphenylbut-2-en-1-yl)oxy)triisopropylsilane

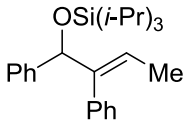

Table 2.6, Entry 1: Following a modified procedure B, $Ni(COD)_2$ (16.5 mg, 0.06 mmol), SIPr·HCl salt (21.3 mg, 0.05 mmol), and *t*-BuOK (5.6 mg, 0.05 mmol) were dissolved in 38 mL THF. Triisopropylsilane (158 mg, 1 mmol), prop-1-yn-1-ylbenzene (58 mg, 0.5 mmol), benzaldehyde (53 mg, 0.5 mmol) were combined with 2 mL THF and added to the reaction over 1 hour. This gave a crude residue which was purified via flash chromatography (100 % hexanes) to afford a single regioisomer in a >98:2 isolated regioselectivity (>98:2 crude regioselectivity) (157 mg, 0.41 mmol, 82 % yield).

Spectra data as previously reported[28]

(E)-((1-(4-fluorophenyl)-2-phenylbut-2-en-1-yl)oxy)triisopropylsilane.

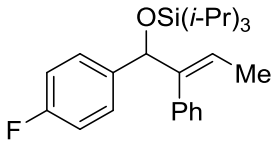

Table 2.6, Entry 2: Following Procedure A, $Ni(COD)_2$ (16.5 mg, 0.06 mmol), SIPr·HCl salt (21.3 mg, 0.05 mmol), *t*-BuOK (5.6 mg, 0.05 mmol), triisopropylsilane (158 mg, 1 mmol), prop-1-yn-1-ylbenzene (58 mg, 0.5 mmol), 4-fluorobenzaldehyde (62 mg, 0.5 mmol) gave a crude residue which was purified via flash chromatography (100 % hexanes) to afford a single regioisomer in a >98:2 isolated regioselectivity (93:7 crude regioselectivity) (169 mg, 0.43 mmol, 85 % yield).

^{1}H NMR (700 MHz, $CDCl_3$) δ 7.18-7.14 (m, 3H), 7.04-7.00 (m, 2H), 6.84-6.80 (m, 2H), 6.79-6.76 (m, 2H), 6.03 (qd, *J* = 7.0 Hz, 0.7 Hz, 1H), 5.36 (s, 1H), 1.49 (dd, *J* = 7.0 Hz, 0.7 Hz, 3H), 1.13-1.07 (m, 3H), 1.02 (d, *J* = 7.0 Hz, 9H), 0.97 (d, *J* = 7.7 Hz, 9H)

^{13}C NMR (175 MHz, $CDCl_3$): δ 161.6 (d, *J* = 242.6 Hz), 144.7, 139.5 (d, *J* = 2.8 Hz), 138.0, 129.6, 128.0 (d, *J* = 8.1 Hz), 127.5, 126.5, 121.2, 114.3 (d, *J* = 21.0 Hz), 78.7, 18.02, 17.95, 14.1, 12.3

IR (film, cm^{-1}): 2943, 2865, 1602, 1506, 1463

HRMS (EI) (m/z): [M-^{i}Pr]$^{+}$ calcd for $C_{22}H_{28}FOSi$ 355.1893; found 355.1888

(E)-triisopropyl((3-phenylundec-2-en-4-yl)oxy)silane. *Major Regioiosmer*

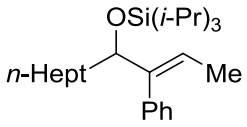

Table 2.6, Entry 3: Following Procedure A, Ni(COD)$_2$ (16.5 mg, 0.06 mmol), SIPr·HCl salt (21.3 mg, 0.05 mmol), *t*-BuOK (5.6 mg, 0.05 mmol), triisopropylsilane (158 mg, 1 mmol), prop-1-yn-1-ylbenzene (58 mg, 0.5 mmol), octanal (64 mg, 0.5 mmol) gave a crude residue which was purified via flash chromatography (100 % hexanes) to afford a single regioisomer in a >98:2 isolated regioselectivity (>98:2 crude regioselectivity) (156 mg, 0.39 mmol, 77 % yield).

^{1}H NMR (500 MHz, $CDCl_3$) δ 7.32-7.28 (m, 2H), 7.24-7.20 (m, 1H), 7.18-7.12 (m, 2H), 5.76 (q, *J* = 7.0 Hz, 1H), 4.45 (t, *J* = 5.0 Hz, 1H), 1.54 (d, *J* = 7.0 Hz, 3H), 1.43-1.04 (m, 33H), 0.84 (t, *J* = 7.0 Hz, 3 H)

^{13}C NMR (125 MHz, $CDCl_3$): δ 143.2, 138.9, 129.3, 127.8, 126.4, 122.6, 77.3 35.7, 31.8, 29.6, 29.2, 23.9, 22.6, 18.20, 18.18, 14.13, 14.08, 12.5

IR (film, cm^{-1}): 2925, 2864, 1493, 1463, 1382

HRMS (EI) (m/z): [M-^{i}Pr]$^{+}$ calcd for$C_{23}H_{39}OSi$ 359.2770; found 359.2772

(E)-((1-cyclohexyl-2-phenylbut-2-en-1-yl)oxy)triisopropylsilane.

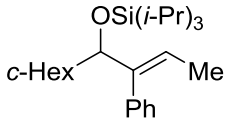

Table 2.6, Entry 4: Following Procedure A, Ni(COD)$_2$ (16.5 mg, 0.06 mmol), SIPr·HCl salt (21.3 mg, 0.05 mmol), *t*-BuOK (5.6 mg, 0.05 mmol), triisopropylsilane (158 mg, 1 mmol), prop-1-yn-1-ylbenzene (58 mg, 0.5 mmol), cyclohexanecarbaldehyde (56 mg, 0.5 mmol) gave a crude residue which was purified via flash chromatography (100 % hexanes) to afford a single

regioisomer in a >98:2 isolated regioselectivity (>98:2 crude regioselectivity) (174 mg, 0.45 mmol, 90 % yield).

^{1}H NMR (500 MHz, $CDCl_3$) δ 7.32-7.28 (m, 2H), 7.24-7.18 (m, 3H), 5.74 (q, *J* = 7.0 Hz, 1H), 4.30 (d, *J* = 4.5 Hz, 1H), 1.70-1.47 (m, 8H), 1.25-0.86 (m, 27 H)

^{13}C NMR (175 MHz, $CDCl_3$): δ 142.2, 139.5, 129.3, 127.8, 126.4, 123.1, 81.6, 42.5, 30.0, 27.2, 26.7, 26.5, 26.4, 18.4, 18.3, 14.2, 12.9

IR (film, cm^{-1}): 2924, 2864, 1492, 1449, 1387

HRMS (EI) (*m/z*): $[M]^+$ calcd for $C_{25}H_{42}OSi$ 386.3005; found 386.2996

(E)-((2-isobutyl-1-phenylpent-2-en-1-yl)oxy)triisopropylsilane Major Regioisomer

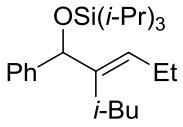

(E)-((2-ethyl-5-methyl-1-phenylhex-2-en-1-yl)oxy)triisopropylsilane Minor regioisomer

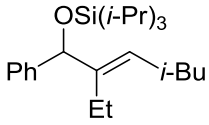

Table 2.6, Entry 5: Following Procedure A, $Ni(COD)_2$ (16.5 mg, 0.06 mmol), SIPr·HCl salt (21.3 mg, 0.05 mmol), *t*-BuOK (5.6 mg, 0.05 mmol), triisopropylsilane (158 mg, 1 mmol), 6-methylhept-3-yne (55 mg, 0.5 mmol), benzaldehyde (53 mg, 0.5 mmol) gave a crude residue which was purified via flash chromatography (100 % hexanes) to afford a mixture of regioisomers in a 95:5 regioselectivity (94:6 crude regioselectivity) (161 mg, 0.43 mmol, 86 % yield).

^{1}H NMR (700 MHz, $CDCl_3$) δ 7.33-7.30 (m, 2 H), 7.26-7.22 (m, 2 H), 7.19-7.15 (m, 1 H), 5.79 (t, *J* = 7 Hz, 1 H), 5.14 (s, 1 H), 2.09-1.99 (m, 2 H), 1.78 (dd, *J* = 14, 8.4 Hz, 1 H), 1.66 (dd, *J* = 14 Hz, 6.3 Hz, 1 H), 1.57-1.51 (m, 1 H), 1.1-1.03 (m, 3 H), 1.02-0.94 (m, 21 H), 0.75 (d, *J* = 6.3 Hz, 3 H), 0.72 (d, J = 6.3 Hz, 3 H)

^{13}C NMR (175 MHz, $CDCl_3$): δ 144.8, 139.6, 128.3, 127.6, 126.6, 126.5, 78.9, 36.1, 27.4, 23.2, 22.3, 21.2, 18.04, 17.97, 14.3, 12.3

IR (film, cm^{-1}): 2945, 2866, 1463

HRMS (EI) (*m/z*): $[M]^+$ calcd for $C_{24}H_{42}OSi$ 374.3005; found 374.2991

Characteristic ^{1}H NMR of minor isomer: 5.64 (t, *J* = 7.7 Hz, 1 H), 5.17 (s, 1 H)

(E)-((4-isobutyldodec-3-en-5-yl)oxy)triisopropylsilane Major regioiosmer

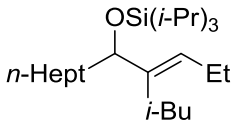

(E)-((5-ethyl-2-methyltridec-4-en-6-yl)oxy)triisopropylsilane Minor regioisomer

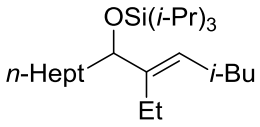

Table 2.6, Entry 6: Following Procedure A, $Ni(COD)_2$ (16.5 mg, 0.06 mmol), SIPr·HCl salt (21.3 mg, 0.05 mmol), *t*-BuOK (5.6 mg, 0.05 mmol), triisopropylsilane (158 mg, 1 mmol), 6-methylhept-3-yne (55 mg, 0.5 mmol), octanal (64 mg, 0.5 mmol) gave a crude residue which was purified via flash chromatography (100 % hexanes) to afford a mixture of regioisomers in 94:6 regioselectivity (96:4 crude regioselectivity) (132 mg, 0.33 mmol, 66 % yield).

^{1}H NMR (700 MHz, $CDCl_3$) δ 5.40 (t, *J* = 7.0 Hz, 1 H), 4.13 (t, *J* = 4.0 Hz, 1 H), 2.07-1.97 (m, 2 H), 1.89 (dd, *J* = 14.0, 8.4 Hz, 1 Hz), 1.84 (dd, *J* = 14.0, 6.3 Hz, 1 H), 1.80-1.74 (m, 1 H), 1.62-1.46 (m, 2 H), 1.31-1.10 (m, 10 H), 1.08-1.00 (m, 21 H), 0.91 (t, *J* = 7 Hz, 3 H), 0.87 (d, *J* = 6.3 Hz, 3 H), 0.85 (t, *J* = 7.0 Hz, 3 H), 0.84 (d, *J* = 7 Hz, 3 H)

^{13}C NMR (125 MHz, $CDCl_3$): δ 138.3, 129.3, 76.96, 36.6, 36.5, 31.8, 29.7, 29.3, 27.8, 24.5, 23.3, 22.7, 22.6, 21.2, 18.17, 18.15, 14.3, 14.1, 12.5

IR (film, cm^{-1}): 2926, 2865, 1463

HRMS (EI) (*m/z*): $[M\text{-}iPr]^+$ calcd for $C_{22}H_{45}OSi$ 353.3240; found 353.3233

Characteristic ^{1}H NMR of minor isomer: 5.24 (t, *J* = 7.7 Hz, 1 H), 4.09 (t, *J* = 6.3 Hz, 1 H)

(E)-1-phenyl-2-propylpent-2-en-1-ol Major regioisomer

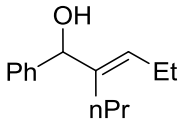

(E)-2-ethyl-1-phenylhex-2-en-1-ol Minor regioisomer

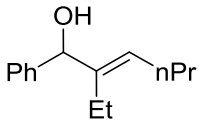

Table 2.6, Entry 7: Following Procedure A, $Ni(COD)_2$ (16.5 mg, 0.06 mmol), SIPr·HCl salt (21.3 mg, 0.05 mmol), *t*-BuOK (5.6 mg, 0.05 mmol), triisopropylsilane (158 mg, 1 mmol), hept-3-yne (48 mg, 0.5 mmol), benzaldehyde (53 mg, 0.5 mmol) gave a crude residue which was purified via flash chromatography (100 % hexanes) to afford a mixture of regioisomers in a 68:32 regioselectivity (68:32 crude regioselectivity). The product was subjected to tetra-*n*-butylammonium fluoride deprotection for characterization purposes. (57 mg, 0.28 mmol, 56 % yield). Spectral data is provided for the mixture of regioisomers.

^{1}H NMR (700 MHz, $CDCl_3$): 7.36-7.33 (m, 2.8 H), 7.32-7.29 (m, 2.9 H), 7.25-7.24 (m, 0.6 H), 7.23-7.22 (m, 0.3 H), 5.59 (t, *J* = 7 Hz, 1 H), 5.58 (t, *J* = 7 Hz, 0.44 H), 5.15 (d, *J* = 2.1 Hz, 0.47 H), 5.13 (d, *J* = 2.1 Hz, 1 H), 2.11-2.03 (m, 3 H), 2.00 (dd, *J* = 14, 7.7 Hz, 0.5 H), 1.98-1.93 (m, 1.16 H), 1.91-1.85 (m, 0.56 H), 1.84-1.79 (m 1.1 H), 1.75 (br s, 1.35 H), 1.42 (sex, 7.7 Hz, 1 H), 1.30-1.23 (m , 1.32 H), 1.22-1.15 (m, 1.15 H), 0.995 (t = 7.7 Hz, 3 H), 0.92 (t, *J* = 7.7 Hz, 1.65 H), 0.82 (t, *J* = 7.7 Hz, 1.65 H), 0.80 (t, *J* = 7 Hz, 3 H)

^{13}C NMR (175 MHz, $CDCl_3$): 142.79, 142.78, 142.75, 140.6, 129.1, 128.2, 127.3, 127.3, 126.8, 126.54, 126.53, 78.2, 78.1, 29.9, 29.5, 22.9, 22.8, 21.0, 20.6, 14.41, 14.36, 14.15, 13.95

IR (film, cm^{-1}): 3362, 2958, 2930, 2869, 1492, 1451

HRMS (EI) (*m/z*): calcd for $C_{14}H_{20}O$ 204.1514; found 204.1516

(E)-3-(phenyl((triisopropylsilyl)oxy)methyl)hex-2-en-1-ol Major Regioisomer

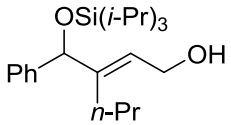

Table 2.6, Entry 8: Following a modified procedure A, $Ni(COD)_2$ (16.5 mg, 0.06 mmol), SIPr·HCl salt (21.3 mg, 0.05 mmol),PPh_3 (15.7 mg, 0.06 mmol), *t*-BuOK (5.6 mg, 0.05 mmol) were dissolved in 2 mL 1,4-dioxane and stirred for 10 min at rt and then heated to 90 °C. Triisopropylsilane (158 mg, 1 mmol), hex-2-yn-1-ol (74 mg, 0.75 mmol), benzaldehyde (53 mg, 0.5 mmol) were dissolved in 2 mL 1,4-dioxane and added to the reaction over 60 minutes. This gave a crude residue which was purified via flash chromatography (10 % EtOAC in hexanes) to afford two regioisomers in a 90:10 regioselectivity (89:11 crude regioselectivity) (107 mg, 0.296 mmol, 59 % yield): Major (97 mg, 0.27 mmol), Minor (10 mg, 0.03 mmol)

^{1}H NMR (700 MHz, $CDCl_3$) δ 7.34-7.32 (m, 2 H), 7.27-7.24 (m, 2 H), 7.21-7.18 (m, 1 H), 5.95 (t, *J* = 7 Hz, 1 H), 5.16 (s, 1 H), 4.23-4.16 (m, 2 H), 1.92 (ddd, J= 13.5, 10.3, 6.3 Hz, 1 H), 1.82 (ddd, *J* = 13.5, 10.3, 5.6 Hz, 1 H), 1.18-1.04 (m, 6 H), 1.00 (d, *J* = 7.7 Hz, 9 H), 0.96 (d, *J* = 7.7 Hz, 9 H), 0.76 (t, *J* = 7 Hz, 3 H)

^{13}C NMR (175 MHz, $CDCl_3$): δ 145.6, 143.7, 127.8, 127.0, 126.4, 123.8, 78.3, 59.4, 29.3, 23.1, 18.05, 17.97, 14.4, 12.2

IR (film, cm^{-1}): 3298, 2944, 2867, 1464

HRMS (EI) (*m/z*): $[M\text{-}iPr]^+$ calcd for $C_{19}H_{31}O_2Si$ 319.2093, found 319.2079

(E)-2-(phenyl((triisopropylsilyl)oxy)methyl)hex-2-en-1-ol Minor Regioisomer

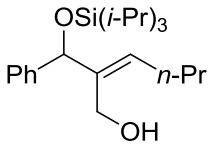

^{1}H NMR (500 MHz, $CDCl_3$) δ 7.40-7.36 (m, 2 H), 7.32-7.27 (m, 2 H), 7.23-7.19 (m, 1H), 5.72 (t, *J* = 7.5 Hz, 1 H), 5.37 (s, 1 H), 4.09 (dd, *J* = 12, 6.5 Hz, 1 H), 3.95 (d, *J* = 12 Hz, 1 H), 2.33 (m, 1 H), 2.14 (dq, *J* = 14.5, 8 Hz, 1 H), 2.04 (dq, *J* = 14.5, 7 Hz, 1 H), 1.46-1.37 (m, 2 H), 1.16-1.06 (m, 3 H), 1.02 (d, *J* = 7 Hz, 9 H), 0.99 (d, *J* = 7 Hz, 9 H), 0.90 (t, *J* = 7 Hz, 3 H)

^{13}C NMR (125 MHz, $CDCl_3$): δ 143.2, 139.8, 131.0, 128.1, 127.1, 125.7, 81.0, 57.7, 29.5, 22.8, 17.99, 17.96, 13.8, 12.1

IR (film, cm^{-1}): 3401, 2944, 2866, 1464

HRMS (EI) (*m/z*): $[M\text{-}iPr]^+$ calcd for $C_{19}H_{31}O_2Si$ 319.2093, found 319.2098

(E)-((2-ethylidene-1-(furan-2-yl)pentyl)oxy)triisopropylsilane Major regioisomer

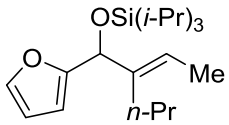

(E)-((1-(furan-2-yl)-2-methylhex-2-en-1-yl)oxy)triisopropylsilane Minor regioisomer

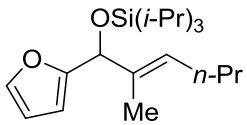

Table 2.6, Entry 9: Following Procedure A, $Ni(COD)_2$ (16.5 mg, 0.06 mmol), SIPr·HCl salt (21.3 mg, 0.05 mmol), ^{t}BuOK (5.6 mg, 0.1 mmol), triisopropylsilane (158 mg, 1 mmol), 2-hexyne (41 mg, 0.5 mmol),2-furancarboxaldehyde (48 mg, 0.5 mmol) gave a crude residue which was purified via flash chromatography (100 % hexanes) to afford a mixture of regioisomers in 92:8 regioselectivity (93:7 crude regioselectivity) (128 mg, 0.38 mmol, 76 % yield).

^{1}H NMR (700 MHz, $CDCl_3$) δ 7.28 (dd, *J* = 1.4, 0.7 Hz, 1 H), 6.27 (dd, *J* = 3.5, 1.4 Hz, 1 H), 6.19-6.18 (m, 1 H), 5.73 (q, *J* =7.0 Hz, 1 H), 5.14 (s, 1H), 1.97 (ddd, *J* = 13.3, 10.5, 6.3 Hz, 1 H), 1.87 (ddd, *J* = 13.7, 10.5, 5.6, 1 H) (m, 1 H), 1.64 (d, *J* = 7.0 Hz, 3H), 1.22-1.16 (m, 1 H), 1.13-1.03 (m, 4H), 1.01 (d, *J* = 7.7 Hz, 9H), 0.99 (d, *J* = 7.0 Hz, 9 H), 0.80 (t, *J* = 7.0 Hz, 3 Hz)

^{13}C NMR (175 MHz, $CDCl_3$): δ 156.9, 141.0, 140.4, 121.2, 110.0, 105.9, 73.3, 29.1, 21.9, 18.0, 17.9, 14.5, 13.1, 12.3

IR (film, cm^{-1}): 2943, 2866, 1464

HRMS (ESI+) (*m/z*): $[M+H]^+$ calcd for$C_{20}H_{40}O_2Si$ 337.2557; found 337.2549

Characteristic ^{1}H NMR of minor isomer: 5.58 (t, *J* = 7 Hz, 1 H), 5.13 (s, 1 H), 0.89 (t, *J* = 7.0 Hz, 3 H)

(E)-triisopropyl((2-isopropyl-1-phenylbut-2-en-1-yl)oxy)silane

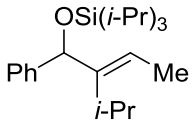

Table 2.6, Entry 11: Following Procedure A, Ni(COD)$_2$ (16.5 mg, 0.06 mmol), SIPr·HCl salt (21.3 mg, 0.05 mmol), *t*-BuOK (5.6 mg, 0.05 mmol), triisopropylsilane (158 mg, 1 mmol), 4-methylpent-2-yne (41 mg, 0.5 mmol), benzaldehyde (53 mg, 0.5 mmol) gave a crude residue which was purified via flash chromatography (100 % hexanes) to afford a single regioisomer in a >98:2 isolated regioselectivity (>98:2 crude regioselectivity) (135 mg, 0.39 mmol, 78 % yield).

Spectral data as previously reported[28]

(E)-((1-cyclohexyl-2-isopropylbut-2-en-1-yl)oxy)triisopropylsilane

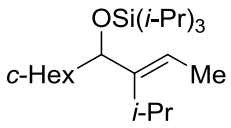

Table 2.6, Entry 12: Following Procedure A, Ni(COD)$_2$ (16.5 mg, 0.06 mmol), SIPr·HCl salt (21.3 mg, 0.05 mmol), *t*-BuOK (5.6 mg, 0.05 mmol), triisopropylsilane (158 mg, 1 mmol), 4-methylpent-2-yne (41 mg, 0.5 mmol), cyclohexanecarbaldehyde (56 mg, 0.5 mmol) gave a crude residue which was purified via flash chromatography (100 % hexanes) to afford a single regioisomer in a >98:2 isolated regioselectivity (>98:2 crude regioselectivity) (133 mg, 0.38 mmol, 75 % yield).

^{1}H NMR (500 MHz, $CDCl_3$) δ 5.31 (q, *J* = 7 Hz, 1H), 3.93 (d, *J* = 5 Hz, 1 H), 2.46 (sept, *J* = 7 Hz, 1H), 1.75-1.68 (m, 3H), 1.66 (d, *J* = 7.0 Hz), 1.64-1.57 (m, 2H), 1.34-0.88 (m, 33H)

^{13}C NMR (125 MHz, $CDCl_3$): δ 144.8, 120.3, 81.3, 42.9, 31.0, 28.0, 26.81, 26.78, 26.6, 21.4, 21.2, 18.4, 18.3, 13.5, 13.0

IR (film, cm^{-1}): 2925, 2865, 1464

HRMS (EI) (*m/z*): $[M]^+$ calcd for$C_{22}H_{44}OSi$ 352.3161; found 352.3151

Di-tert-butyl(methyl)(3-methyl-2-methylene-1-phenylbutoxy)silane

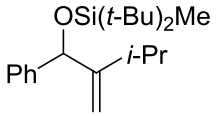

Table 2.8, Entry 1: Following Procedure B, $Ni(COD)_2$ (30.2 mg, 0.11 mmol), SIPr·HCl salt (42.6 mg, 0.1 mmol), *t*-BuOK (11.2 mg, 0.1 mmol), Di-t-butylmethylsilane (158 mg, 1 mmol), 3-methylbut-1-yne (41 mg, 0.6 mmol), benzaldehyde (53 mg, 0.5 mmol) gave a crude residue which was purified via flash chromatography (100 % hexanes) to afford a single regioisomer in a >98:2 isolated regioselectivity (>98:2 crude regioselectivity) (101 mg, 0.30 mmol, 61 % yield).

^{1}H NMR (700 MHz, $CDCl_3$) δ 7.32-7.30 (m, 2H), 7.27-7.24 (m, 2H), 7.20-7.17 (m, 1 H), 5.38 (s, 1 H), 5.16 (s, 1 H), 4.9 (s, 1 H), 2.04 (sept, *J* = 7.0 Hz, 1 H), 0.99 (s, 9 H), 0.89 (d, *J* = 7.0 Hz, 3 H), 0.84 (s, 9 H), 0.83 (d, *J* = 7 Hz, 3 H), -0.04 (s, 3 H)

^{13}C NMR (175 MHz, $CDCl_3$): δ 158.2, 143.6, 127.8, 126.98, 126.97, 106.6, 78.4, 28.8, 27.8, 27.6, 23.7, 22.3, 21.1, 20.5, -8.6

IR (film, cm^{-1}): 2960, 2857, 1471

HRMS (EI) (m/z): $[M-{}^tBu]^+$ calcd for $C_{17}H_{27}OSi$ 275.1813; found 275.1833

Di-tert-butyl(methyl)((2-methylene-1-phenyloctyl)oxy)silane

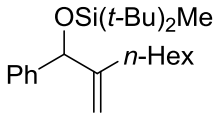

Table 4, Entry 2: Following Procedure B, $Ni(COD)_2$ (30.2 mg, 0.11 mmol), SIPr·HCl salt (42.6 mg, 0.1 mmol), *t*-BuOK (11.2 mg, 0.1 mmol), Di-t-butylmethylsilane (158 mg, 1 mmol), 1-octyne (66 mg, 0.6 mmol), benzaldehyde (53 mg, 0.5 mmol) gave a crude residue which was purified via flash chromatography (100 % hexanes) to give a mixture of regioisomers in 95:5 isolated regioselectivity (95:5 crude regioselectivity) (121 mg, 0.32 mmol, 65 % yield) Major (115 mg, 0.31 mmol), Minor (6 mg, 0.016 mmol)

^{1}H NMR (700 MHz, $CDCl_3$) δ 7.33-7.31 (m, 2 H), 7.28 (t, *J* = 7.7 Hz, 2 H), 7.21-7.18 (m, 1 H), 5.29 (s, 1 H), 5.15 (s, 1 H), 4.82 (d, *J* = 1.4 Hz, 1 H), 1.91 (dt, *J* =16.1, 7.7 Hz, 1 H), 1.70 (dt, *J* =16.1, 7.7 Hz, 1 H), 1.32-1.26 (m, 2 H), 1.26-1.13 (m, 6 H), 1.00 (s, 9 H), 0.87 (s, 9 H), 0.82 (t, *J* = 7 Hz, 3 H), -0.01 (s, 3 H)

^{13}C NMR (175 MHz, $CDCl_3$): δ 151.9, 143.6, 127.8, 126.8, 126.5, 108.8, 79.3, 31.7, 30.3, 29.1, 27.8, 27.7, 27.5, 22.5, 20.9, 20.7, 14.0, -8.7

IR (film, cm^{-1}): 2930, 2856, 1471

HRMS (EI) (*m/z*): $[M-{}^{t}Bu]^{+}$ calcd for$C_{20}H_{33}OSi$ 317.2301; found 317.2305

(E)-di-tert-butyl(methyl)((1-phenylnon-2-en-1-yl)oxy)silane

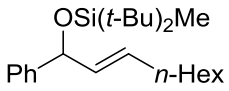

Kinetics experiments

Initial Rates using iPr_3SiH

Following a modified method A, $Ni(COD)_2$ (16.5 mg, 0.06 mmol), SIPr·HCl salt (21.3 mg, 0.05 mmol), and *t*-BuOK (5.6 mg, 0.05 mmol) were dissolved in 38 mL THF. The mixture was stirred for approximately 15 min until the solution turned light brown. Triisopropylsilane (2, 3 ,4, 6 equiv), prop-1-yn-1-ylbenzene (58 mg, 0.5 mmol), benzaldehyde (53 mg, 0.5 mmol), and octadecane (95 mg, 0.0375 mmol) were combined with THF to a total volume of 2 mL. This mixture was injected into the reaction as quickly as possible. Reaction aliquots (1.0 mL) were taken every 10 seconds, diluted in CH_2Cl_2 (0.8 mL), and shaken. Aliquots were then filtered through a pipette of silica gel. Samples were analyzed by GCFID and product concentration was determined using a calibration curve. The first 6 data points were used for initial rates.

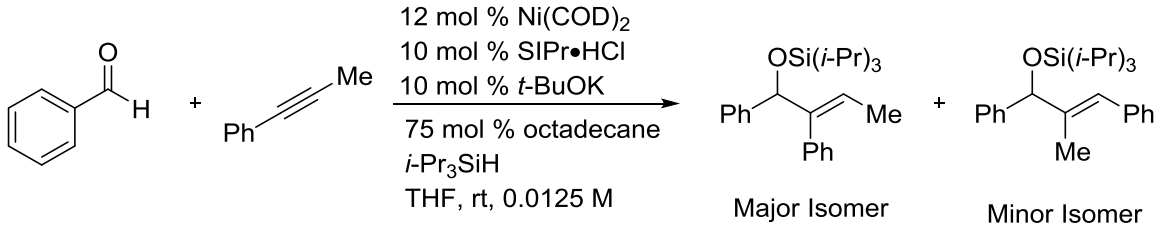

Example plot of reaction progression for both regioisomers using 2 equiv *i*-Pr_3SiH

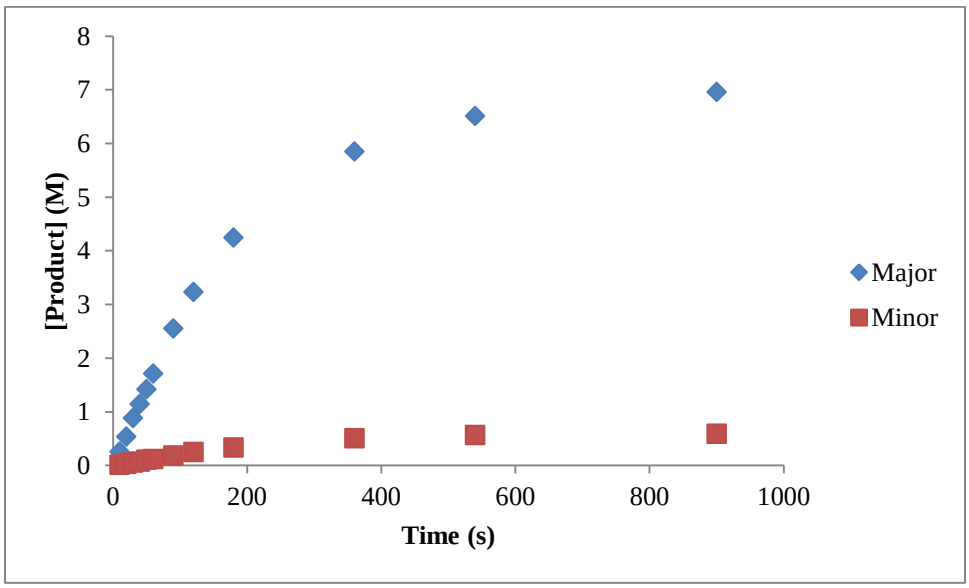

Initial rates of Major regioisomer

Equiv iPr3SiH	Δ[Major]/Δt (M/Sec)*10^{-5}	Avg. Δ[Major]/Δt	Std. Dev.
2	2.87	2.71	0.22
	2.48		
	2.91		
	2.56		
3	2.60	3.21	0.46
	3.11		
	3.61		
	3.51		
4	3.44	3.03	0.56
	2.47		
	2.64		
	3.57		
6	3.51	3.21	0.90
	4.33		
	2.67		
	2.32		

Initial rates of Minor regioisomer

Equiv iPr3SiH	Δ[Minor]/Δt (M/Sec)*10^{-5}	Avg. Δ[Minor]/Δt	Std. Dev.
2	0.206	0.207	0.016
	0.202		
	0.228		
	0.190		
3	0.251	0.332	0.058
	0.329		
	0.373		
	0.374		
4	0.457	0.405	0.058
	0.352		
	0.359		
	0.453		
6	0.638	0.582	0.156
	0.777		
	0.473		
	0.441		

2 equiv *i*-Pr_3SiH

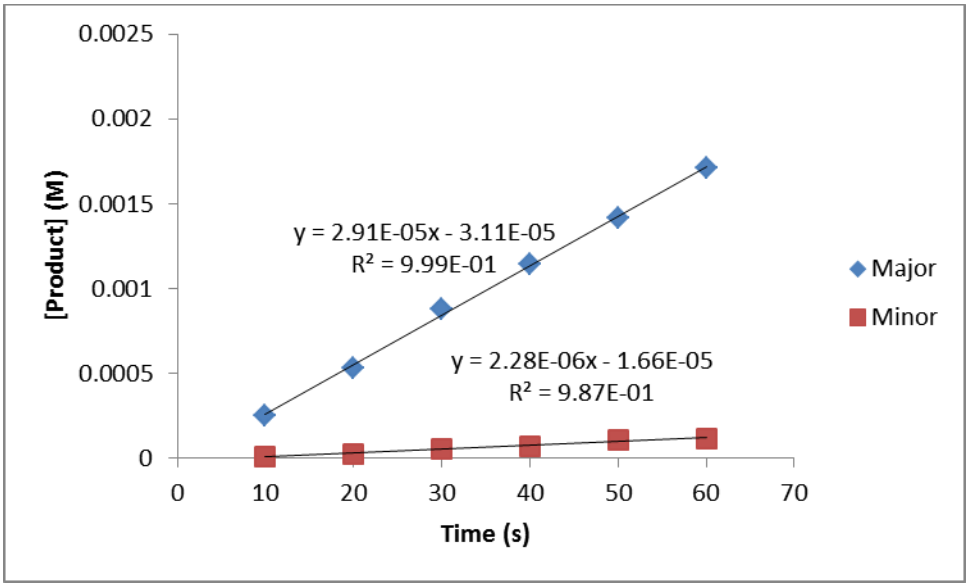

3 equiv *i*-Pr_3SiH

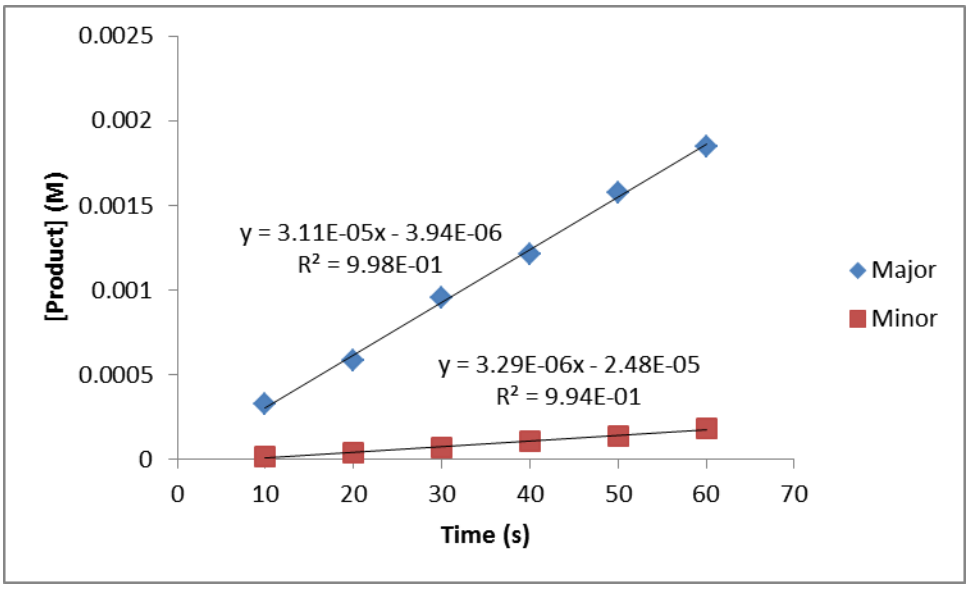

4 equiv *i*-Pr_3SiH

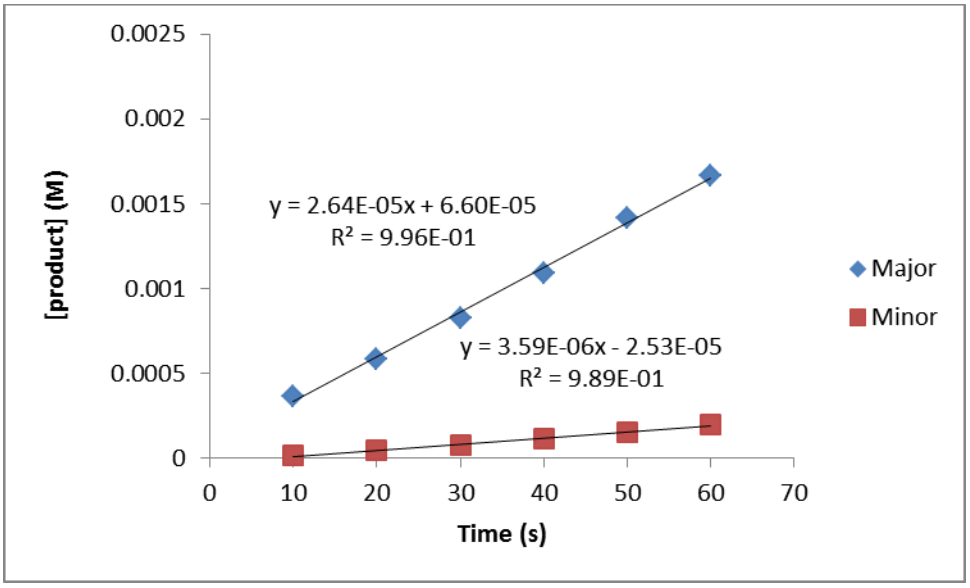

6 equiv *i*-Pr_3SiH

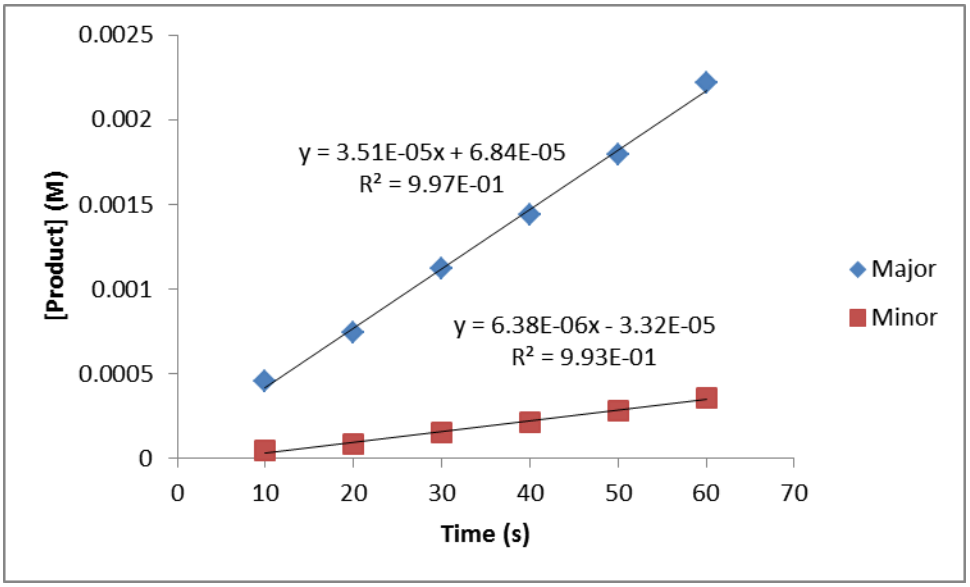

Initial Rates using Et_3SiH

Following a modified method A, $Ni(COD)_2$ (16.5 mg, 0.06 mmol), SIPr·HCl salt (21.3 mg, 0.05 mmol), and *t*-BuOK (5.6 mg, 0.05 mmol) were dissolved in 38 mL THF. The mixture was stirred for approximately 15 min until the solution turned light brown. Triethylsilane (2, 3 ,4, 6 equiv),

prop-1-yn-1-ylbenzene (58 mg, 0.5 mmol), benzaldehyde (53 mg, 0.5 mmol), and octadecane (95 mg, 0.0375 mmol) were combined with THF to a total volume of 2 mL. This mixture was injected into the reaction as quickly as possible. Reaction aliquots (1.0 mL) were taken every 10 seconds, diluted in CH_2Cl_2 (0.8 mL), and shaken. Aliquots were then filtered through a pipette of silica gel. Samples were analyzed by GCFID and product concentration was determined using a calibration curve. The first 6 data points were used for initial rates.

Initial rate major using Et_3SiH

Equiv Et3SiH	Δ[Major]/Δt (M/Sec)*10^{-5}	Avg. Δ[Major]/Δt	Std. Dev.
2	0.74	0.79	0.11
	0.92		
	0.72		
3	0.83	0.89	0.26
	1.17		
	0.67		
4	0.83	0.98	0.13
	1.09		
	1.01		
6	1.22	1.01	0.22
	0.78		
	1.03		

Initial rate minor using Et_3SiH

Equiv iPr3SiH	Δ[Minor]/Δt (M/Sec)*10^{-5}	Avg. Δ[Minor]/Δt	Std. Dev.
2	0.990	1.053	0.108
	1.178		
	0.990		
3	1.103	1.206	0.168
	1.400		
	1.115		
4	1.080	1.173	0.086
	1.250		
	1.188		
6	1.268	1.212	0.090
	1.108		
	1.260		

^{1}H and ^{13}C Spectra

Table 2.6, Entry 2 (E)-((1-(4-fluorophenyl)-2-phenylbut-2-en-1-yl)oxy)triisopropylsilane

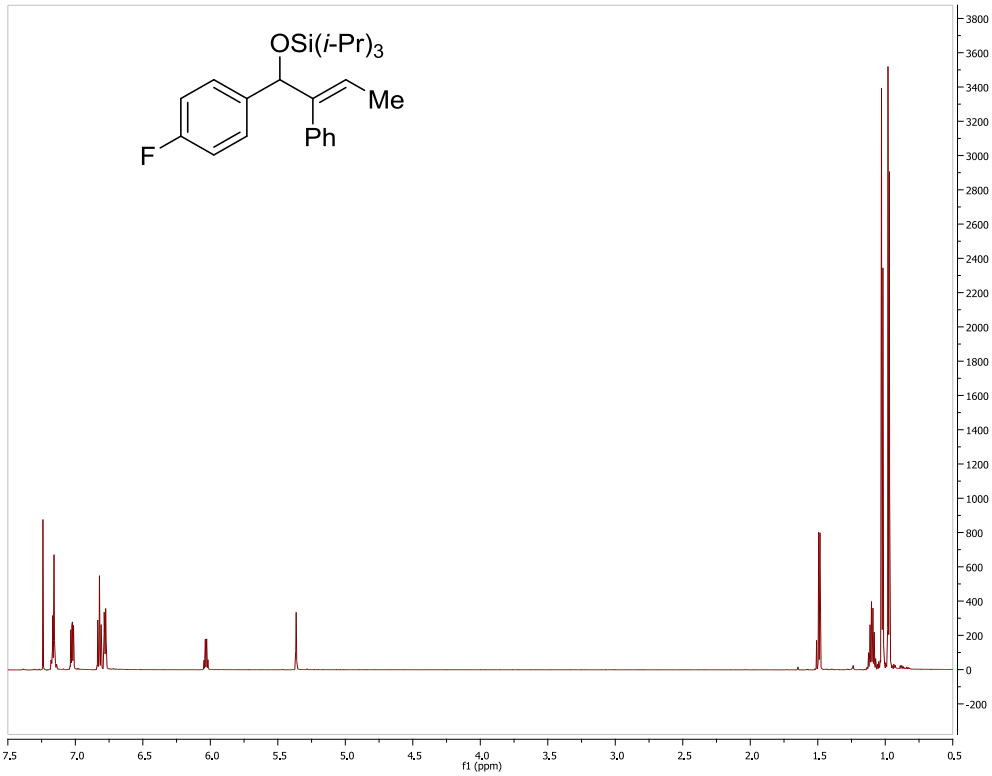

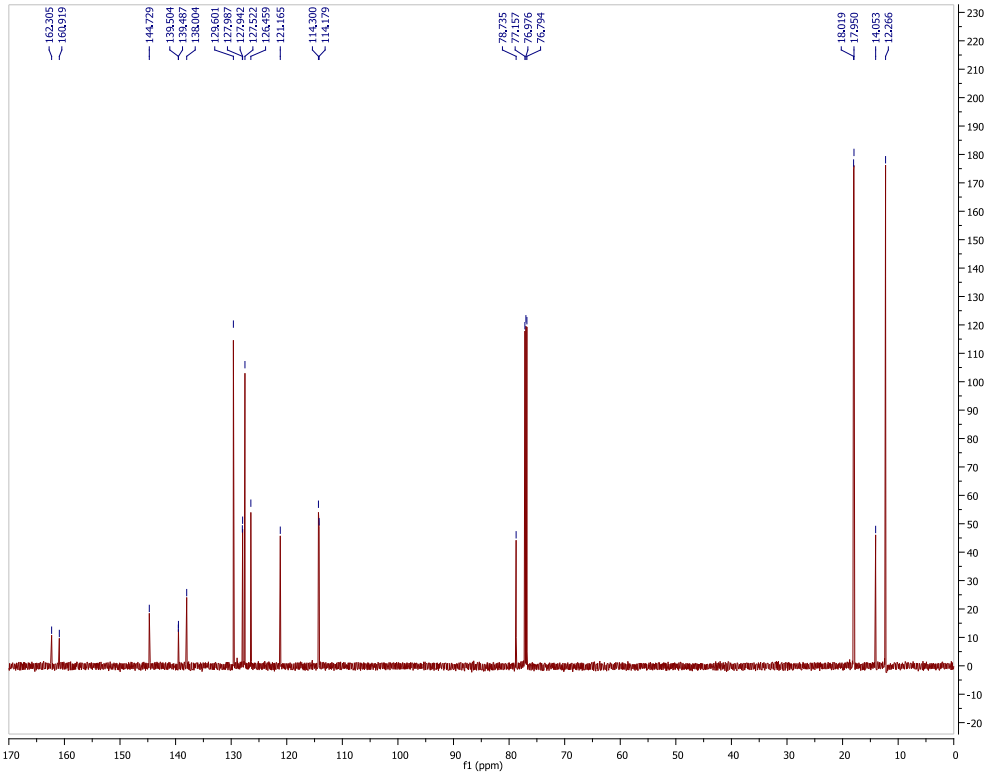

Table 2.6, Entry 3 (E)-triisopropyl((3-phenylundec-2-en-4-yl)oxy)silane

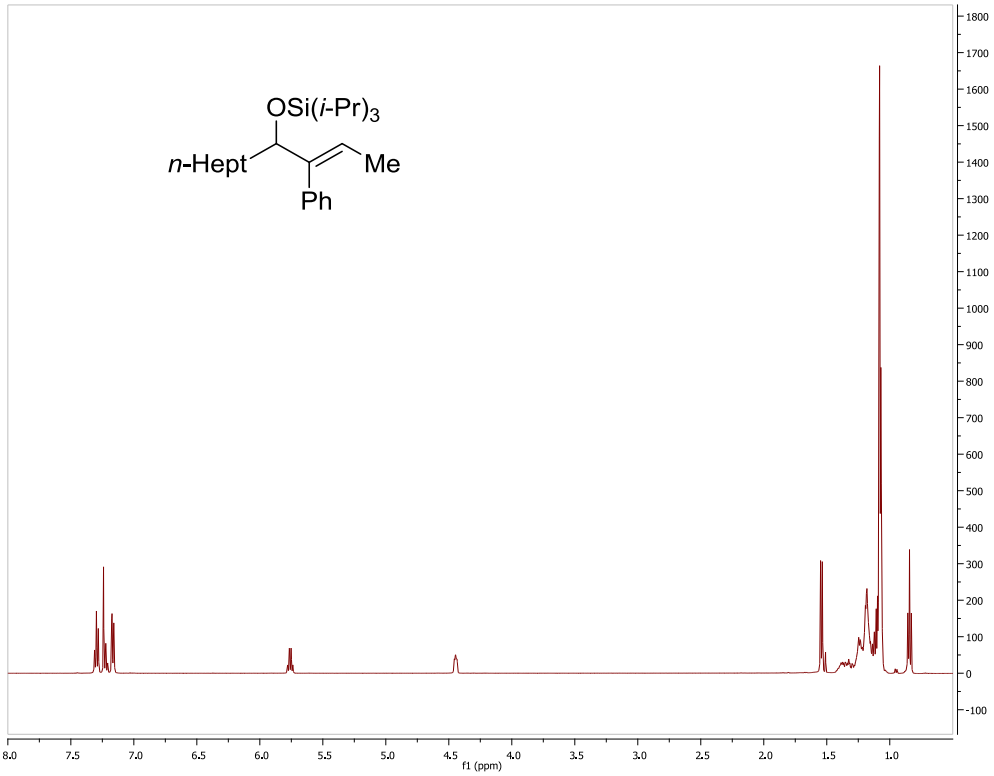

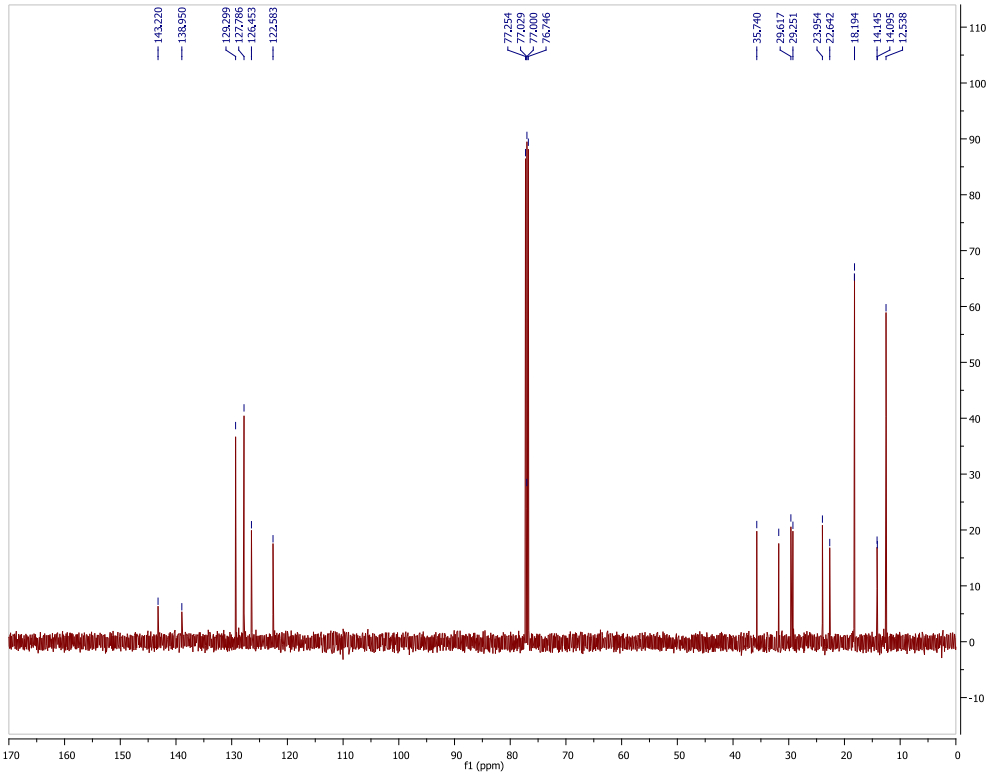

Table 2.6, Entry 4 (E)-((1-cyclohexyl-2-phenylbut-2-en-1-yl)oxy)triisopropylsilane

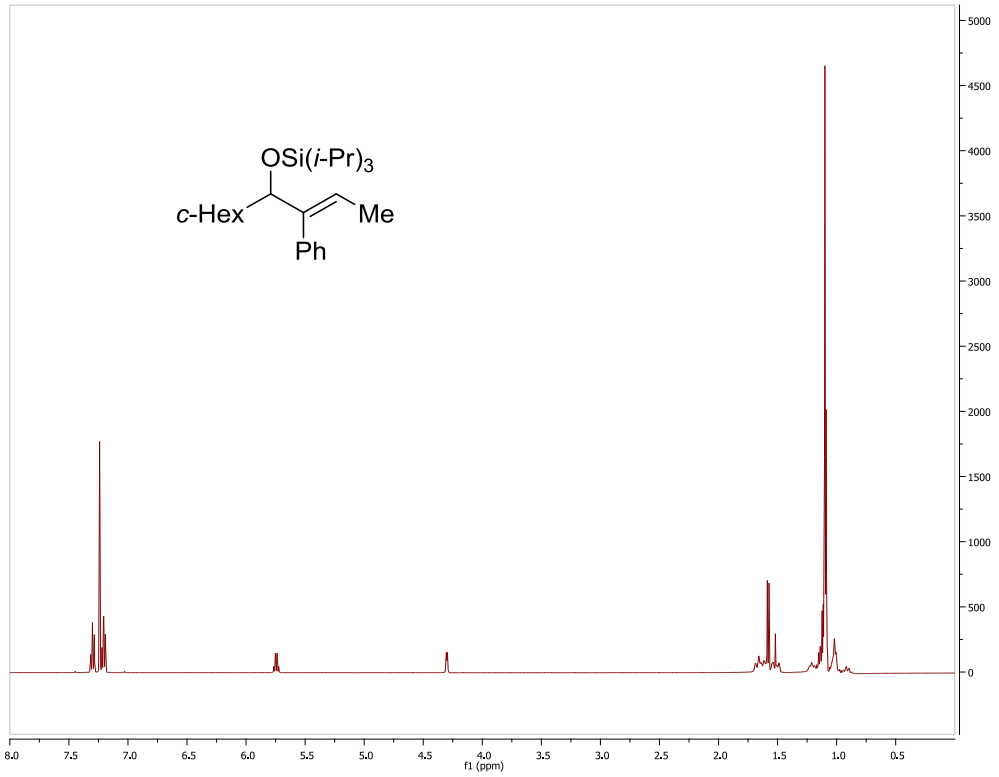

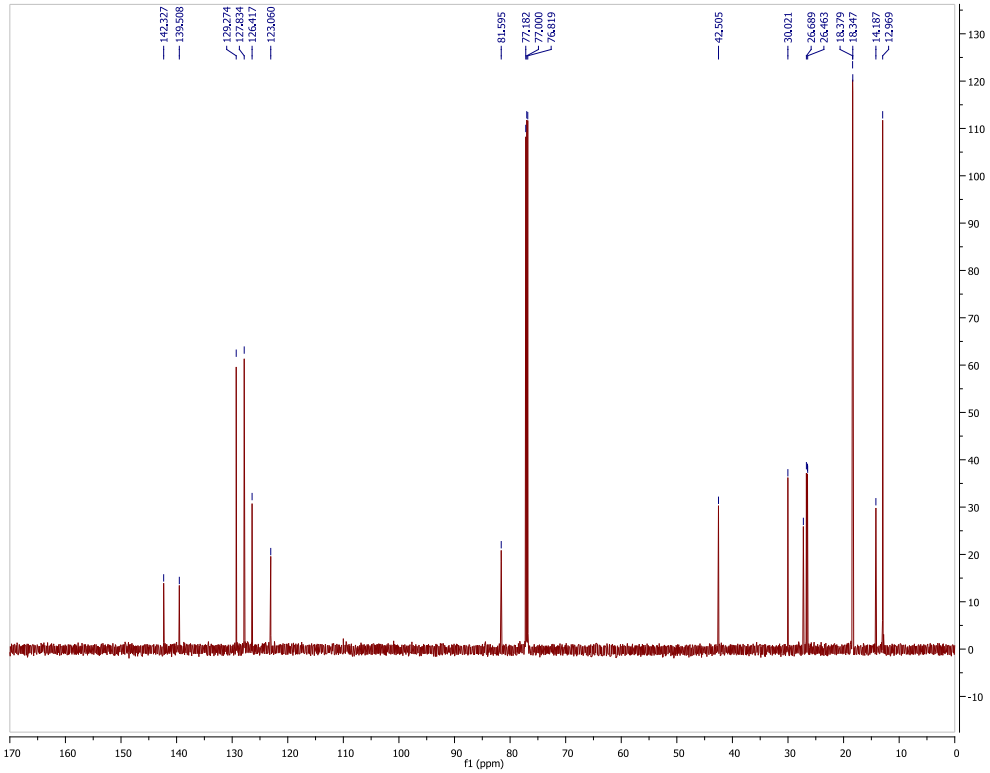

Table 2.6, Entry 5
Major isomer (E)-((2-isobutyl-1-phenylpent-2-en-1-yl)oxy)triisopropylsilane
Minor isomer (E)-((2-ethyl-5-methyl-1-phenylhex-2-en-1-yl)oxy)triisopropylsilane

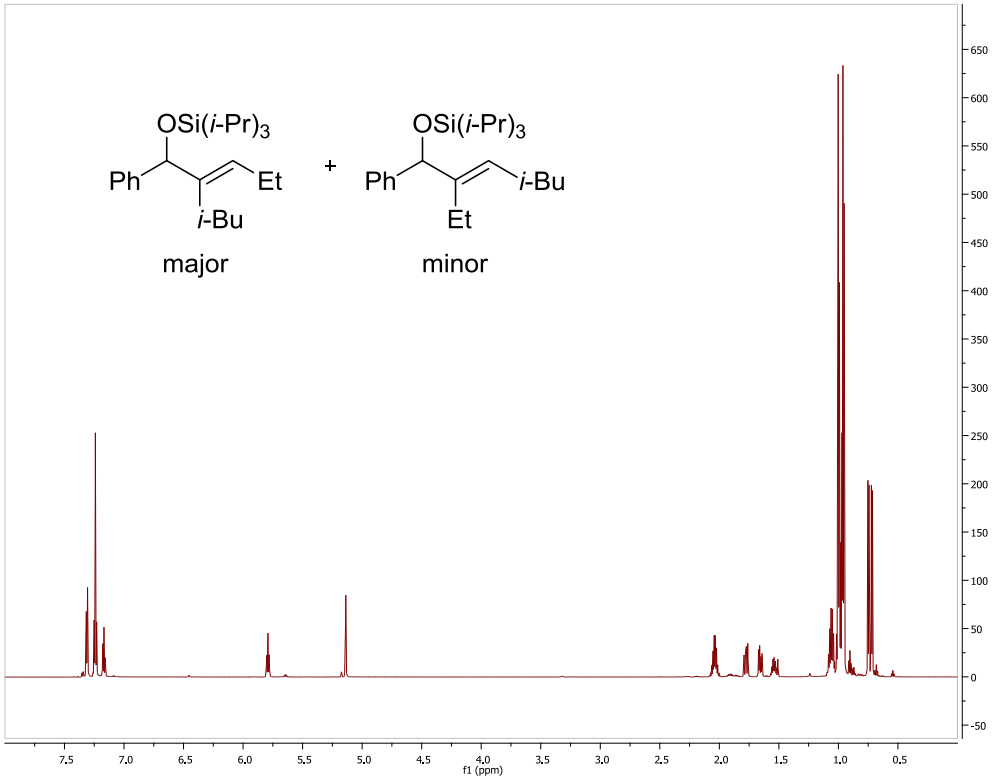

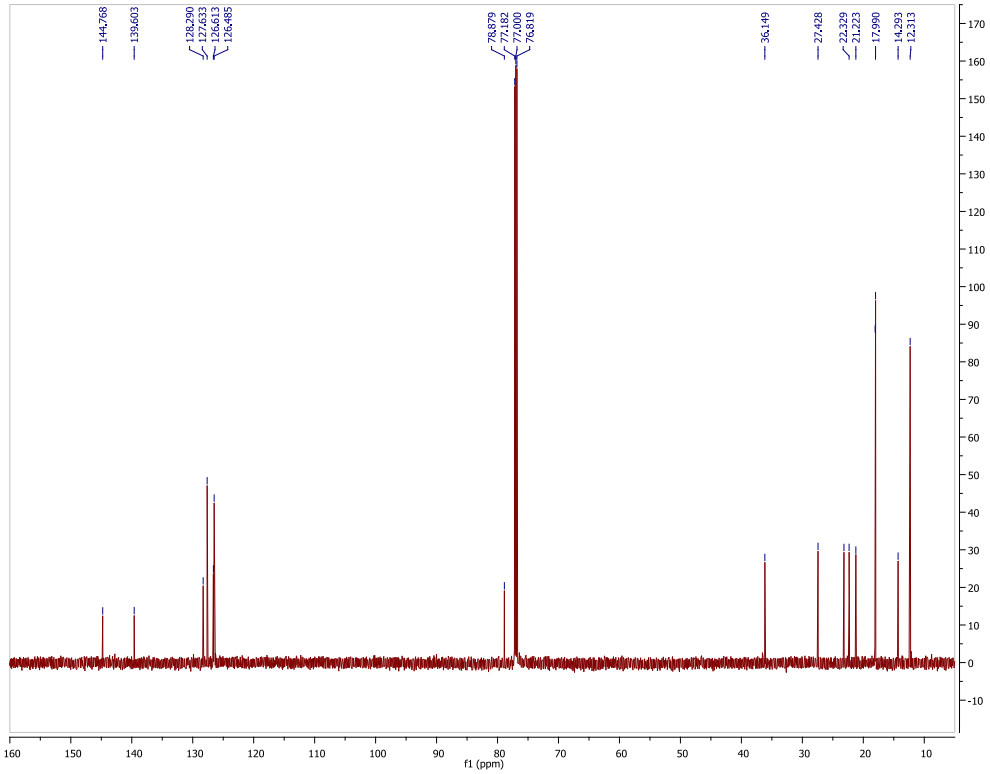

Table 2.6, Entry 6
Major regioisomer (E)-((4-isobutyldodec-3-en-5-yl)oxy)triisopropylsilane
Minor regioisomer (E)-((5-ethyl-2-methyltridec-4-en-6-yl)oxy)triisopropylsilane

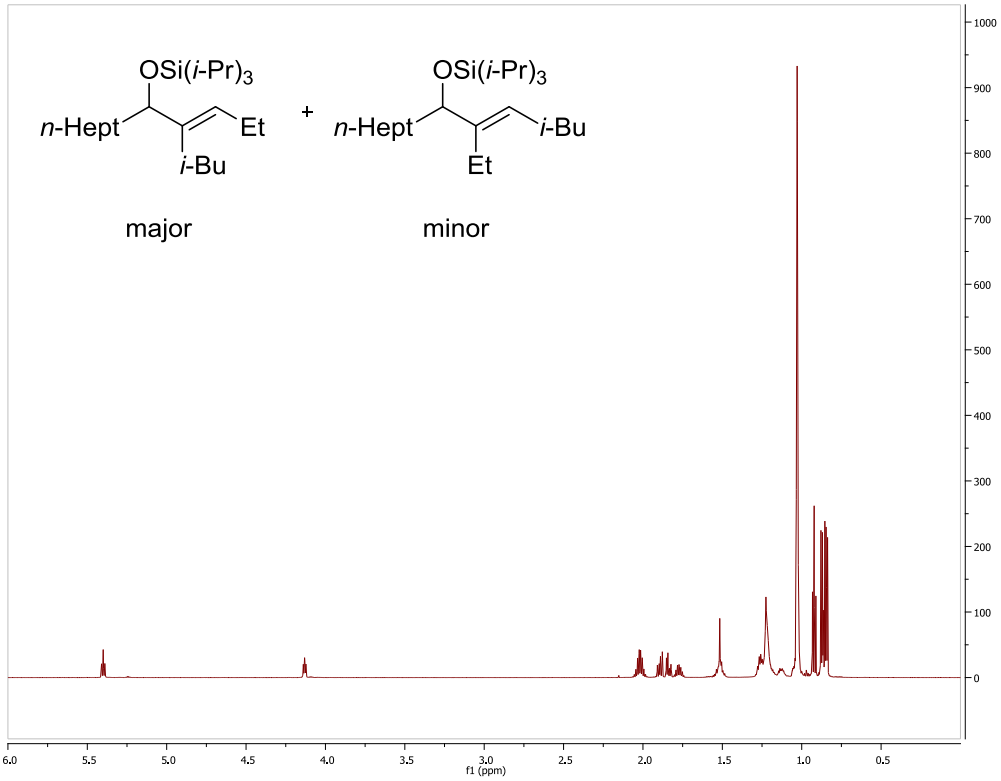

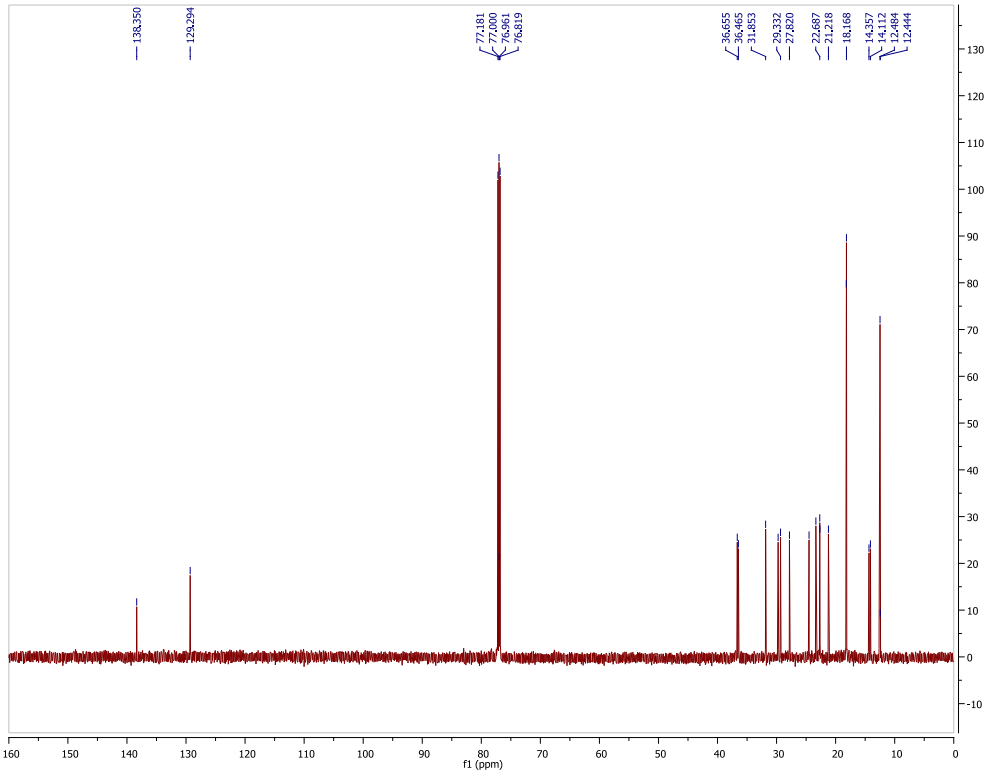

Table 2.6, Entry 7
Major regiosiomer (E)-1-phenyl-2-propylpent-2-en-1-ol
Minor regioisomer (E)-2-ethyl-1-phenylhex-2-en-1-ol

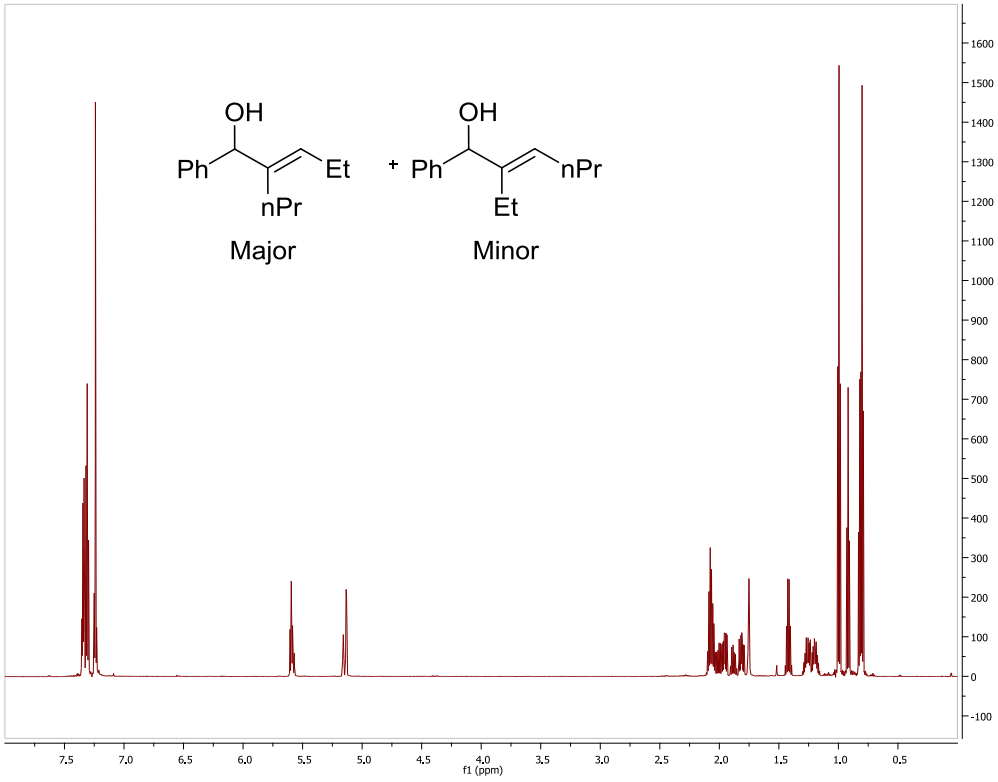

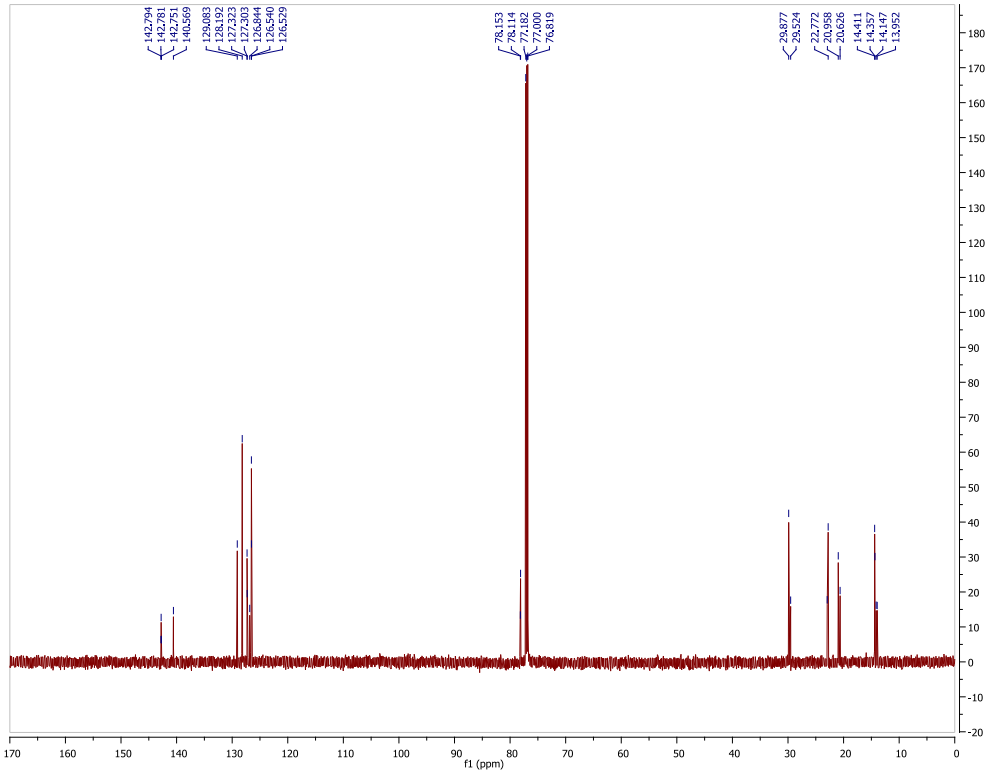

Table 2.6, Entry 8 (E)-3-(phenyl((triisopropylsilyl)oxy)methyl)hex-2-en-1-ol Major isomer

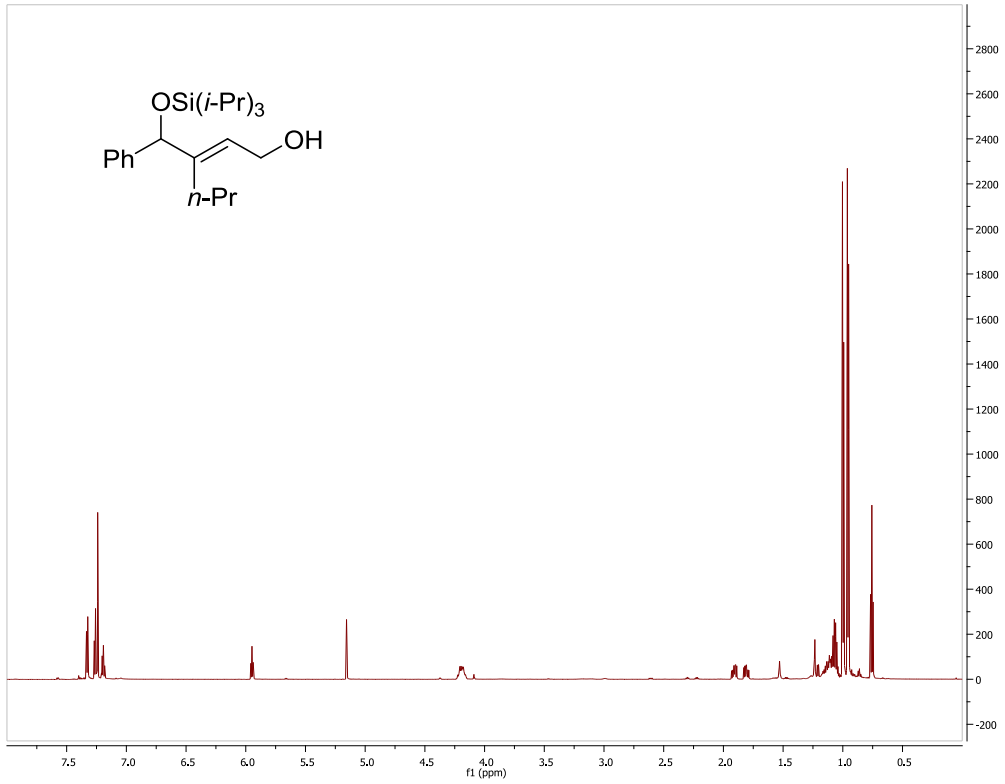

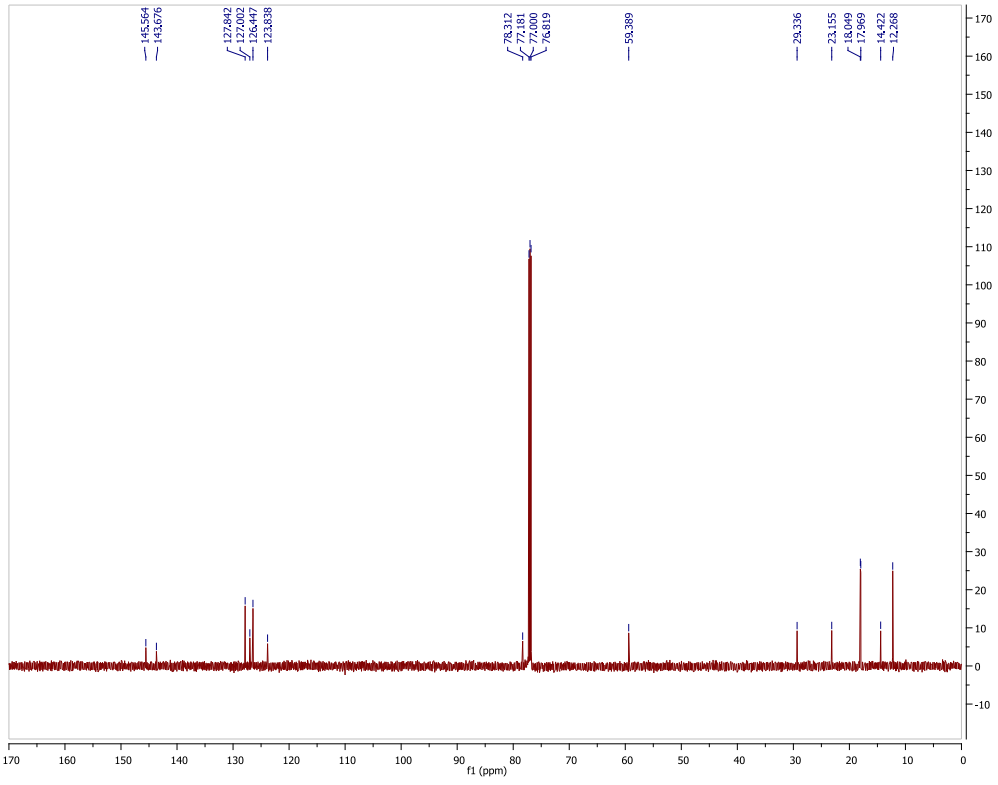

(E)-2-(phenyl((triisopropylsilyl)oxy)methyl)hex-2-en-1-ol Minor Regioisomer

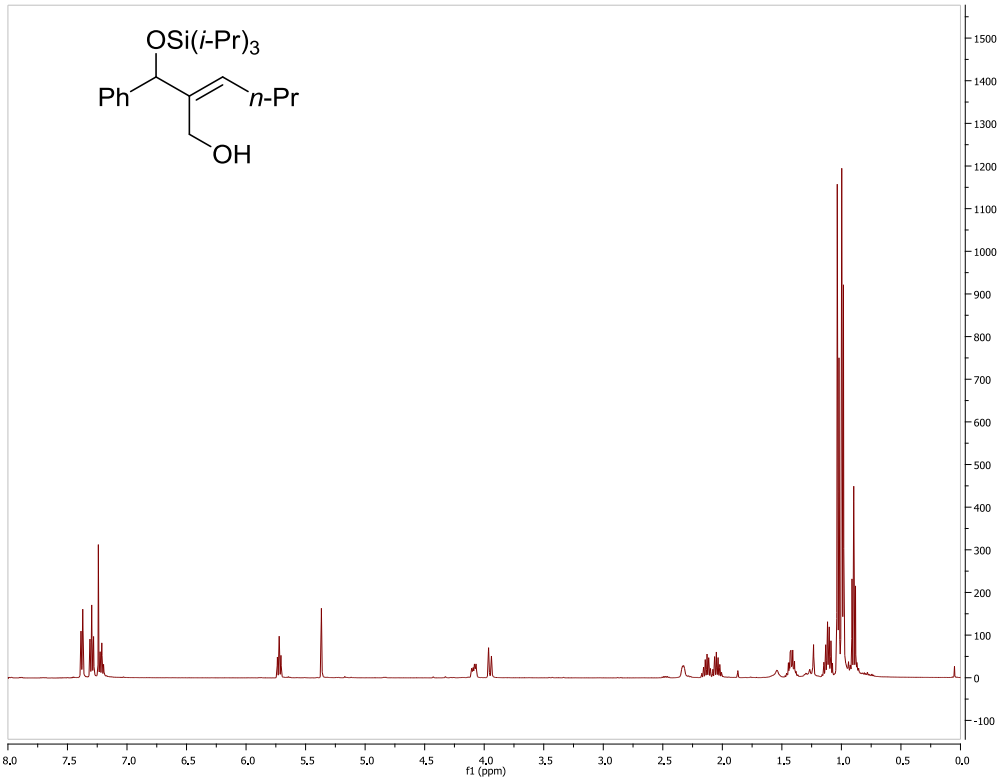

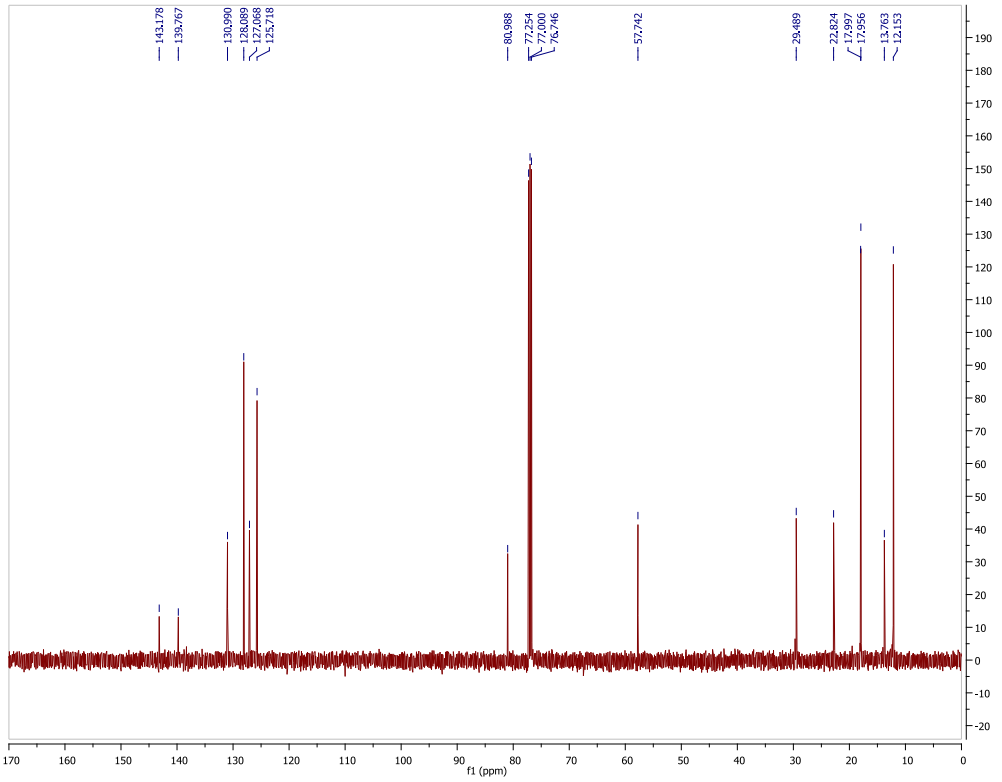

Table 2.6, Entry 9
Major regioisomer (E)-((2-ethylidene-1-(furan-2-yl)pentyl)oxy)triisopropylsilane
Minor regioisomer (E)-((1-(furan-2-yl)-2-methylhex-2-en-1-yl)oxy)triisopropylsilane

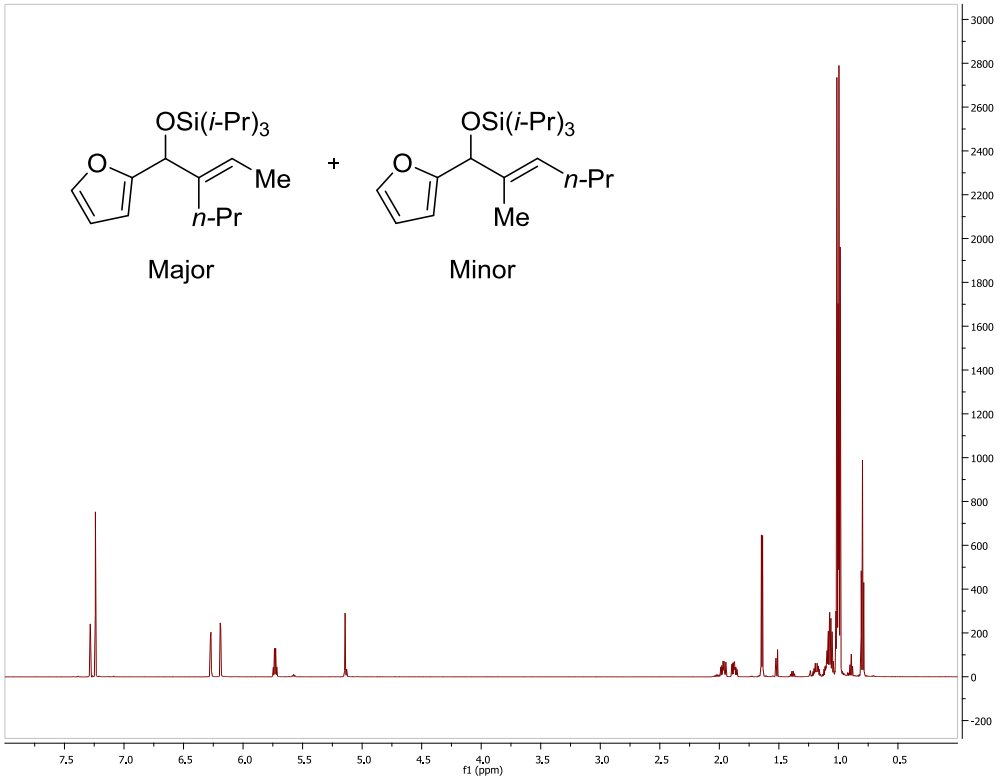

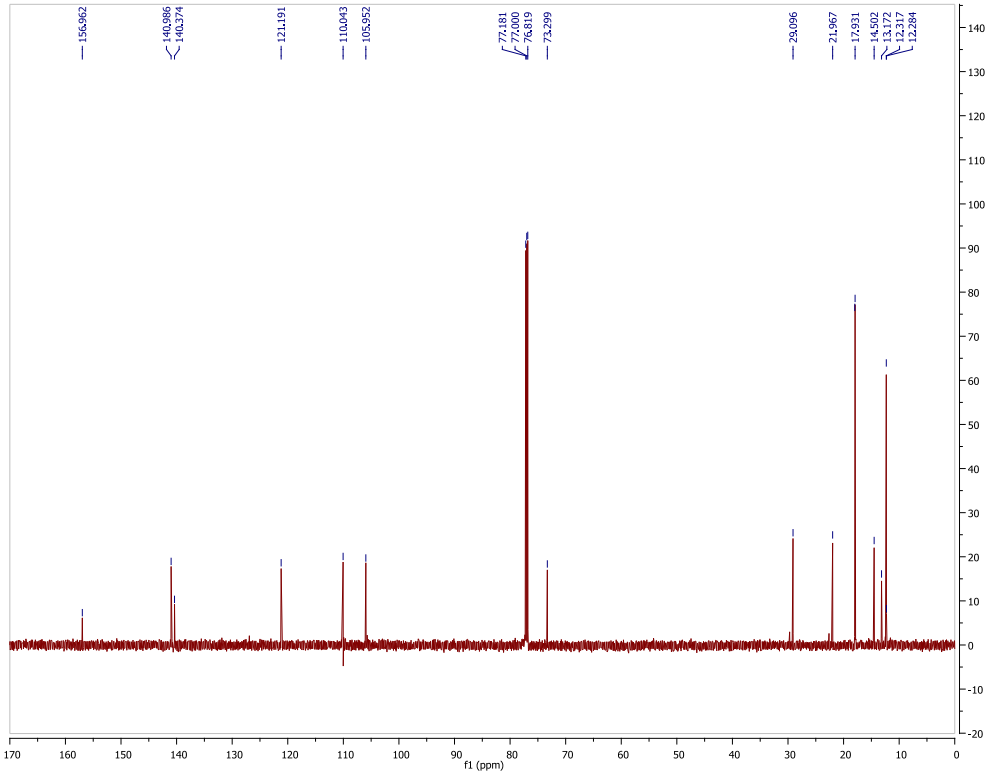

Table 2.6, Entry 11 (E)-((1-cyclohexyl-2-isopropylbut-2-en-1-yl)oxy)triisopropylsilane

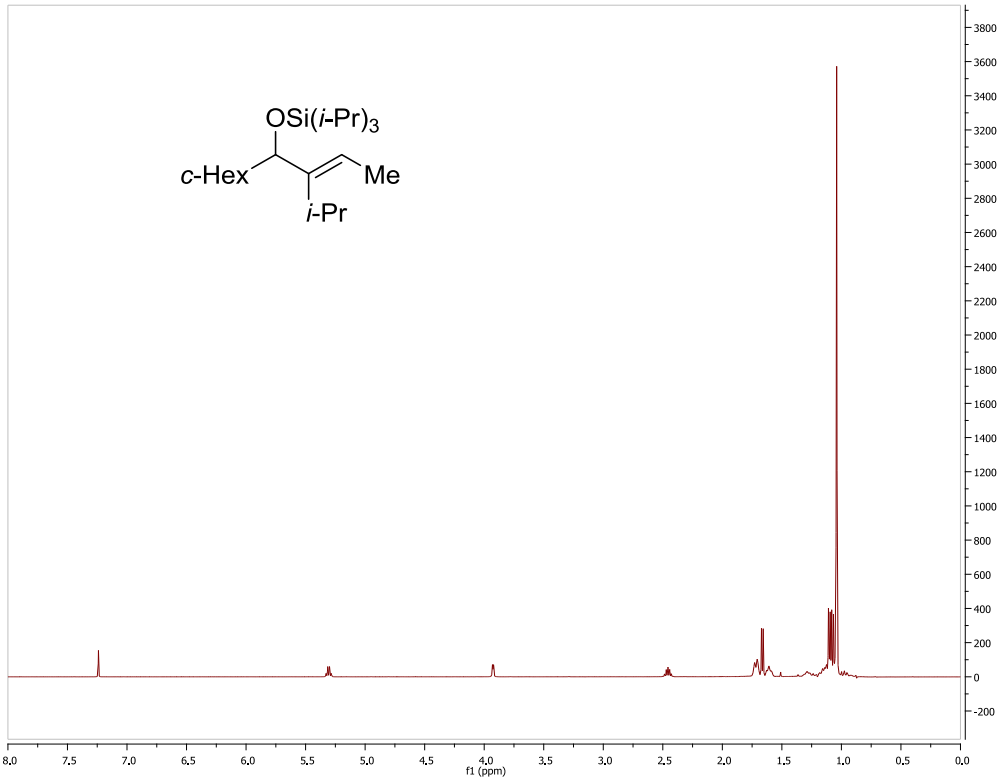

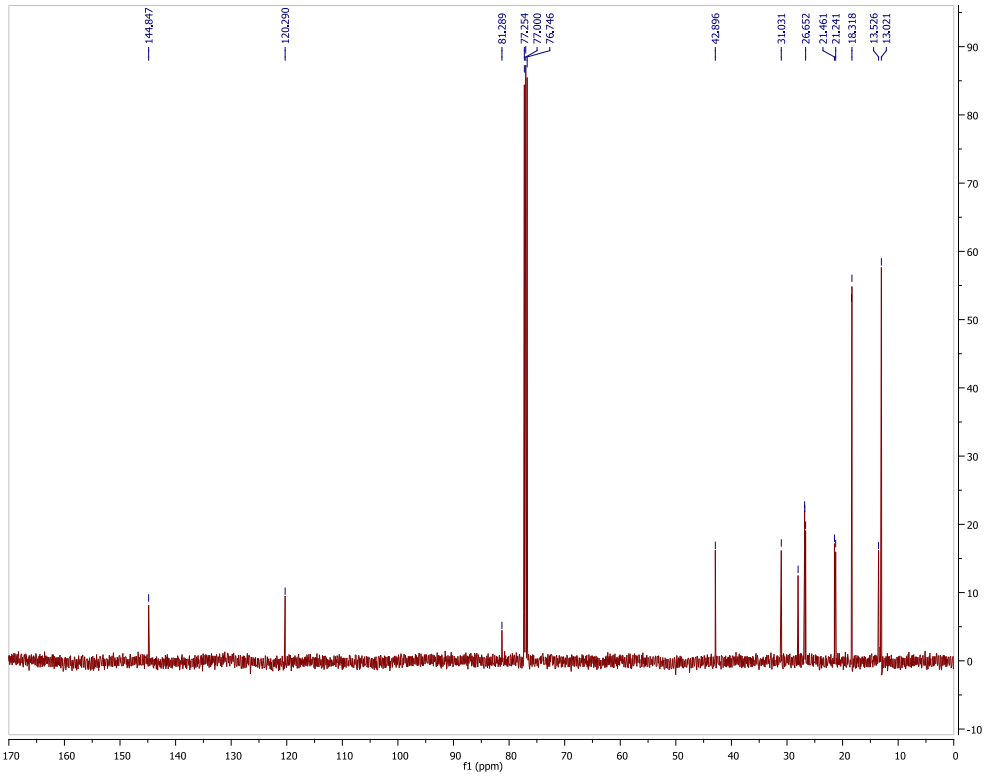

Table 2.8, Entry 1 Di-tert-butyl(methyl)(3-methyl-2-methylene-1-phenylbutoxy)silane

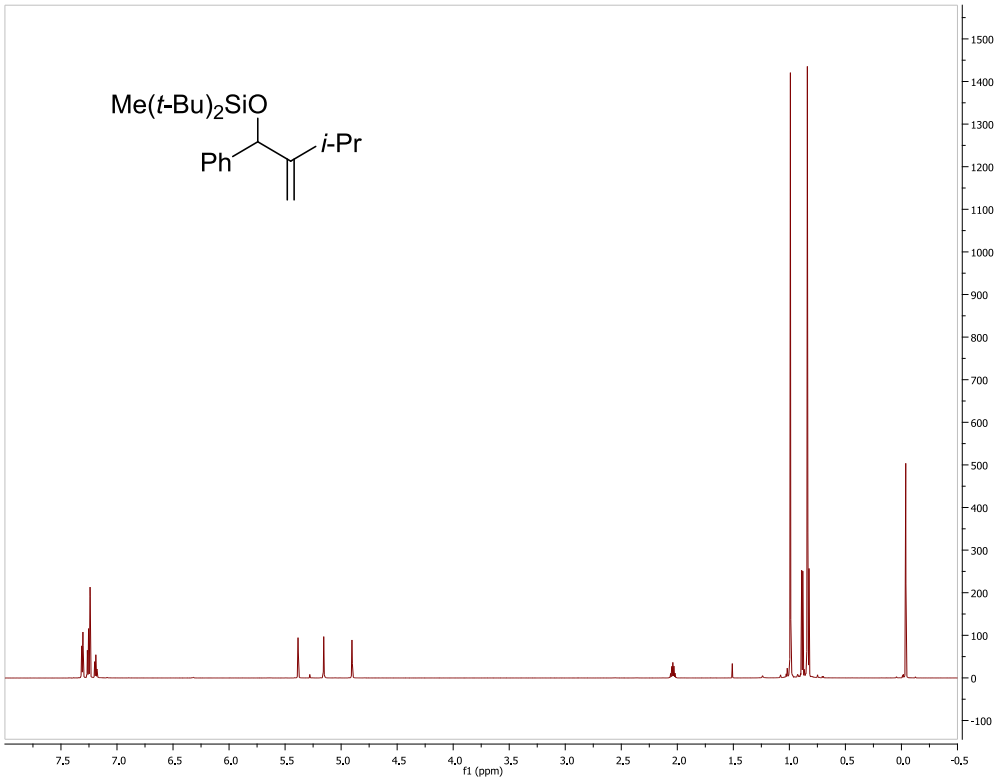

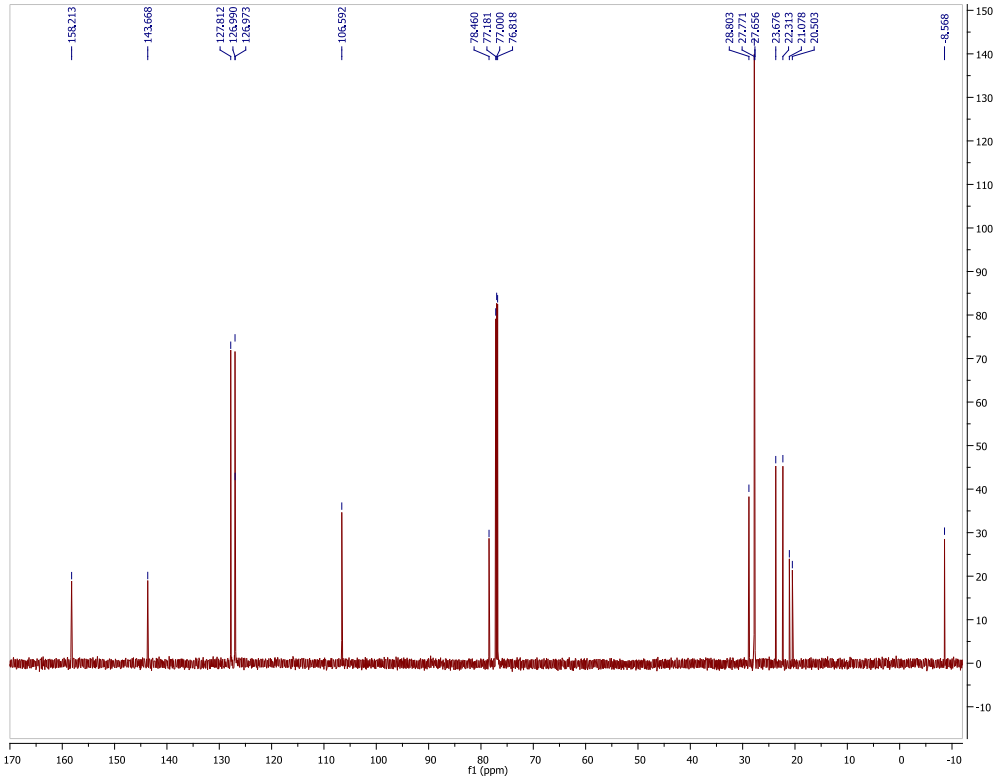

Table 2.8, Entry 2 Di-tert-butyl(methyl)((2-methylene-1-phenyloctyl)oxy)silane Major regioisomer

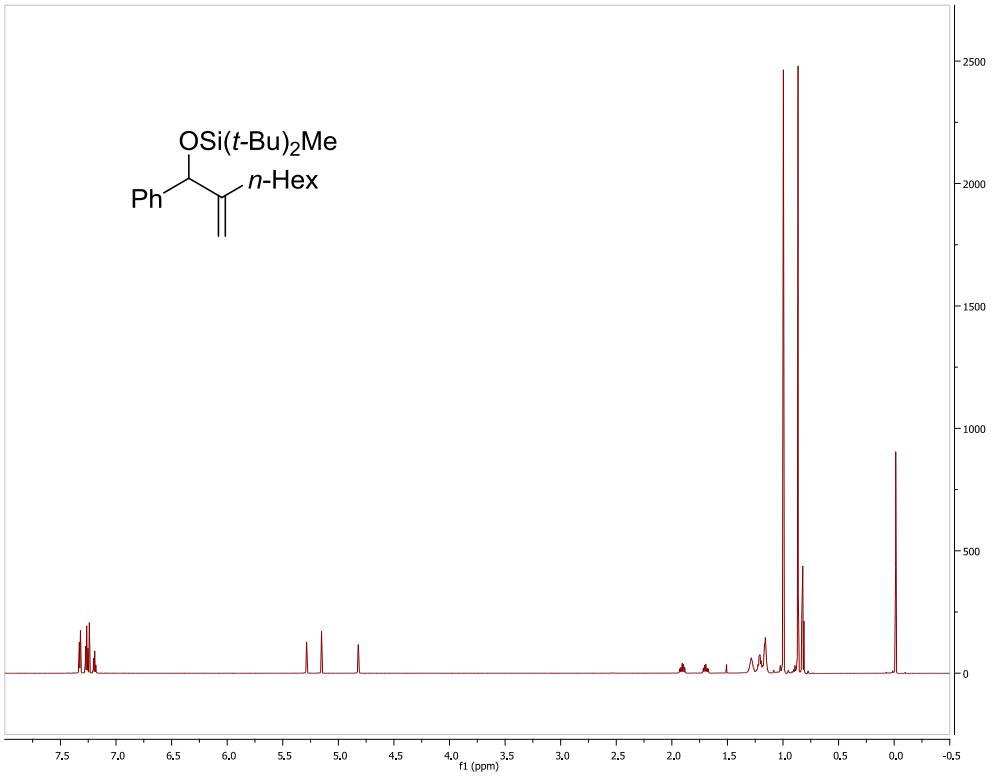

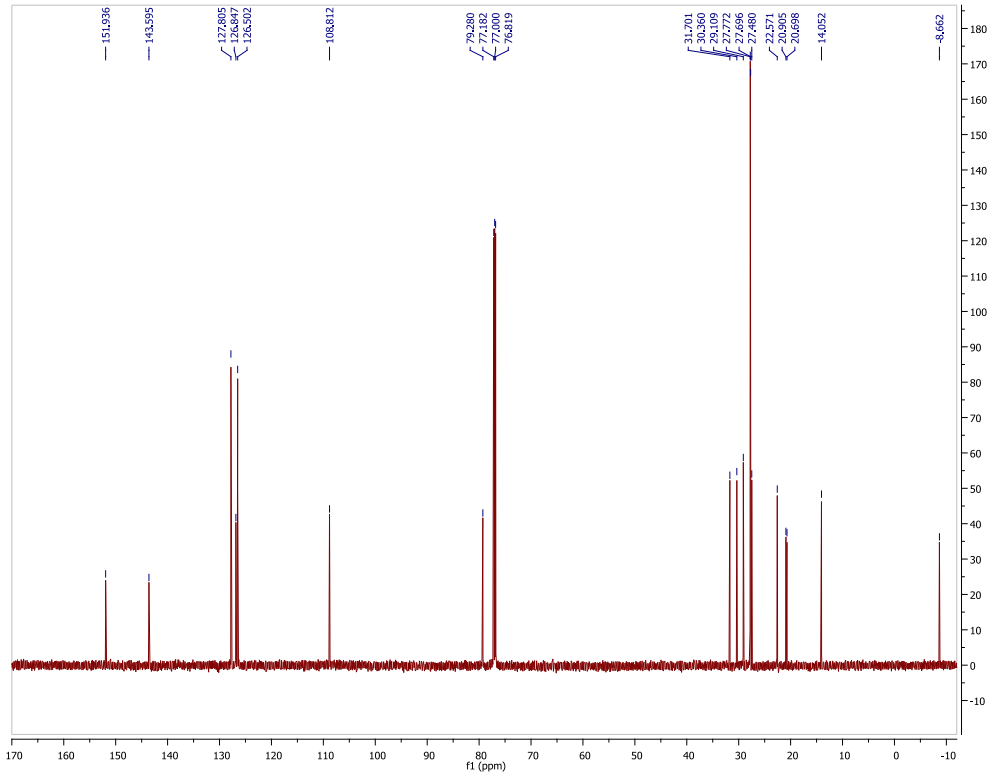

5.2 General Experimental Details Chapter 3

All reactions were conducted in flame-dried or oven dried (120 °C) glassware with magnetic stirring under an atmosphere of dry nitrogen. Solvents were purified under nitrogen using a solvent purification system (Innovative Technology, Inc. Model # SPS-400-3 and PS-400-3). Unless otherwise noted, alkynes were used as received. Aldehydes were distilled prior to use. Et_3SiH and $tBuMe_2SiH$ (Aldrich) were passed through basic alumina before use and stored under nitrogen. $Ni(acac)_2XH_2O$ (Strem Chemicals, Inc), *N*-heterocyclic carbene salts (Sigma Aldrich, Strem), and *t*-BuOK were stored in a desiccator and used on the bench. $Ni(COD)_2$, $NiBr_2$glyme, and $Ni(acac)_2$, (strem) and Mn (Aldrich) were stored and used in an inert atmosphere glovebox.

^1H and ^{13}C were obtained in $CDCl_3$ at rt on a Varian Unity 500 MHz or Varian Unity 700 MHz instrument. Chemical shifts of ^1H NMR spectra were recorded in parts per million (ppm) on the δ scale from an internal standard of residual chloroform (7.24 ppm). Chemical shifts of ^{13}C NMR spectra were recorded in ppm from the central peak of $CDCl_3$ (77.0 ppm) on the δ scale. High resolution mass spectra (HRMS were obtained at the University of Michigan Mass Spectrometry Laboratory on a VG-70-250-s spectrometer manufactured by Micromass Corp. (Manchester UK). Regioisomeric ratios were determined on crude reaction mixtures using either ^1H NMR or GC. GCMS analysis was carried out on a HP 6980 Series GC system with HP-5MS column (30 m x 0.250 mm x 0.25 μm). GCFID analysis was carried out on a HP 6980N Series GC system with a HP-5 column (30 m x 0.32 mm x 0.25 μm).

General Procedure A for $Ni(acac)_2XH_2O$/IMes Promoted Reductive Coupling of Benzaldhyde, Alkynes, and Triethylsilane:

$Ni(acac)_2 \bullet XH_2O$ (0.05 mmol), IMes•HCl salt (0.05 mmol), and *t*-BuOK (0.05 mmol) were weighed out on the bench into a screw capped vial with septum. The vial was evacuated to a pressure <1.0 mmHg and backfilled with dry N_2. This process was repeated a total of 3 times. 4 mL of Toluene was added to the catalyst mixture and the resulting solution was stirred for 15 min at rt until the solution turned golden yellow. Triethylsilane (1.0 mmol), aldehyde (0.75 mmol), and alkyne (0.5 mmol) were added sequentially The reaction mixture was stirred for 18 hours and then filtered through silica gel eluting with 50 % v/v EtOAc/hexanes. The solvent was removed *in vacuo*, and the crude residue was purified via flash chromatography on silica gel to afford the desired product.

General Procedure B for $Ni(acac)_2XH_2O$/IMes Promoted Reductive Coupling of Aliphatic Aldehydes, Alkynes, and Triethylsilane:

$Ni(acac)_2 \bullet XH_2O$ (0.05 mmol), IMes•HCl salt (0.05 mmol), and *t*-BuOK (0.05 mmol) were weighed out on the bench into a screw capped vial with septum. The vial was evacuated to a pressure <1.0 mmHg and backfilled with dry N_2. This process was repeated a total of 3 times. 2 mL of Toluene was added to the catalyst mixture and the resulting solution was stirred for 15 min at rt until the solution turned golden yellow. Triethylsilane (1.0 mmol) was added to the catalyst mixture. The aldehyde (0.75 mmol), and alkyne (0.5 mmol) were combined with 2 mL toluene and added over the course of an hour by syringe pump. The reaction mixture was stirred for 18 hours and then filtered through silica gel eluting with 50 % v/v EtOAc/hexanes. The solvent was removed *in vacuo*, and the crude residue was purified via flash chromatography on silica gel to afford the desired product.

(E)-triethyl((2-methyl-1,3-diphenylallyl)oxy)silane

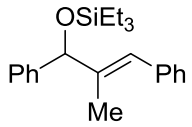

Table 3.4, 3a: Following Procedure A, $Ni(acac)_2 \bullet XH_2O$ (14.6 mg 0.05 mmol), IMes•HCl salt (17 mg, 0.05 mmol), *t*-BuOK (19.6 mg, 0.175 mmol), triethylsilane (116 mg, 1.0 mmol), benzaldehyde (79.5 mg, 0.75 mmol), and prop-1-yn-1-ylbenzene (58 mg, 0.5 mmol) gave a crude residue which was purified via flash chromatography (100 % Hexanes) to afford a mixture of regioisomers in a >98:2 regioselectivity (97:3 crude regioselectivity) as a clear oil (150 mg, 0.44 mmol, 88 %).

Spectral data as previously reported.[40] ^{1}H NMR spectrum is included below.

(E)-triethyl((2-ethyl-4-methyl-1-phenylpenta-2,4-dien-1-yl)oxy)silane

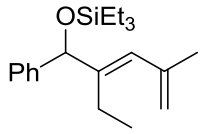

Table 3.4, 3b: Following Procedure A, $Ni(acac)_2 \bullet XH_2O$ (14.6 mg 0.05 mmol), IMes•HCl salt (17 mg, 0.05 mmol), *t*-BuOK (19.6 mg, 0.175 mmol), triethylsilane (116 mg, 1.0 mmol), benzaldehyde (79.5 mg, 0.75 mmol), and 2-methylhex-1-en-3-yne (47 mg, 0.5 mmol) gave a crude residue which was purified via flash chromatography (100 % Hexanes) to afford a single isomer in >98:2 regioselectivity (>98:2 crude regioselectivity) as a clear oil (148 mg, 0.47 mmol, 94 %)

^{1}H NMR (500 MHz, $CDCl_3$) δ 7.34 (d, *J* = 7.5 Hz, 2 H), 7.27 (t, *J* = 7.5 Hz, 2 H), 7.21-7.18 (m, 1 H), 6.12 (s, 1 H), 5.1 (s, 1 H), 4.93 (s, 1 H), 4.86 (s, 1 H), 2.20-2.12 (m, 1 H), 1.97-1.91 (m, 1 H), 1.88 (s, 3 H), 0.89 (t, *J* = 8 Hz, 9 H), 0.82 (t, *J* = 8 Hz, 3 H), 0.57 (q, *J* = 8 Hz, 6 H).

^{13}C NMR (175 MHz, $CDCl_3$) δ 144.9, 143.8, 141.9, 127.8, 127.2, 126.9, 126.5, 114.2, 78.6, 23.5, 20.7, 14.6, 6.8, 4.9

HRMS (EI) (*m/z*): $[M]^+$ calcd for $C_{20}H_{32}OSi$ 316.2222, found 316.2213

(E)-triethyl((2-methyl-1-phenylnon-1-en-3-yl)oxy)silane

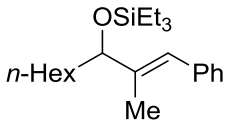

Table 3.4, 3c: Following Procedure B, $Ni(acac)_2 \bullet XH_2O$ (14.6 mg 0.05 mmol), IMes•HCl salt (17 mg, 0.05 mmol), *t*-BuOK (19.6 mg, 0.175 mmol), triethylsilane (116 mg, 1.0 mmol), heptanal (86 mg, 0.75 mmol), and prop-1-yn-1-ylbenzene (58 mg, 0.5 mmol) gave a crude residue which was purified via flash chromatography (100 % Hexanes) to afford a mixture of regioisomers in a 96:4 regioselectivity (93**:**7 crude regioselectivity) as a clear oil (122 mg, 0.35 mmol, 71 %).

Spectral data as previously reported.[40] ^{1}H NMR spectrum is included below.

(E)-triethyl((1-phenylnon-2-en-1-yl)oxy)silane

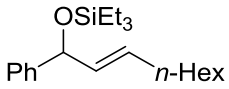

Table 3.4, 3d: Following Procedure A, $Ni(acac)_2 \bullet XH_2O$ (14.6 mg 0.05 mmol), IMes•HCl salt (17 mg, 0.05 mmol), *t*-BuOK (19.6 mg, 0.175 mmol), triethylsilane (116 mg, 1.0 mmol), benzaldehyde (79.5 mg, 0.75 mmol), and oct-1-yne (55 mg, 0.5 mmol) gave a crude residue which was purified via flash chromatography (100 % Hexanes) to afford a mixture of regioisomers in a >98:2 regioselectivity (98:2 crude regioselectivity) as a clear oil (108 mg, 0.33 mmol, 65 %).

Spectral data as previously reported. ^{1}H NMR spectrum is included below.

(E)-triethyl(pentadec-8-en-7-yloxy)silane

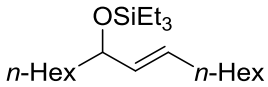

Table 3.4, 3e Following Procedure B, $Ni(acac)_2 \bullet XH_2O$ (14.6 mg 0.05 mmol), IMes•HCl salt (17 mg, 0.05 mmol), *t*-BuOK (19.6 mg, 0.175 mmol), triethylsilane (116 mg, 1.0 mmol), heptanal (86 mg, 0.75 mmol), and oct-1-yne (55 mg, 0.5 mmol) gave a crude residue which was purified

via flash chromatography (100 % Hexanes) to afford a single isomer in >98:2 regioselectivity (>98:2 crude regioselectivity) as a clear oil (69 mg, 0.20 mmol, 41 %).

^{1}H NMR (500 MHz, $CDCl_3$) δ 5.48 (dt, *J* = 15, 7 Hz, 1 H), 5.36 (dd, *J* = 15, 7 Hz, 1 H), 3.97 (q, *J* = 6.5 Hz, 1 H), 1.97 (q, *J* = 7 Hz, 2 H), 1.50-1.21 (m, 18 H), 0.92 (t, *J* = 8 Hz, 9 H), 0.88-0.83 (m, 6 H), 0.56 (q, *J* = 8 Hz, 6 H)

^{13}C NMR (175 MHz, $CDCl_3$) δ 133.6, 130.5, 73.8, 38.6, 32.2, 31.9, 31.7, 29.3, 29.2, 28.8, 25.4, 22.64, 22.63, 14.10, 14.09, 6.7, 5.0

HRMS (EI) (*m/z*): $[M]^+$ calcd for $C_{21}H_{44}OSi$ 340.3161, found 340.3159

(E)-7-phenyl-7-((triethylsilyl)oxy)hept-5-en-1-ol

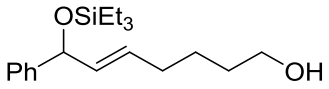

Table 3.4, 3f: Following Procedure A, $Ni(acac)_2 \bullet XH_2O$ (14.6 mg 0.05 mmol), IMes•HCl salt (17 mg, 0.05 mmol), *t*-BuOK (19.6 mg, 0.175 mmol), triethylsilane (116 mg, 1.0 mmol), benzaldehyde (79.5 mg, 0.75 mmol), and hex-5-yn-1-ol (49 mg, 0.5 mmol) gave a crude residue which was purified via flash chromatography (85/15 % Hexanes/EtOAc) to afford a single isomer in a >98:2 regioselectivity (>98:2 crude regioselectivity) as a clear oil (86 mg, 0.27 mmol, 54 %).

Spectral data as previously reported.[40] ^{1}H NMR spectrum is included below.

(E)-4-(2-methyl-3-phenyl-1-((triethylsilyl)oxy)allyl)pyridine Major regioisomer

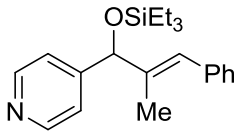

(E)-4-(2-phenyl-1-((triethylsilyl)oxy)but-2-en-1-yl)pyridine Minor regioisomer

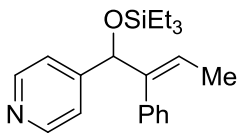

Table 3.4, 3g: Following a modified Procedure B, Ni(acac)2•XH_2O (14.6 mg 0.05 mmol), IMes•HCl salt (17 mg, 0.05 mmol),*t*-BuOK (19.6 mg, 0.175 mmol), and PPh_3 (13.1 mg, 0.05 mmol) were combined with 2 mL PhMe and stirred 15 min. $AlMe_3$ (2 M in Toluene, 0.05 mmol) and triethylsilane (116 mg, 1.0 mmol) were added and the vial was heated to 100 C. Isonicotinaldehyde (54 mg, 0.5 mmol) and prop-1-yn-1-ylbenzene (58 mg, 0.5 mmol) were combined with 2 mL PhMe and added to the reaction over 1 hour. The reaction gave a crude residue which was purified via flash chromatography (35 % v/v EtOAc/Hexanes) to afford a mixture of regioisomers in a 96:4 regioselectivity (97:3 crude regioselectivity) as a clear oil (117 mg, 0.35 mmol, 69 %).

^{1}H NMR (700 MHz, $CDCl_3$) δ 8.54 (d, *J* = 5.6 Hz, 2H), 7.34-7.32 (m ,4 H), 7.27-7.26 (m, 2 H), 7.23-7.21 (m, 1 H), 6.68 (s, 1H), 5.21 (s, 1H), 1.63, (s, 1H), 0.95 (t, *J* = 7.7 Hz, 9H), 0.646 (q, *J* = 7.7, 6H)

^{13}C NMR (175 MHz, $CDCl_3$) 152.3, 149.6, 139.5, 137.1, 128.9, 128.2, 127.1, 126.7, 121.0, 79.1, 12.6, 6.8, 4.8

HRMS (ESI+) (*m/z*): $[M]^+$ calcd for $C_{22}H_{29}NOSi$ 340.2091, found; 340.2090

Characteristic ^{1}H NMR of minor isomer: 5.31 (s, 1 H), 1.53 (d, J = 7.0 Hz, 1 H)

(E)-3-(2-methyl-3-phenyl-1-((triethylsilyl)oxy)allyl)pyridine

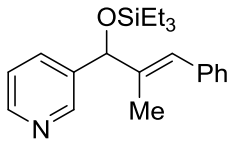

Table 3.4, 3h: Following a modified Procedure B, Ni(acac)2•XH_2O (14.6 mg 0.05 mmol), IMes•HCl salt (17 mg, 0.05 mmol),*t*-BuOK (19.6 mg, 0.175 mmol), and PPh_3 (13.1 mg, 0.05 mmol) were combined with 2 mL PhMe and stirred 15 min. $AlMe_3$ (2 M in Toluene, 0.05 mmol) and triethylsilane (116 mg, 1.0 mmol) were added and the vial was heated to 100 C. Nicotinaldehyde (54 mg, 0.5 mmol) and prop-1-yn-1-ylbenzene (58 mg, 0.5 mmol) were combined with 2 mL PhMe and added to the reaction over 1 hour. The reaction gave a crude residue which was purified via flash chromatography (15 % v/v EtOAc/Hexanes) to afford a

mixture of regioisomers in a 98:2 regioselectivity (97:3 crude regioselectivity) as a clear oil (95 mg, 0.28 mmol, 56 %).

^{1}H NMR (500 MHz, $CDCl_3$) δ 8.65 (s, 1 H), 8.49 (d, *J* = 3.5 Hz, 1 H), 7.74-7.71 (m, 1 H), 7.35-7.30 (m, 2 H), 7.27-7.19 (m , 4 H), 6.72 (s, 1 H), 5.26 (s, 1 H), 1.64 (s, 3 H), 0.94 (t, *J* = 8.5 Hz, 9 H), 0.64 (q, J = 8.5 Hz, 6 H)

^{13}C NMR (125 MHz, $CDCl_3$): δ 148.5, 148.1, 139.8, 138.6, 137.3 133.7, 128.9, 128.2, 126.6, 126.3, 123.1, 78.1, 13.0, 6.8, 4.8

HRMS (ESI+) (*m/z*): $[M]^+$ calcd for $C_{22}H_{29}NOSi$ 340.2091; found 340.2090

tert-butyl((2-(cyclohexylmethyl)-1-phenylallyl)oxy)dimethylsilane

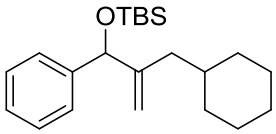

Table 3.4, 3i: Following a modified procedure A, $Ni(acac)_2 \bullet XH_2O$ (14.6 mg 0.05 mmol), IMes•HCl salt (17 mg, 0.05 mmol), and *t*-BuOK (19.6 mg, 0.175 mmol) were combined and the flask was evacuated and backfilled with N_2. 4 mL of toluene was added and the solution was stirred for 15 min at rt. The solution was then cooled to -78 °C and tert-butyldimethylsilane (174 mg, 1.5 mmol), benzaldehyde (159 mg, 1.5 mmol), and cyclohexylallene (61 mg, 0.5 mmol) were added sequentially. The mixture was allowed to react overnight and warm to rt. The reaction gave a crude residue which was purified via flash chromatography (100 % Hexanes) to afford a mixture of regioisomers in a >98:2 regioselectivity (>98:2 crude regioselectivity) as a clear oil (89 mg, 0.26 mmol, 52 %).

Spectral data as previously reported.[99] ^{1}H NMR spectrum is included below.

^{1}H and ^{13}C Spectra

Table 3.4, 1a (E)-triethyl((2-methyl-1,3-diphenylallyl)oxy)silane

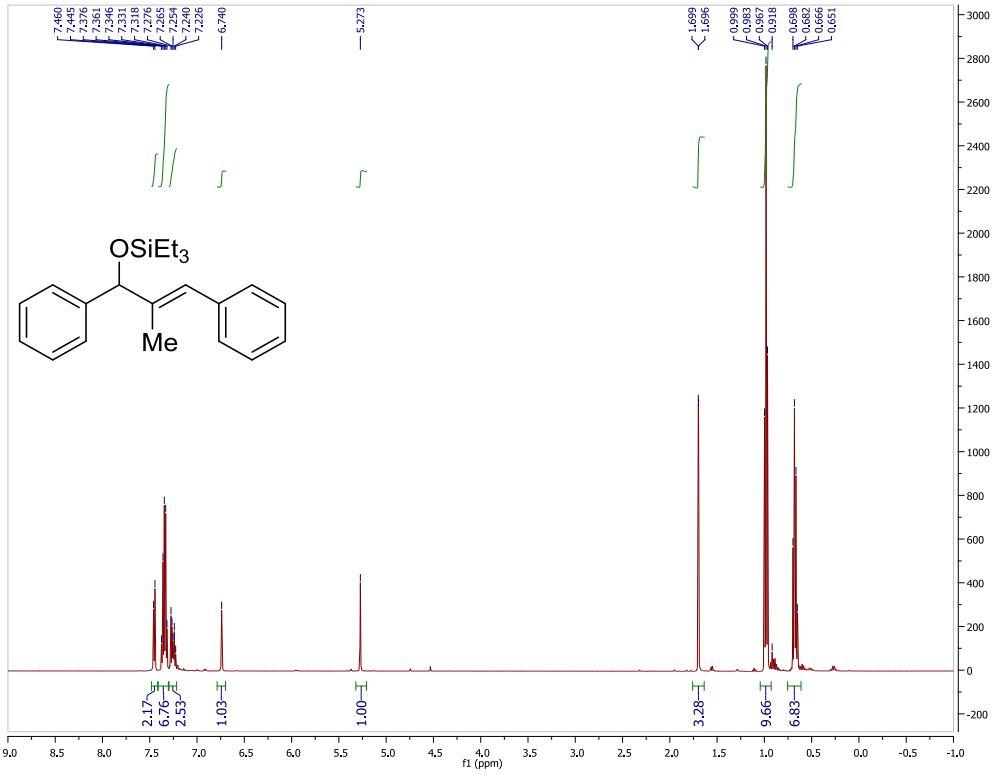

Table 3.4, (E)-triethyl((2-ethyl-4-methyl-1-phenylpenta-2,4-dien-1-yl)oxy)silane

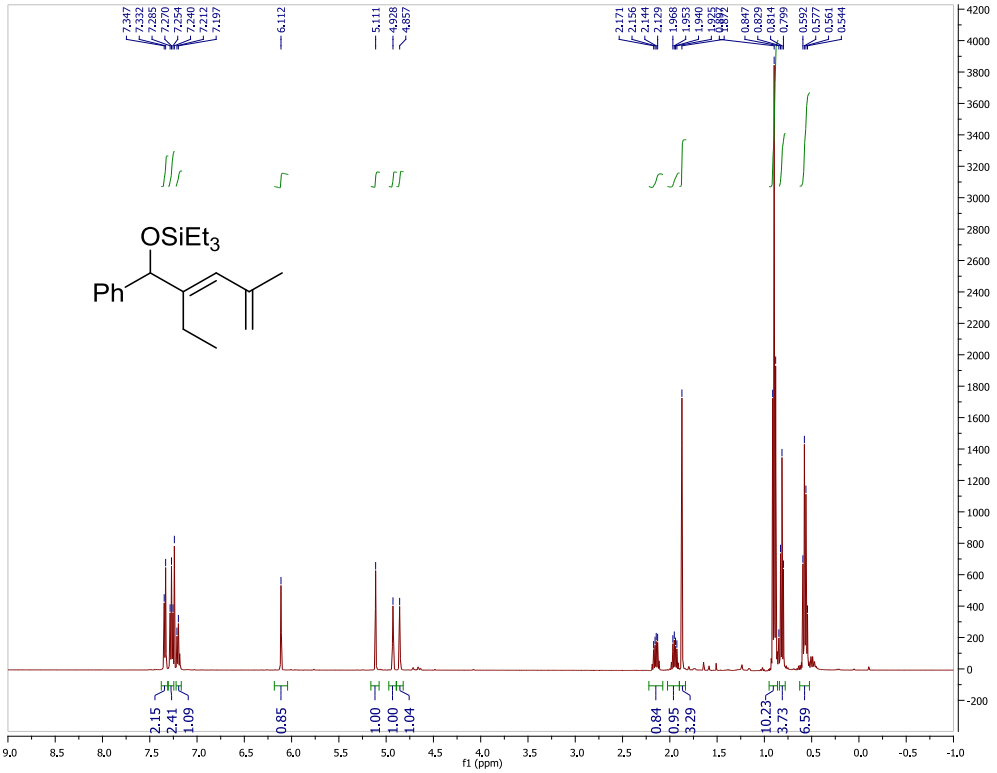

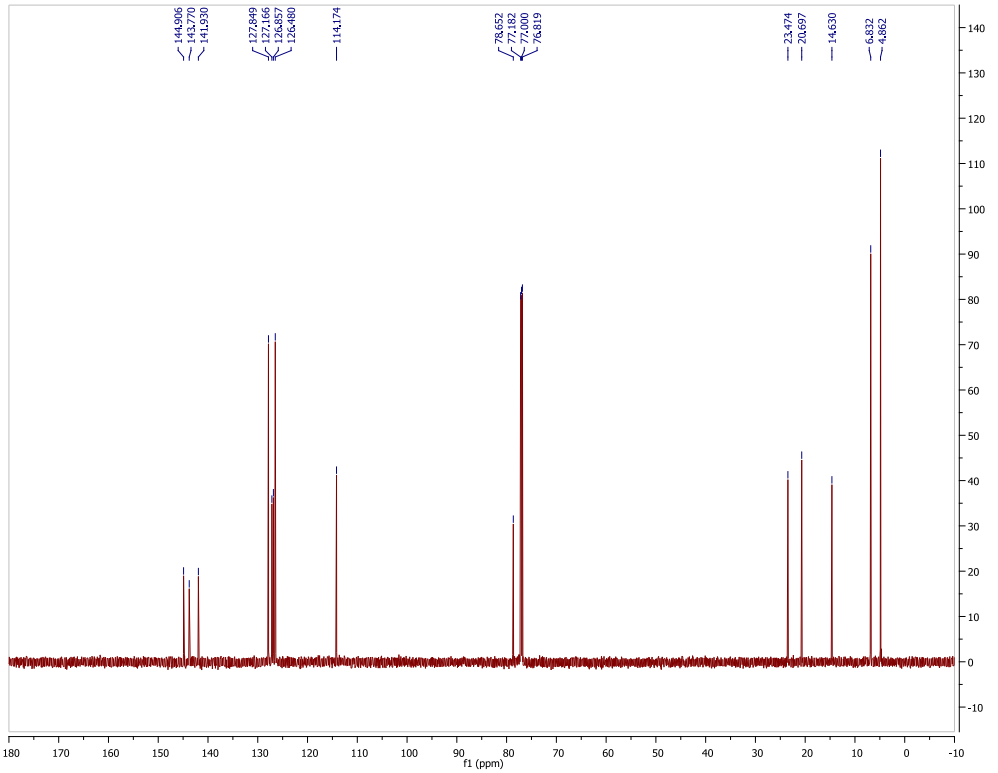

Table 3.4, 3c (E)-triethyl((2-methyl-1-phenylnon-1-en-3-yl)oxy)silane

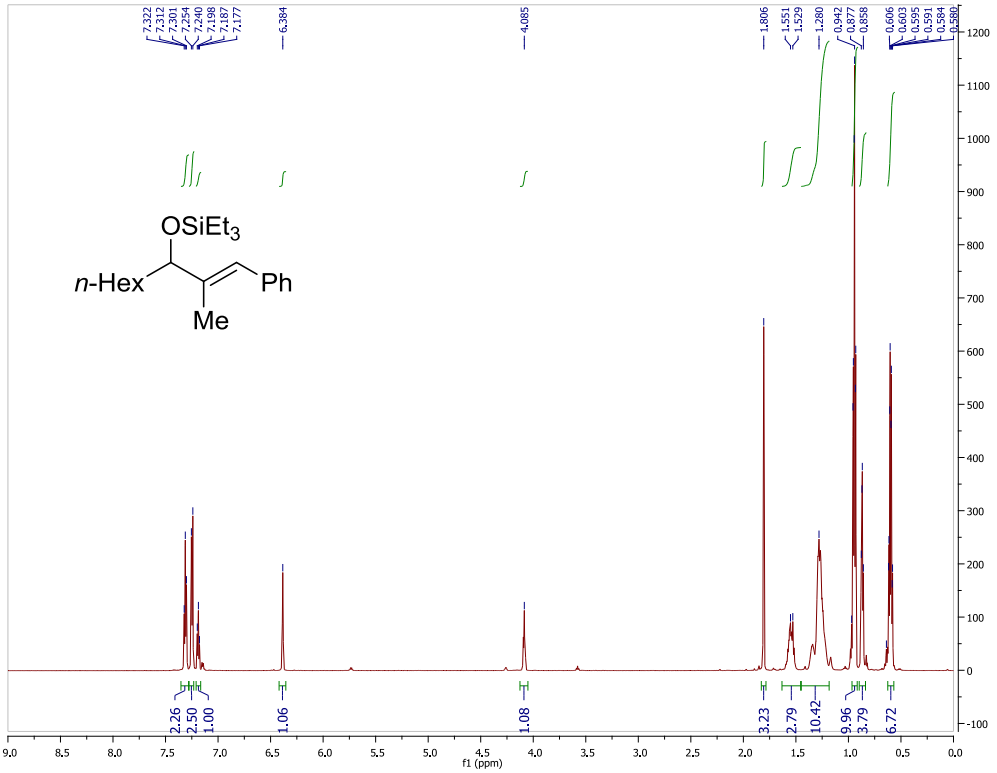

Table 3.4, 3d (E)-triethyl(pentadec-8-en-7-yloxy)silane

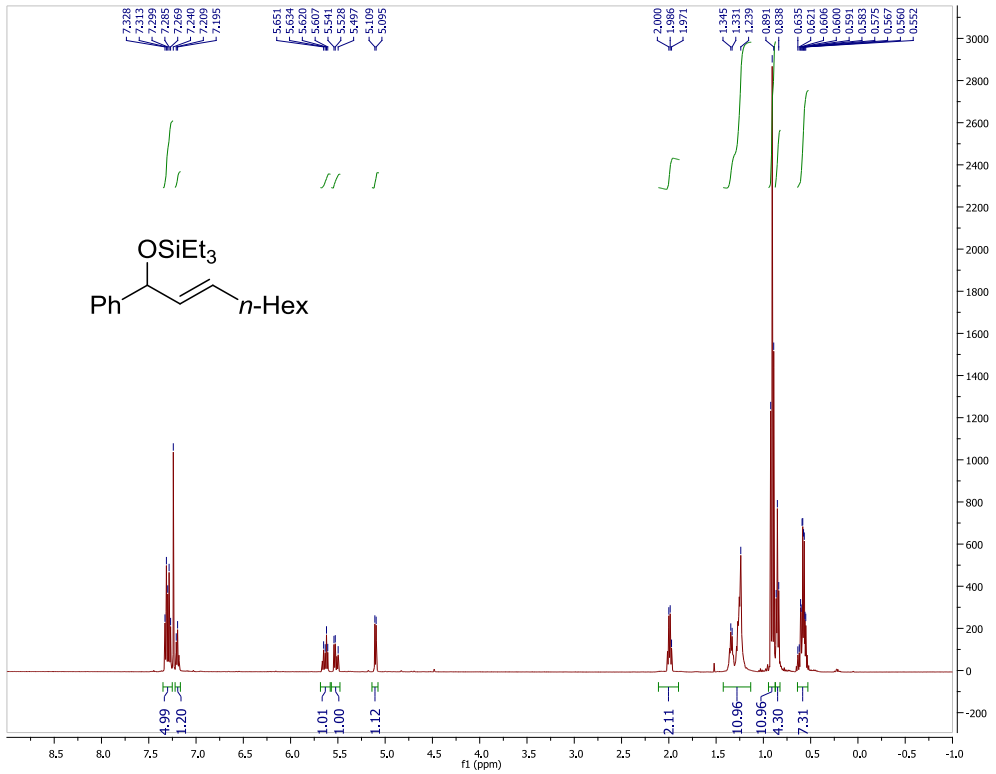

Table 3.4, 3e (E)-triethyl(pentadec-8-en-7-yloxy)silane

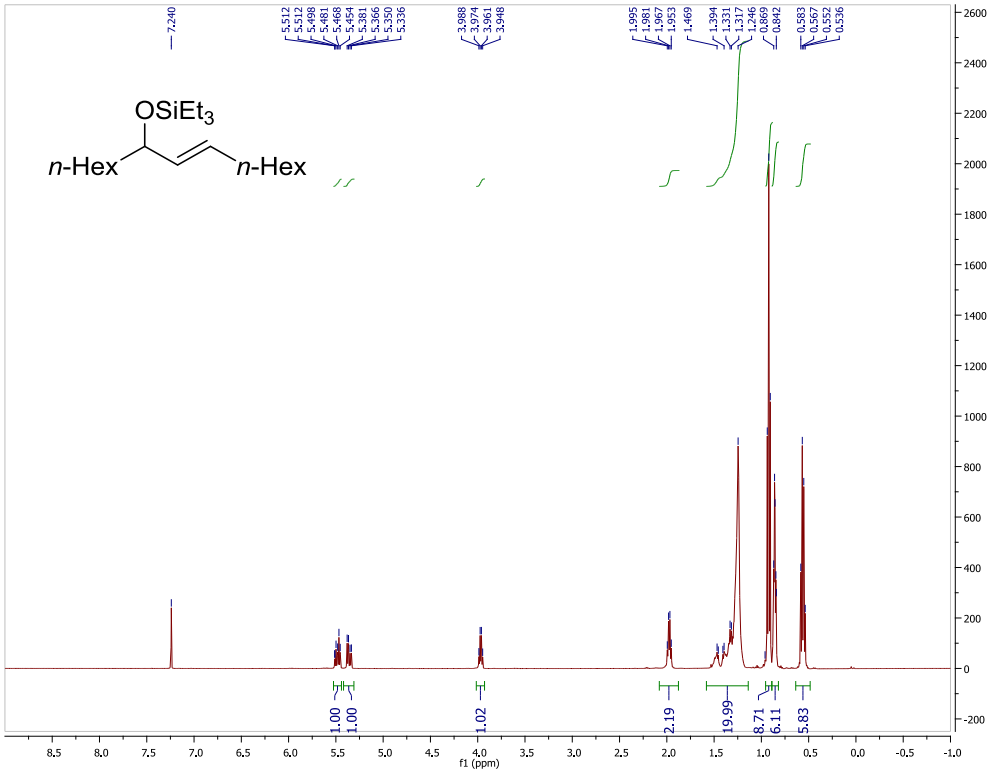

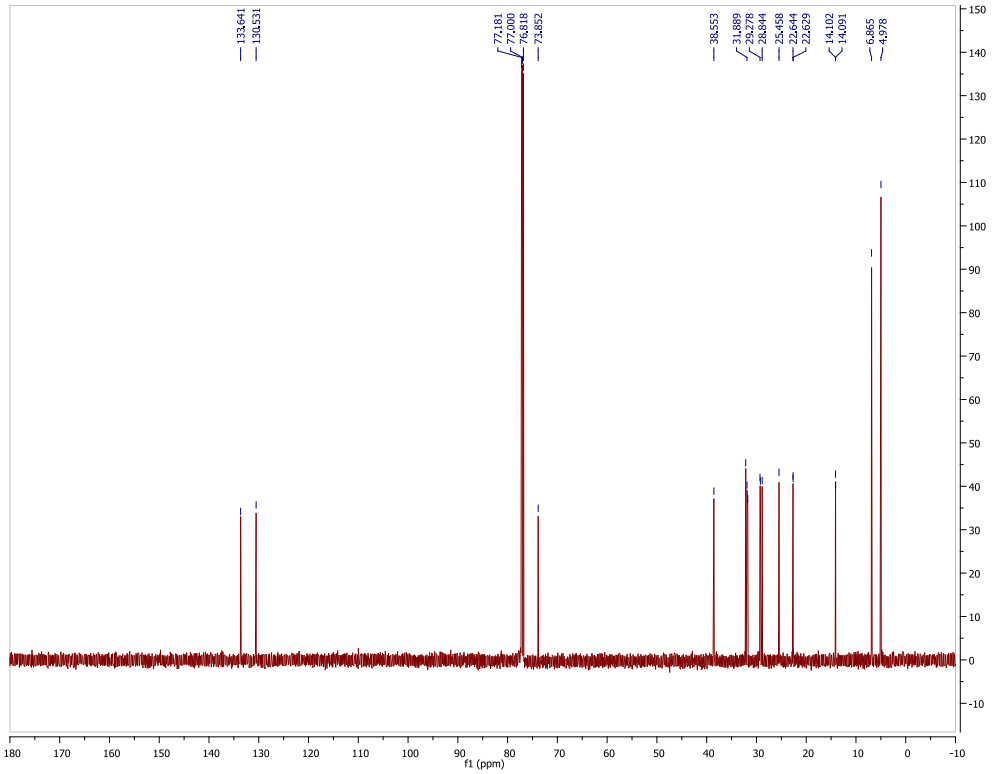

Table 3.4, Entry 3f (E)-7-phenyl-7-((triethylsilyl)oxy)hept-5-en-1-ol

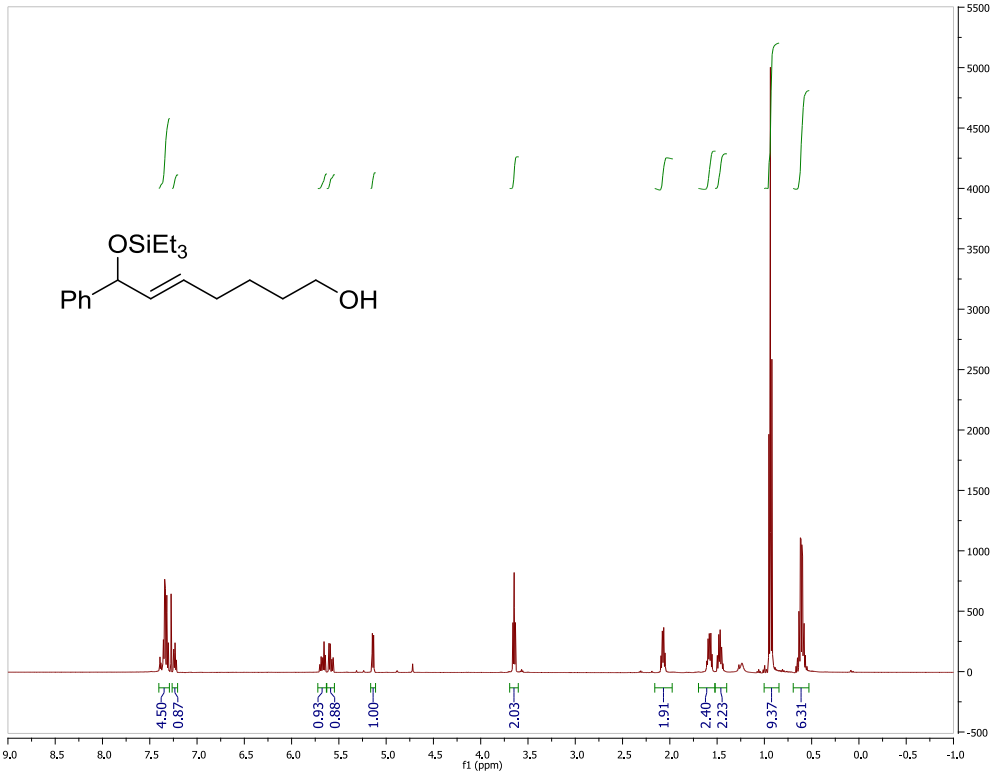

Table 3.4, 3g
(E)-3-(2-methyl-3-phenyl-1-((triethylsilyl)oxy)allyl)pyridine

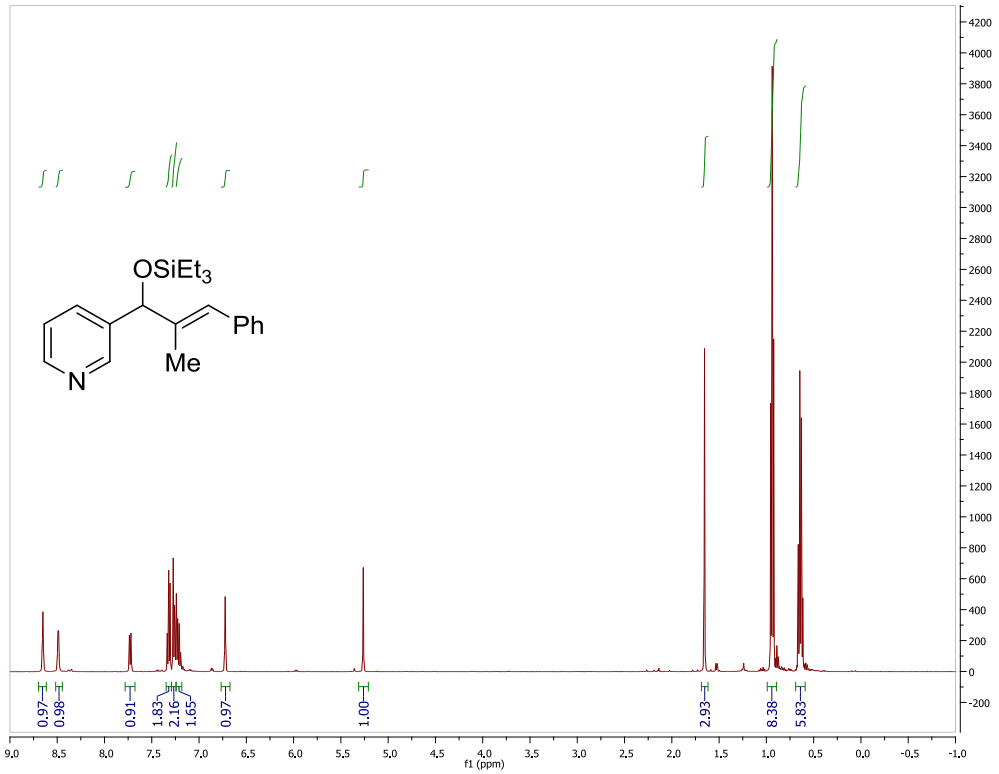

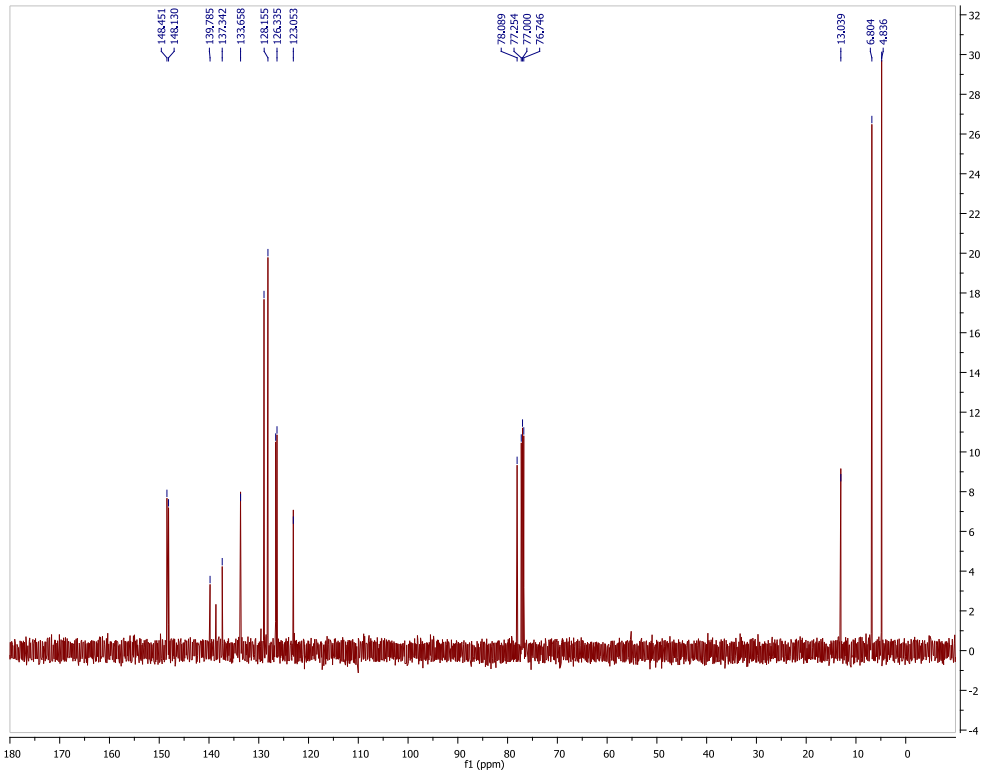

Table 3.4, 3h
(E)-4-(2-methyl-3-phenyl-1-((triethylsilyl)oxy)allyl)pyridine Major isomer
(E)-4-(2-phenyl-1-((triethylsilyl)oxy)but-2-en-1-yl)pyridine Minor regioisomer

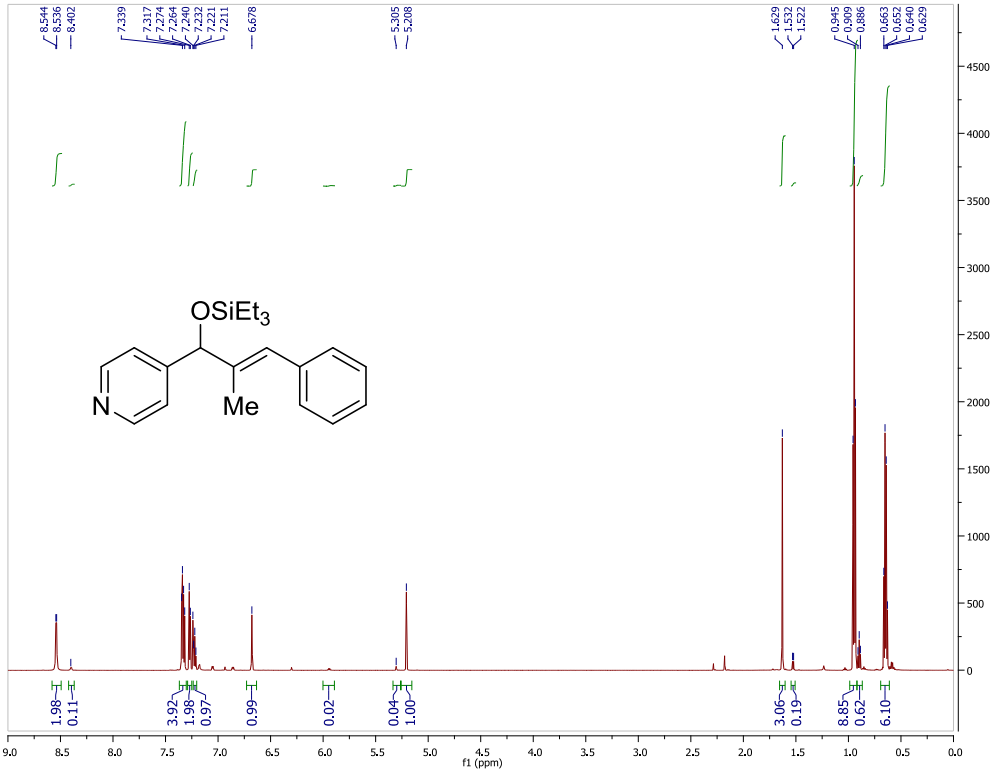

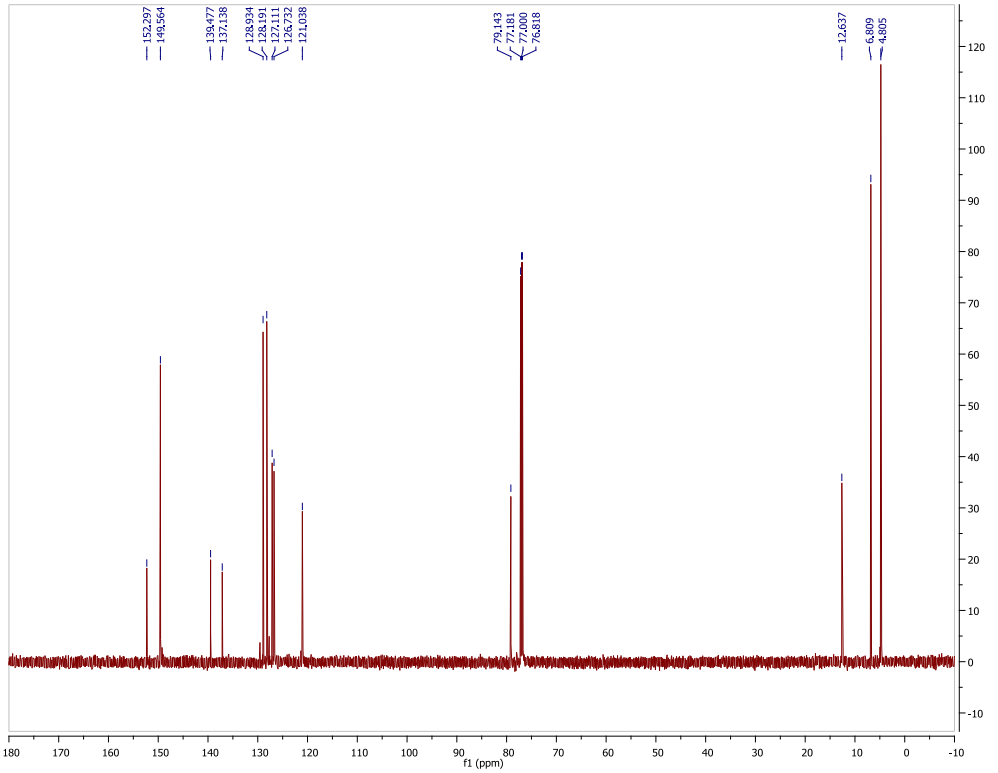

Table 3.4, 3i tert-butyl((2-(cyclohexylmethyl)-1-phenylallyl)oxy)dimethylsilane

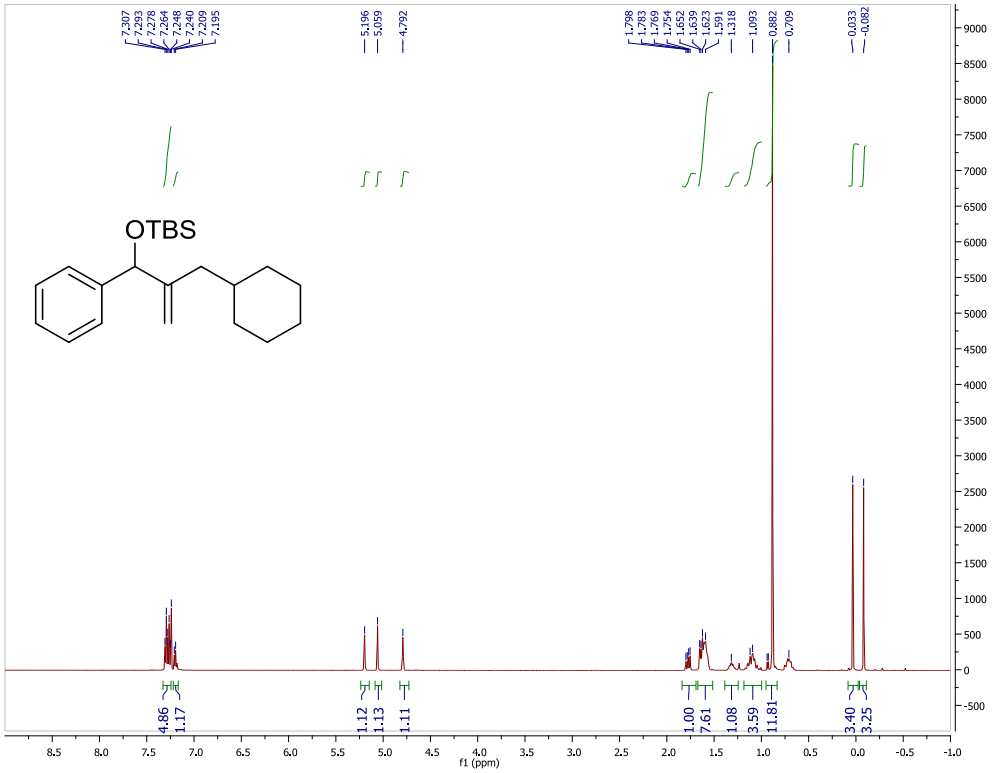

References

1. Mahatthananchai, J.; Dumas, A. M.; Bode, J. W. *Angew. Chem. Int. Ed.* **2012**, *51*, 10954–10990.

2. Hoveyda, A. H.; Evans, D. A.; Fu, G. C. *Chem. Rev.* **1993**, *93*, 1307–1370.

3. Boren, B. C.; Narayan, S.; Rasmussen, L. K.; Zhang, L.; Zhao, H.; Lin, Z.; Jia, G.; Fokin, V. V. *J. Am. Chem. Soc.* **2008**, *130*, 8923–8930.

4. Hein, J. E.; Fokin, V. V. *Chem. Soc. Rev.* **2010**, *39*, 1302–1315.

5. Marion, N.; Ramón, R. S.; Nolan, S. P. *J. Am. Chem. Soc.* **2009**, *131*, 448–449.

6. Tokunaga, M.; Wakatsuki, Y. *Angew. Chem. Int. Ed.* **1998**, *37*, 2867–2869.

7. Gainer, M. J.; Bennett, N. R.; Takahashi, Y.; Looper, R. E. *Angew. Chem. Int. Ed.* **2011**, *50*, 684–687.

8. Smith, N. D.; Mancuso, J.; Lautens, M. *Chem. Rev.* **2000**, *100*, 3257–3282.

9. Darwish, A.; Lang, A.; Kim, T.; Chong, J. M. *Org. Lett.* **2008**, *10*, 861–864.

10. Kazmaier, U.; Pohlman, M.; Schauß, D. *Eur. J. Org. Chem.* **2000**, *2000*, 2761–2766.

11. Bausch, C. C.; Patman, R. L.; Breit, B.; Krische, M. J. *Angew. Chem. Int. Ed.* **2011**, *50*, 5687–5690.

12. Ogoshi, S.; Arai, T.; Ohashi, M.; Kurosawa, H. *Chem. Commun.* **2008**, 1347–1349.

13. Santos, A.; Lopez, J.; Montoya, J.; Noheda, P.; Romero, A.; Echavarren, A. M. *Organometallics* **1994**, *13*, 3605–3615.

14. Brown, H. C.; Rao, B. C. S. *J. Am. Chem. Soc.* **1956**, *78*, 5694–5695.

15. Jang, H.; Zhugralin, A. R.; Lee, Y.; Hoveyda, A. H. *J. Am. Chem. Soc.* **2011**, *133*, 7859–7871.

16. Gao, F.; Hoveyda, A. H. *J. Am. Chem. Soc.* **2010**, *132*, 10961–10963.

17. Trost, B. M.; Ball, Z. T. *Synthesis.* **2005**, 853–887.

18. Chung, L. W.; Wu, Y.-D.; Trost, B. M.; Ball, Z. T. *J. Am. Chem. Soc.* **2003**, *125*, 11578–11582.

19. Yang, Y.-F.; Chung, L. W.; Zhang, X.; Houk, K. N.; Wu, Y.-D. *J. Org. Chem.* **2014**, *79*, 8856–8864.

20. Ding, S.; Song, L.-J.; Chung, L. W.; Zhang, X.; Sun, J.; Wu, Y.-D. *J. Am. Chem. Soc.* **2013**, *135*, 13835–13842.

21. Ohmura, T.; Oshima, K.; Suginome, M. *Chem. Commun.* **2008**, 1416–1418.

22. Ohmura, T.; Oshima, K.; Taniguchi, H.; Suginome, M. *J. Am. Chem. Soc.* **2010**, *132*, 12194–12196.

23. Kezuka, S.; Tanaka, S.; Ohe, T.; Nakaya, Y.; Takeuchi, R. *J. Org. Chem.* **2006**, *71*, 543–552.

24. Fujino, D.; Yorimitsu, H.; Osuka, A. *J. Am. Chem. Soc.* **2014**, *136*, 6255–6258.

25. Miller, K. M.; Jamison, T. F. *J. Am. Chem. Soc.* **2004**, *126*, 15342–15343.

26. Moslin, R. M.; Jamison, T. F. *Org. Lett.* **2006**, *8*, 455–458.

27. Knapp-Reed, B.; Mahandru, G. M.; Montgomery, J. *J. Am. Chem. Soc.* **2005**, *127*, 13156–13157.

28. Malik, H. A.; Sormunen, G. J.; Montgomery, J. *J. Am. Chem. Soc.* **2010**, *132*, 6304–6305.

29. Liu, P.; Montgomery, J.; Houk, K. N. J. Am. Chem. Soc. **2011**, 133, 6956–6959.

30. Tang, X.-Q.; Montgomery, J. *J. Am. Chem. Soc.* **2000**, *122*, 6950–6954.

31. Wender, P. A.; Hegde, S. G.; Hubbard, R. D.; Zhang, L. *J. Am. Chem. Soc.* **2002**, *124*, 4956–4957.

32. Suh, E. M.; Kishi, Y. *J. Am. Chem. Soc.* **1994**, *116*, 11205–11206.

33. Katsuki, T.; Sharpless, K. B. *J. Am. Chem. Soc.* **1980**, *102*, 5974–5976.

34. Denmark, S. E.; O'Connor, S. P. *J. Org. Chem.* **1997**, *62*, 584–594.

35. Trost, B. M.; Van Vranken, D. L. *Chem. Rev.* **1996**, *96*, 395–422.

36. Claisen, L. *Berichte der Dtsch. Chem. Gesellschaft* **1912**, *45*, 3157–3166.

37. Fürstner, A. *Chem. Rev.* **1999**, *99*, 991–1046.

38. Oblinger, E.; Montgomery, J. *J. Am. Chem. Soc.* **1997**, *119*, 9065–9066.

39. Huang, W.-S.; Chan, J.; Jamison, T. F. *Org. Lett.* **2000**, *2*, 4221–4223.

40. Mahandru, G. M.; Liu, G.; Montgomery, J. *J. Am. Chem. Soc.* **2004**, *126*, 3698–3699.

41. Sa-ei, K.; Montgomery, J. *Org. Lett.* **2006**, *8*, 4441–4443.

42. Chaulagain, M. R.; Sormunen, G. J.; Montgomery, J. *J. Am. Chem. Soc.* **2007**, *129*, 9568–9569.

43. Haynes, M. T.; Liu, P.; Baxter, R. D.; Nett, A. J.; Houk, K. N.; Montgomery, J. *J. Am. Chem. Soc.* **2014**, *136*, 17495–17504.

44. McCarren, P. R.; Liu, P.; Cheong, P. H.-Y.; Jamison, T. F.; Houk, K. N. *J. Am. Chem. Soc.* **2009**, *131*, 6654–6655.

45. Liu, P.; McCarren, P.; Cheong, P. H.-Y.; Jamison, T. F.; Houk, K. N. *J. Am. Chem. Soc.* **2010**, *132* (6), 2050–2057.

46. Liu, P.; Krische, M. J.; Houk, K. N. *Chem. Eur. J.* **2011**, *17*, 4021–4029.

47. Baxter, R. D.; Montgomery, J. *J. Am. Chem. Soc.* **2011**, *133*, 5728–5731.

48. Ogoshi, S.; Tonomori, K.; Oka, M.; Kurosawa, H. *J. Am. Chem. Soc.* **2006**, *128*, 7077–7086.

49. Park, B. Y.; Montgomery, T. P.; Garza, V. J.; Krische, M. J. *J. Am. Chem. Soc.* **2013**, *135*, 16320–16323.

50. Jackson, E. P.; Montgomery, J. *J. Am. Chem. Soc.* **2015**, *137*, 958–963.

51. Malik, H. A.; Chaulagain, M. R.; Montgomery, J. *Org. Lett.* **2009**, *11*, 5734–5737.

52. Sadow, A. D.; Tilley, T. D. *J. Am. Chem. Soc.* **2004**, *127*, 643–656.

53. Baxter, R. D. PhD. Dissertation, University of Michigan 2010.

54. Haynes, M.T. PhD. Dissertation, University of Michigan 2014.

55. Corey, J. Y.; Braddock-Wilking, J. *Chem. Rev.* **1999**, *99*, 175–292.

56. Ampt, K. A. M.; Duckett, S. B.; Perutz, R. N. *Dalt. Trans.* **2007**, 2993–2996.

57. Hester, D. M.; Sun, J.; Harper, A. W.; Yang, G. K. *J. Am. Chem. Soc.* **1992**, *114*, 5234–5240.

58. Hill, R. H.; Wrighton, M. S. *Organometallics* **1987**, *6*, 632–638.

59. Lage, M. L.; Bader, S. J.; Sa-Ei, K.; Montgomery, J. *Tetrahedron* **2013**, *69*, 5609–5613.

60. Chaulagain, M. R.; Mahandru, G. M.; Montgomery, J. *Tetrahedron* **2006**, *62*, 7560–7566.

61. Montgomery, J. In *Organometallics in Synthesis*; John Wiley & Sons, Inc., 2013; pp 319–428.

62. Tamaru, Y. (Ed) *Modern Organonickel Chemistry*; Wiley-VCH Verlag GmbH & Co. KGaA, 2005

63. Wilke, G. *Angew. Chem. Int. Ed.* **1988**, *27*, 185–206.

64. Rosen, B. M.; Quasdorf, K. W.; Wilson, D. A.; Zhang, N.; Resmerita, A.-M.; Garg, N. K.; Percec, V. *Chem. Rev.* **2011**, *111*, 1346–1416.

65. Krysan, D. J.; Mackenzie, P. B. *J. Org. Chem.* **1990**, *55*, 4229–4230.

66. Bogdanović, B.; Kröner, M.; Wilke, G. *Justus Liebigs Ann. Chem.* **1966**, *699*, 1–23.

67. Tamao, K.; Sumitani, K.; Kumada, M. *J. Am. Chem. Soc.* **1972**, *94*, 4374–4376.

68. Corriu, R. J. P.; Masse, J. P. *J. Chem. Soc. Chem. Commum.* **1972**, 144a – 144a.

69. Baba, S.; Negishi, E. *J. Am. Chem. Soc.* **1976**, *98*, 6729–6731.

70. Negishi, E.; King, A. O.; Okukado, N. *J. Org. Chem.* **1977**, *42*, 1821–1823.

71. Giovannini, R.; Stüdemann, T.; Dussin, G.; Knochel, P. *Angew. Chem. Int. Ed.* **1998**, *37*, 2387–2390.

72. Wolfe, J. P.; Buchwald, S. L. *J. Am. Chem. Soc.* **1997**, *119*, 6054–6058.

73. Standley, E. A.; Jamison, T. F. *J. Am. Chem. Soc.* **2013**, *135*, 1585–1592.

74. Cornella, J.; Gómez-Bengoa, E.; Martin, R. *J. Am. Chem. Soc.* **2013**, *135*, 1997–2009.

75. Watson, M. P.; Jacobsen, E. N. *J. Am. Chem. Soc.* **2008**, *130*, 12594–12595.

76. Åkermark, B.; Martin, J.; Nyström, J.-E.; Strömberg, S.; Svensson, M.; Zetterberg, K.; Zuber, M. *Organometallics* **1998**, *17*, 367–5373.

77. Han, F.-S. *Chem. Soc. Rev.* **2013**, *42*, 14422–14423.

78. Zhao, Y.-L.; Li, Y.; Li, S.-M.; Zhou, Y.-G.; Sun, F.-Y.; Gao, L.-X.; Han, F.-S. *Adv. Synth. Catal.* **2011**, *353*, 1543–1550.

79. Molander, G. A.; Argintaru, O. A.; Aron, I.; Dreher, S. D. *Org. Lett.* **2010**, *12*, 5783–5785.

80. Molander, G. A.; Argintaru, O. A. *Org. Lett.* **2014**, *16*, 1904–1907.

81. Kende, A. S.; Liebeskind, L. S.; Braitsch, D. M. *Tetrahedron Lett.* **1975**, *16*, 3375–3378.

82. Colon, I.; Kelsey, D. R. *J. Org. Chem.* **1986**, *51*, 2627–2637.

83. Everson, D. A.; Jones, B. A.; Weix, D. J. *J. Am. Chem. Soc.* **2012**, *134* , 6146–6159.

84. Everson, D. A.; Shrestha, R.; Weix, D. J. *J. Am. Chem. Soc.* **2010**, *132*, 920–921.

85. Everson, D. A.; Weix, D. J. *J. Org. Chem.* **2014**, *79*, 4793–4798.

86. Moragas, T.; Cornella, J.; Martin, R. *J. Am. Chem. Soc.* **2014**, *136*, 17702–17705.

87. Correa, A.; León, T.; Martin, R. *J. Am. Chem. Soc.* **2014**, *136*, 1062–1069.

88. León, T.; Correa, A.; Martin, R. *J. Am. Chem. Soc.* **2013**, *135*, 1221–1224.

89. Herath, A.; Li, W.; Montgomery, J. *J. Am. Chem. Soc.* **2008**, *130*, 469–471.

90. Li, W.; Herath, A.; Montgomery, J. *J. Am. Chem. Soc.* **2009**, *131*, 17024–17029.

91. Phillips, J. H.; Montgomery, J. *Org. Lett.* **2010**, *12*, 4556–4559.

92. Beaver, M. G.; Jamison, T. F. *Org. Lett.* **2011**, *13*, 4140–4143.

93. Molinaro, C.; Jamison, T. F. *J. Am. Chem. Soc.* **2003**, *125*, 8076–8077.

94. Mahandru, G. M.; Skauge, A. R. L.; Chowdhury, S. K.; Amarasinghe, K. K. D.; Heeg, M. J.; Montgomery, J. *J. Am. Chem. Soc.* **2003**, *125*, 13481–13485.

95. Díez-González, S.; Kaur, H.; Zinn, F. K.; Stevens, E. D.; Nolan, S. P. *J. Org. Chem.* **2005**, *70*, 4784–4796.

96. Chakraborty, S.; Krause, J. A.; Guan, H. *Organometallics* **2009**, *28*, 582–586.

97. Nakao, Y.; Yamada, Y.; Kashihara, N.; Hiyama, T. *J. Am. Chem. Soc.* **2010**, *132*, 13666–13668.

98. Ng, S.-S.; Jamison, T. F. *J. Am. Chem. Soc.* **2005**, *127*, 7320–7321.

99. Ng, S.-S.; Jamison, T. F. *Tetrahedron* **2006**, *62*, 11350–11359.

100. Sergeev, A. G.; Hartwig, J. F. *Science* **2011**, *332*, 439–443.

101. Álvarez-Bercedo, P.; Martin, R. *J. Am. Chem. Soc.* **2010**, *132*, 17352–17353.

102. Chaulagain, M. R.; Mahandru, G. M.; Montgomery, J. *Tetrahedron* **2006**, *62*, 7560–7566.

103. Matsubara, K.; Miyazaki, S.; Koga, Y.; Nibu, Y.; Hashimura, T.; Matsumoto, T. *Organometallics* **2008**, *27*, 6020–6024.

104. Nakai, K.; Yoshida, Y.; Kurahashi, T.; Matsubara, S. *J. Am. Chem. Soc.* **2014**, *136*, 7797–7800.